

High Resolution Imaging Ground Penetrating Radar Design and Simulation

Charles Phillip Saunders II

Thesis submitted to the faculty of the Virginia Polytechnic Institute and State
University in partial fulfillment of the requirements for the degree of

Master of Science in Mechanical Engineering

Alfred L. Wicks, Chair

Kathleen Meehan

John P. Bird

10APR2014

Blacksburg, VA

Keywords: High Resolution, Ground Penetrating, Radar, Fundamentals, Concepts, Landmines

High Resolution Imaging Ground Penetrating Radar Design and Simulation

Charles Phillip Saunders II

ABSTRACT

This paper describes the design and simulation of a microwave band, high resolution imaging ground penetrating radar. A conceptual explanation is given on the mechanics of wave-based imaging, followed by the governing radar equations. The performance specifications for the imaging system are given as inputs to the radar equations, which output the full system specifications. Those specifications are entered into a MATLAB simulation, and the simulation results are discussed with respect to both the mechanics and the desired performance. Finally, this paper discusses limitations of the design, both with the simulations and anticipated issues if the device is fully realized.

PREFACE

This thesis is the result of research in support of an imaging metal detector. I knew that early radar and sonar systems produced a “ping” that corresponded to the target distance when the antenna or transducer was pointed in the correct direction. When installed in arrays, those systems were capable of generating detailed, sometimes photorealistic, images instead of just “blips” on an operator screen.

I spent a great deal of time trying to grasp the fundamental concepts of how an array allows a system to produce images. There were, in general, two types of literature that I could find on array-based imaging: the first group assumed you already knew how imaging worked and offered advanced processing techniques; and the other, which decided that the best way to explain imaging is with differential equations and as little supporting explanatory text as possible.

The very best papers I have read were written in a more relaxed, informal manner, and attempted to explain the fundamental concepts before or while introducing the governing mathematics. I believe that a more conversational tone helps to put the reader at ease, and I have emulated this style in this paper in the hopes that you, the reader, can focus more on what I’m saying instead of how I’m saying it.

Please feel free to contact me with any questions or feedback regarding this paper. I have had my civilian email address, “goband@gmail.com”, for nearly a decade now, and intend to keep it for the foreseeable future. Please be sure to reference radar imaging, or I may mistakenly regard your message as spam.

ACKNOWLEDGEMENTS

I would like to dedicate this paper to my Grandfather, who died around the time the first successful simulations were being performed. Words cannot express how much his love and support meant to me and everyone else in my family. He often said he didn't understand the finer points of my research, but he was always eager to hear about the latest progress, shared joy in my breakthroughs, and offered words of encouragement during my setbacks. He will be sorely missed.

I would also like to thank my advisors, friends, family, and of course, my wife Kristine ♥

TABLE OF CONTENTS

Abstract	iv
Preface	iii
Acknowledgements	iv
Table of Contents	v
List of Figures	viii
List of Tables	x
Acronymns and Abbreviations	xi
CHAPTER 1 THESIS PROBLEM DEFINITION AND APPROACH	1
Chapter Summary	1
The Landmine Problem	1
Initial Approach	1
Existing Mine Detection Systems	2
Performance Requirements - The Need for Something New	6
CHAPTER 2 RADAR MECHANICS CONCEPTUAL DESCRIPTION	8
Chapter Summary	8
Isotropic Radiators	8
Multiple Radiators	9
Continuous and Discrete Apertures	12
Beamwidth	13
Beam Steering	20
Pulsed vs. Continuous Wave Radar	21
Processing the Returned Signal	22
Sidelobes and Phantom Images	25
Spherical vs. Cartesian Resolution	27
Range Resolution	28
Basic Operation Recap	29
CHAPTER 3 RADAR MECHANICS MATHEMATICAL DESCRIPTION	31
Chapter Summary	31
Performance Metrics	31
Detection and the Signal to Noise Ratio	31

The Pulse - Range, Range Resolution, Pulse Repetition Frequency and Bandwidth	33
Aperture Size Calculation	34
Beam Width Calculation	35
Operating Frequency Selection	36
Transmitter Power Estimation.....	36
Threshold Selection.....	38
CHAPTER 4 DESIGN CRITERIA, FULL SYSTEM SPECS, AND TARGETS	39
Chapter Summary.....	39
System Design.....	39
Overview.....	39
The Minimum Target.....	40
Operating Frequency.....	42
Beam Width	43
Detection Probabilities.....	43
Antenna Selection	44
Full System Specifications	45
Targets for a Crowded Scene	46
Scanning Method and Expected Simulation Results.....	51
CHAPTER 5 SIMULATION RESULTS AND DISCUSSION.....	56
Chapter Summary.....	56
Method of Simulation.....	56
Non-Imaging Specifications.....	57
Transmission Power.....	57
Revisit Time.....	57
Small Scene Response.....	58
Varying Scan Step Size.....	58
Varying Target Size	60
Crowded Scene Response	63
CHAPTER 6 LIMITATIONS AND FUTURE WORK.....	69
Chapter Summary.....	69
Health and Safety Considerations	69

Propagation Models and Noise	70
Simulation Limitations	71
Potential Construction Issues	72
Conclusion.....	73
REFERENCES.....	75
APPENDIX A.1 – MAIN SIMULATION CODE	79
APPENDIX A.2 – TARGET FETCHING CODE	89
APPENDIX A.3 – CUSTOM DATA PLOTTER	97
APPENDIX A.4 – CUSTOM GRID OVERLAYS	98

LIST OF FIGURES

Figure 1-1. The ODIS landmine detection system, being pushed by a small vehicle. Borgwardt, C. (1996). High-precision mine detection with real-time imaging. , 2765(1) doi:10.1117/12.241232. Used under fair use, 2014.	2
Figure 1-2. A 5 meter strip of real-time generated ODIS output. Borgwardt, C. (1996). High-precision mine detection with real-time imaging. , 2765(1) doi:10.1117/12.241232. Used under fair use, 2014.....	3
Figure 1-3. The HILTI Ferroskan. HILTI. (Photographer). (2009). HILTI Ferroskan [Web Photo]. Retrieved from https://www.hilti.com/data/product/prodlarge/62304.jpg . Used under fair use, 2014.....	4
Figure 1-4. A PMN landmine, on the left, and the corresponding Ferroskan output, on the right. Bruschini, C. (2000). <i>Metal detectors in civil engineering and humanitarian demining: Overview and tests of a commercial visualizing system</i> . Informally published manuscript, Institute of Electrical Engineering, School of Engineering, École Polytechnique Fédérale de Lausanne & Vrije Universiteit Brussel, Brussels, Belgium. Retrieved from http://citeseerx.ist.psu.edu/viewdoc/download?doi=10.1.1.72.9870&rep=rep1&type=pdf . Used under fair use, 2014.	4
Figure 1-5. Sonar depth sounding, on the left, and sonar imaging, on the right, of a German Do 17 bomber. Port of London Authority. (Photographer). (2013, June 03). Dornier Do 17 bomber [Web Photo]. Retrieved from http://eandt.theiet.org/news/2013/jun/images/640_german-plane-sonar-cropped.jpg . Used under fair use, 2014. Port of London Authority. (Photographer). (2013, May 07). Dornier Do 17 bomber [Web Photo]. Retrieved from http://a57.foxnews.com/global.fncstatic.com/static/managed/img/Scitech/660/371/Possible Do17_Wessex Archaeology side scan.jpg?ve=1&tl=1 . Used under fair use, 2014.	5
Figure 1-6. GPR scans (above) and interpretation of (below) culverts under Fountains Abbey in North Yorkshire, UK. Daniels, D. J., & Institution of Electrical Engineers. (2004). <i>Ground penetrating radar</i> . London: Institution of Engineering and Technology. Used under fair use, 2014.	5
Figure 1-7. A Ditch Witch brand GPR unit. Ditch Witch. (Photographer). (2007, December). Ditch Witch 2450GR [Web Photo]. Retrieved from http://www.ditchwitch.com/sites/default/files/styles/popup/public/pictures/ditch-witch_2450GR_master_03.jpg . Used under fair use, 2014.	6
Figure 2-1. An isotropic radiator. A large positive signal is red, fading to green, and a large negative signal is dark blue, fading to light blue.....	8
Figure 2-2. Two isotropic radiators, above, with a single radiator for comparison, below.	9
Figure 2-3. Two radiators at an arbitrary distance apart.	10
Figure 2-4. Combined outputs for two radiators at various intervals.	11
Figure 2-5. Inter-element spacing of a half wavelength, on the left, and full wavelength, on the right, for an eight element array.	12
Figure 2-6. Two radiators spaced half a wavelength apart.	14
Figure 2-7. The -3dB beamwidth for a two element array.....	15
Figure 2-8. The -3dB beamwidth of a four element array.	16
Figure 2-9. The -3dB beamwidth of an eight element array.	17
Figure 2-10. The side lobes of a four element array. The side lobes have been left with full color detail; the remainder of the image has been desaturated.	18
Figure 2-11. A two element array at a spacing of a half wavelength on the left, and at one-and-a-half on the right. .	19
Figure 2-12. A four element array spaced at a half-wavelength interval is the summation of the two sub-arrays shown in Figure 2-11.	19
Figure 2-13. Continuous wave, frequency modulated radar signals.....	22
Figure 2-14. A recorded signal, in blue, and the output of the convolution, in black.	24
Figure 2-15. Convolved output of a realistic data set.	24
Figure 2-16. Phantom targets generated by side lobes.....	26
Figure 2-17. Range resolution versus pulse duration.....	28
Figure 3-1. Figure 2-17 reproduced for ease of reference.	33
Figure 4-1. Conceptual operation.	39

Figure 4-2. Array beamwidth and target radius, geometric setup.....	42
Figure 4-3. A patch antenna. Tan, Y. C. M., & Tan, Y. C. M. (2010). <i>Computational modelling and simulation to design 60GHz mmWave antenna</i> . 1-4. doi:10.1109/APS.2010.5562035. Used under fair use, 2014.....	44
Figure 4-4. 60 GHz patch antenna radiation pattern. Tan, Y. C. M., & Tan, Y. C. M. (2010). <i>Computational modelling and simulation to design 60GHz mmWave antenna</i> . 1-4. doi:10.1109/APS.2010.5562035. Used under fair use, 2014.....	45
Figure 4-5. NATO 5.56 casing dimensions. Flinch, F. (Artist). (2010, November 19). 5.56 NATO Cartridge Dimensions [Web Drawing]. Retrieved from http://ultimatereloader.com/tag/5-56-x-45mm/ . Used under fair use, 2014.	47
Figure 4-6. Slug lengths for different variations of the 5.56 round. Cooke, G. (Artist). (2005, May 03). 5.56 Ammo [Web Drawing]. Retrieved from http://www.inetres.com/gp/military/infantry/rifle/556mm_amm.html . Used under fair use, 2014.	47
Figure 4-7. A 5.56 NATO casing and its simulation approximation. Flinch, F. (Artist). (2010, November 19). 5.56 NATO Cartridge Dimensions [Web Drawing]. Retrieved from http://ultimatereloader.com/tag/5-56-x-45mm/ . Used under fair use, 2014.	48
Figure 4-8. A complete 5.56 NATO round and the slug without a shell casing. (2010, June 24). 5.56 M855A1 Enhanced Performance Round [Web Photo]. Retrieved from http://usarmy.vo.llnwd.net/e1/-images/2011/05/08/107872/army.mil-107872-2011-05-06-190552.jpg . Used under fair use, 2014.	48
Figure 4-9. A pile of PMN landmines, found outside Fallujah, Iraq, in 2003. Gaines, D. (Photographer). (2003, June 25). EOD personnel evaluating PMN mines in Fallujah, Iraq [Web Photo]. Retrieved from http://www.dodmedia.osd.mil/Assets/2004/Army/DA-SD-04-02138.JPG . Used under fair use, 2014.	49
Figure 4-10. A Russian PMN landmine. Trevelyan, J. (2000, January 01). Photographs of pmn-2 mine. Retrieved from http://school.mech.uwa.edu.au/~jamest/demining/info/pmn-2.html . Used under fair use, 2014.	50
Figure 4-11. A partially disassembled PMN landmine. Trevelyan, J. (2000, January 01). Photographs of pmn-2 mine. Retrieved from http://school.mech.uwa.edu.au/~jamest/demining/info/pmn-2.html . Used under fair use, 2014.	50
Figure 4-12. Sampling techniques.	51
Figure 4-13. An undersampled scene.	52
Figure 4-14. An adequately sampled scene.	52
Figure 4-15. Rendering methods. Left to right: Inscribed circles, bounding boxes, circumscribed circles.	53
Figure 4-16. Oversampling can improve resolution, up to half of the beamwidth.	53
Figure 4-17. Bounding boxes (sample areas) defined in terms of step distances.	54
Figure 5-1. Three targets imaged with undersampled pulse spacing. Spacing is equal to the beam width.....	59
Figure 5-2. Three targets imaged on a coarse pulse spacing grid. Spacing is the minimum necessary to sample every location in the scene.	59
Figure 5-3. Three targets imaged on a medium pulse spacing. This figure is slightly oversampled.	59
Figure 5-4. Three targets imaged on a fine pulse spacing. This figure is highly oversampled.	60
Figure 5-5. Small objects, above, and their representations, below, on a 4.88mm grid	61
Figure 5-6. Large objects, above, and their representations, below, on a 4.88mm grid.....	61
Figure 5-7. Huge objects, above, and their representations and phantom images, below. Grid spacing is 4.88mm. ..	62
Figure 5-8. The "crowded scene".	64
Figure 5-9. Full system results.....	65
Figure 5-10. Erroneous scan width settings.	66
Figure 5-11. Detail of images from Figure 5-9. The images are, top to bottom, a shell casing, a slug, and the landmine springs. From left to right are the simulation models, the optimal system results, and the suboptimal system results.....	67
Figure 6-1. A small display screen installed on the array substrate.	72

LIST OF TABLES

Table 4-1. Full system specifications.	46
---	----

ACRONYMNS AND ABBREVIATIONS

2D	-	Two Dimensional
3D	-	Three Dimensional
AISI	-	American Iron and Steel Institute
AP	-	Associated Press
EM	-	ElectroMagnetic
FCC	-	Federal Communications Commission
FPS	-	Frames Per Second
GPR	-	Ground Penetrating Radar
ISM	-	Industrial, Scientific, and Medical (a band of the EM spectrum for unlicensed use)
PCB	-	Printed Circuit Board
PRF	-	Pulse Repetition Frequency
PRI	-	Pulse Repetition Interval
Radar	-	RADio Detection And Ranging
RCS	-	Radar Cross Section
RF	-	Radio Frequency
ROC	-	Receiver Operating Characteristics
SNR	-	Signal to Noise Ratio
Sonar	-	SONic Detection And Ranging
USAF	-	United States Air Force
UXO	-	UneXploded Ordinance
VMI	-	Virginia Military Institute

Chapter 1 THESIS PROBLEM DEFINITION AND APPROACH

CHAPTER SUMMARY

This chapter details why a new ground penetrating radar (GPR) system needs to be developed, the reasoning for approaching landmines as targets, and researches landmines and current detection methods. An existing GPR system is discussed, and performance requirements show that these existing methods are not truly suitable for real landmine detection.

THE LANDMINE PROBLEM

A report from the Associated Press (AP) says that, *since the end* of the Vietnam War, more than 42,000 people have been killed and more than 62,000 people have been wounded by unexploded ordnance (UXO) and landmines, and more than 350,000 *tons* of landmines and explosives still remain *in Vietnam alone*. [1] Another AP article said, “Vietnamese officials have stated it will take 100 years and \$100,000,000,000 to clear the country of ordnance.” [2]

Outside of Vietnam, consider landmines in general. The numbers get worse. One paper published by Claudio Bruschini of the Swiss Federal Institute of Technology in Lausanne states that landmine clearance, “does not usually exceed 100 m² per deminer per day. Indeed, metal detectors cannot differentiate a mine or UXO from metallic debris.” The latter statement refers to the fact that landmines are typically not placed strictly in civilian areas, but rather in war zones - locations that are rich with shrapnel, bullets, shell casings, and other metallic waste. The paper goes on to say that there are, “between 100 and 1,000 false alarms for each real mine.” [3]

100 m² is about 1,000 square feet, or about the size of a large two bedroom apartment. The slow clearance rate is due to the fact that a deminer cannot see through the ground to identify what is causing the metal detector to alarm. Every one of the false alarms must be treated as though it were a live landmine. A report from the United Nations estimates that it would take 1,100 years to clear all the landmines from the Earth, if no new landmines were placed. Unfortunately, it also estimates that for every landmine that gets removed, 20 more are placed. [4]

INITIAL APPROACH

This project was approached from a mechanical engineering and acoustics background, with the author having little experience in RF systems. The hope was to generate images of buried metallic objects by constructing an array of metal detectors, which operate in the low kilohertz (kHz) range, usually around 1-16 kHz. [5] After initial research into acoustic imaging, the acoustic equations were used to estimate the beamwidth of an array with the hope that the results could be scaled and applied to an imaging metal detector array. This was done by replacing the speed of light for the speed of sound, with the hope that this would give meaningful

direction to guide later research. The purpose was not to try to find accurate results, but to ballpark the operating frequency range to focus research. Initial results suggested the operating frequency would be in the gigahertz range!

This was well above the low kilohertz range in which metal detectors operate. Feedback from master's committee members stated that an inductor operating in the gigahertz range was also called a "microwave transmitter" and that if this is truly the operating band, the project is a form of "ground penetrating radar" (GPR), and the focus of the background research should be directed towards the theory and operation of those systems. The advice was exactly right and that research into radar systems has resulted in this paper.

EXISTING MINE DETECTION SYSTEMS

A system for ordnance detection and identification, ODIS, was developed in the 1990's, and works in a manner similar to the system initially envisioned for this project. An array of metal detectors, referred to in the article as "induction coil sensors," builds an image of metallic objects buried under soil. This system does *not* produce high resolution images because the array performs a sort of "echo sounding," where the physical location of the array element is shaded according to the magnitude of response. This limits the resolution to that of the physical spacing between the array elements.

The system, depicted in Figure 1-1 below being pushed by a vehicle, is touted for its "low weight" of 50 kg, which is about 110 lb. The system is, "usually... pushed in front of a vehicle," likely because of the weight of the system. The system images a swath one meter wide, and generates images in real time.



Figure 1-1. The ODIS landmine detection system, being pushed by a small vehicle. Borgwardt, C. (1996). High-precision mine detection with real-time imaging. , 2765(1) doi:10.1117/12.241232. Used under fair use, 2014.

The output of the ODIS, seen in Figure 1-2 below, works okay, but the images are not crisp enough to be able to differentiate between debris and minimum metal landmines. The images in Figure 1-2 show a 25cm long, (almost 1 ft.), half-inch wide bar, and it appears similar in size as if two rifle casings were located next to each other. [6]

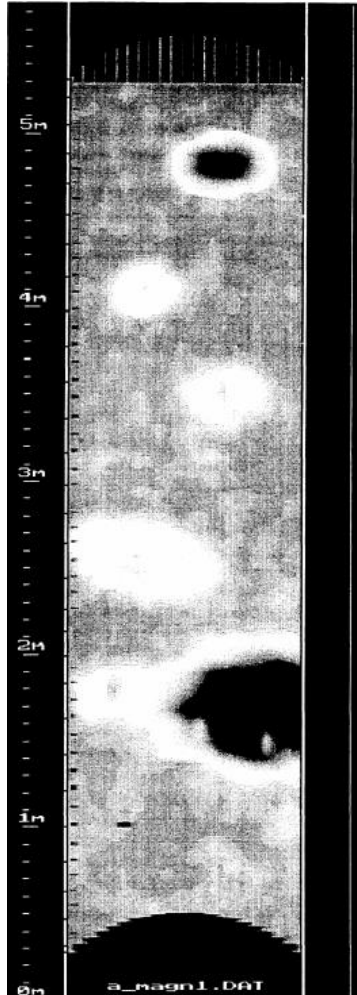


Figure 1-2. A 5 meter strip of real-time generated ODIS output. Borgwardt, C. (1996). High-precision mine detection with real-time imaging. , 2765(1) doi:10.1117/12.241232. Used under fair use, 2014.

From the top down, the objects are: an antipersonnel mine (model PPM2); an iron ball 2 cm in diameter, buried 12 cm deep; a rifle cartridge buried 12 cm deep; an iron bar, 1 cm in diameter, 25 cm long, buried 15 cm deep; and two objects, an iron ball 5 cm in diameter on the left, buried 25 cm deep, and an anti-tank mine on the right, buried 5 cm deep. [6]

Another paper evaluates using a metallic imaging system designed for use in locating rebar in concrete structures to attempt to locate landmines. [3] The HILTI brand “Ferrosan” unit, depicted in Figure 1-3, operates in a manner similar to the ODIS. The user holds the handle of the detector and presses the detector against a wall. The wheels rotate as an area is scanned, and encoders in the wheels log position versus detected response.



Figure 1-3. The HILTI Ferroskan. HILTI. (Photographer). (2009). HILTI Ferroskan [Web Photo]. Retrieved from <https://www.hilti.com/data/product/prodlarge/62304.jpg> . Used under fair use, 2014.

The Ferroskan, operating in a manner similar to the ODIS, produces an output image that is also similar to the ODIS output. Compare Figure 1-4 with the top object from Figure 1-2. The problem with these units is that they cannot resolve small objects because the method of data acquisition does not allow for calculation of information between the data points because the effects of magnetic fields are not suitable for linear interpolation and the correct method of nonlinear interpolation cannot be used without first knowing the orientation and shape of the objects.

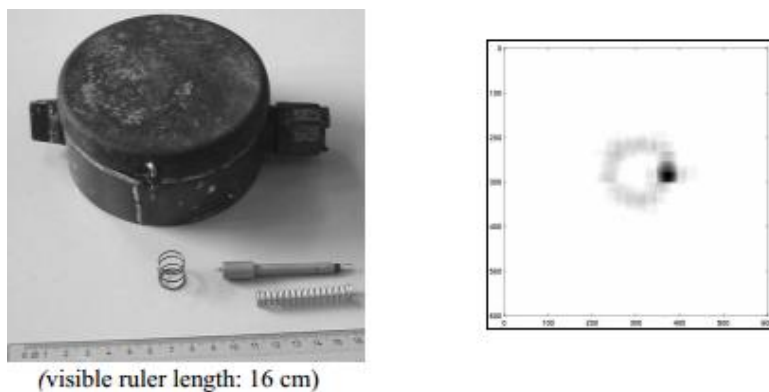


Figure 1-4. A PMN landmine, on the left, and the corresponding Ferroskan output, on the right. Bruschini, C. (2000). *Metal detectors in civil engineering and humanitarian demining: Overview and tests of a commercial visualizing system*. Informally published manuscript, Institute of Electrical Engineering, School of Engineering, École Polytechnique Fédérale de Lausanne & Vrije Universiteit Brussel, Brussels, Belgium. Retrieved from <http://citeseerx.ist.psu.edu/viewdoc/download?doi=10.1.1.72.9870&rep=rep1&type=pdf>. Used under fair use, 2014.

Figure 1-5 below shows two sonar images of a WWII German Do 17 bomber on the bottom of the English Channel. [8][9] The method used by the Ferroskan and ODIS is akin to depth sounding, which produces the image on the left of Figure 1-5 below. The images are blocky and low resolution because there is no image information between discrete points. The result is essentially a point cloud, where it is up to the end user to infer the contours from the points.

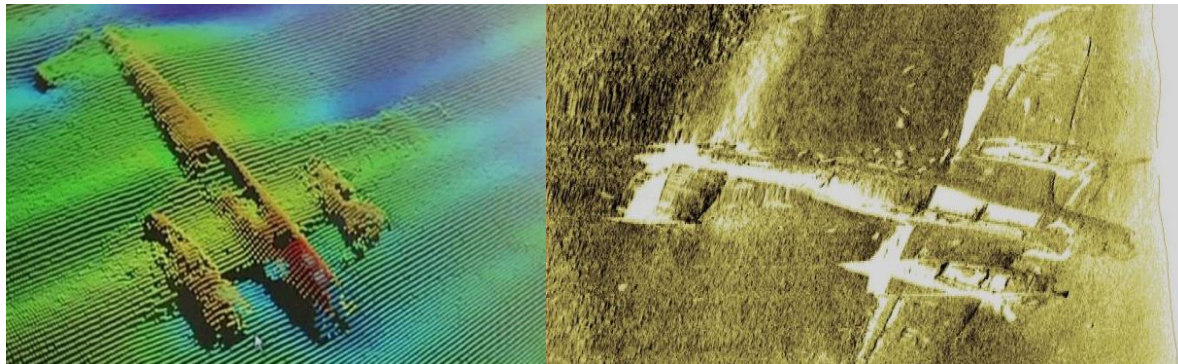


Figure 1-5. Sonar depth sounding, on the left, and sonar imaging, on the right, of a German Do 17 bomber. Port of London Authority. (Photographer). (2013, June 03). Dornier Do 17 bomber [Web Photo]. Retrieved from http://eandt.theiet.org/news/2013/jun/images/640_german-plane-sonar-cropped.jpg. Used under fair use, 2014. Port of London Authority. (Photographer). (2013, May 07). Dornier Do 17 bomber [Web Photo]. Retrieved from http://a57.foxnews.com/global.fncstatic.com/static/managed/img/Scitech/660/371/Possible Do17_Wessex Archaeology side scan.jpg?ve=1&tl=1. Used under fair use, 2014.

A true imaging system uses an array and post-processing to generate a smoother, more detailed image, such as the image on the right in Figure 1-5. [9] As mentioned earlier, the research was guided to ground penetrating radar systems, but the GPR systems researched produced worse images than the Ferroskan or ODIS! Figure 1-6 below shows real GPR data and an interpretation of the scan.

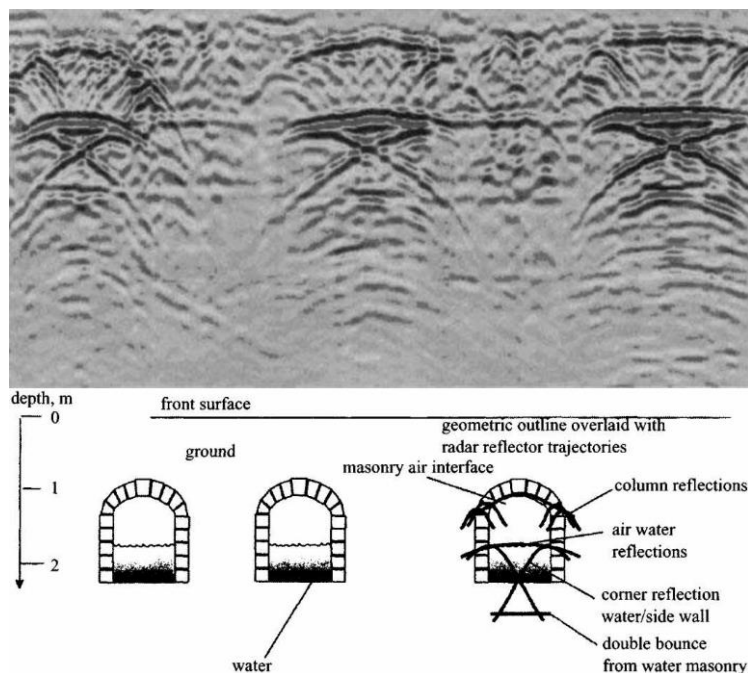


Figure 1-6. GPR scans (above) and interpretation of (below) culverts under Fountains Abbey in North Yorkshire, UK. Daniels, D. J., & Institution of Electrical Engineers. (2004). *Ground penetrating radar*. London: Institution of Engineering and Technology. Used under fair use, 2014.

The data is hard to understand because the images are typically rendered as two dimensional (2D) “slices” of the terrain under the GPR unit. This, in turn, is because GPR units are typically only equipped with one antenna! The relatively low frequencies, in the range of 100MHz to 1GHz, require antennas so large that it is not practical to have a system that uses multiple antennas. [11][12]

Compare the GPR in Figure 1-7 with the Ferrosan in Figure 1-3. Both units use feedback from the wheels to relate sensor data to real, physical coordinates. The only difference is that of scale; the Ferrosan is designed to be handheld, while the GPR units are designed to be pushed by a person. When a GPR unit is advertised as “three dimensional” (3D), the unit is not capable of imaging in 3D in real time, but rather requires the user to generate several “slices” of terrain, by first pushing the GPR in a “mowing the lawn” pattern, and *then* those slices are displayed side-by-side to produce a 3D image.



Figure 1-7. A Ditch Witch brand GPR unit. Ditch Witch. (Photographer). (2007, December). Ditch Witch 2450GR [Web Photo]. Retrieved from http://www.ditchwitch.com/sites/default/files/styles/public/pictures/ditch-witch_2450GR_master_03.jpg. Used under fair use, 2014.

PERFORMANCE REQUIREMENTS - THE NEED FOR SOMETHING NEW

For landmine detection, there is a different set of performance requirements that renders the existing GPR systems useless. First, the system must produce better images than the profile style of imagers shown above. The radar system should be capable of producing images that are easily interpreted. In addition, the radar system should not rely on post-processed results from a large scan area – someone has to walk around a minefield to perform the scan! Additionally, any wheels located on the unit to support the antenna and encoder electronics could inadvertently set

off a landmine. The images should be rendered in real time, and the images should be rendered in a three dimensional (3D) format that lends itself to quick interpretation.

There are practical limitations on range as well. Landmines are found under shallow cover, such that the force of a person above is not dispersed by a large layer of soil, so there is no need to image great distances into the ground, as with surveying equipment. Additionally, unlike surveying equipment, which is expected to locate large underground features, the landmine detector should have a resolution high enough to be able to distinguish between shrapnel, bullets, and the firing pin in a landmine.

A high resolution, low range, handheld, 3D, real-time imaging radar system does not exist. The remainder of this paper describes the technical specifications and signal processing requirements necessary to produce such a device. Chapter 2 describes the concepts behind *how* an imaging radar system works. It is firmly believed that a conceptual understanding is required in order to make sense of the radar equations shown in Chapter 3.

With a firm understanding of the concepts, the usage of the governing equations becomes very straightforward, and, given the required performance specifications, the full system details are derived relatively quickly. Chapter 4 describes the physical constraints that drive the system design and explain the choice of targets, and Chapter 5 discusses the results of the MATLAB simulations under a variety of scenarios. Lastly, Chapter 6 discusses limitations of the system simulations and makes note of practical physical limitations that were not considered as part of the system design.

Chapter 2 RADAR MECHANICS CONCEPTUAL DESCRIPTION

CHAPTER SUMMARY

This chapter explains how an imaging radar system actually works. Discrete and continuous apertures are built up from isotropic radiators, and the relationship between aperture size, operating frequency, and beamwidth is discussed. The mechanics of beam steering are explained, along with reciprocity and the relationship between transmitters and receivers. Finally, this chapter discusses the tradeoff between continuous and pulsed radar systems, and discusses the signal processing needs for the pulsed radar system designed in this paper.

ISOTROPIC RADIATORS

An isotropic radiator, depicted in Figure 2-1 below, is both the simplest form of a radiator and the simplest way of imagining a radiator. An isotropic radiator emits a signal evenly in all directions. Figure 2-1 shows concentric circles, where the dark blue circles represent troughs or minima of the radiated signal, and where the dark red circles represent peaks or maxima of the radiated signal. As the distance from the radiator increases, the signal fades. In this case, the signal fade is not due to any atmospheric attenuation, but instead from the fact that, as distance increases, the same “quantity” of signal must now be “stretched” to occupy a larger space. Conservation of energy dictates that the signal magnitude must be reduced in order to maintain the total signal energy constant.

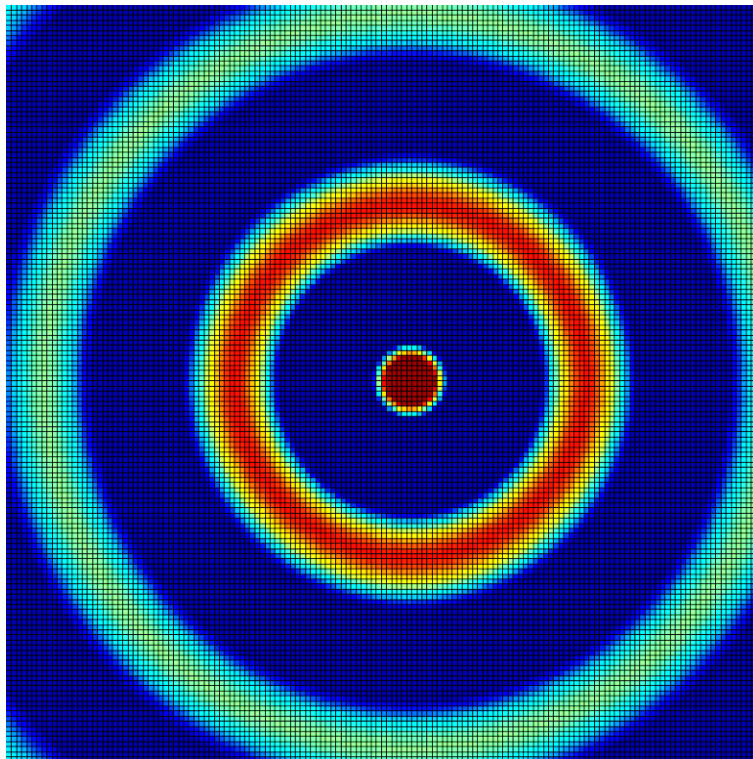


Figure 2-1. An isotropic radiator. A large positive signal is red, fading to green, and a large negative signal is dark blue, fading to light blue.

The isotropic radiator shown appears two dimensional, but a true isotropic radiator emits the signal evenly in *all* directions. That is, the isotropic radiator is actually a stack of concentric *spheres* instead of circles, like an onion, and the view in Figure 2-1 is similar to an onion sliced in half, looking at the sliced surface.

MULTIPLE RADIATORS

When a second radiator is added to the scene, the emissions collide. Where two peaks or two troughs collide, they combine and increase in magnitude. Where a peak and a trough collide, they combine and cancel. The resulting *interference pattern* is the result of the summation of the emitted signal from every radiator at every point in space. That is, the interference pattern is the *superposition* of the output of all radiators. This is seen more clearly in Figure 2-2 below.

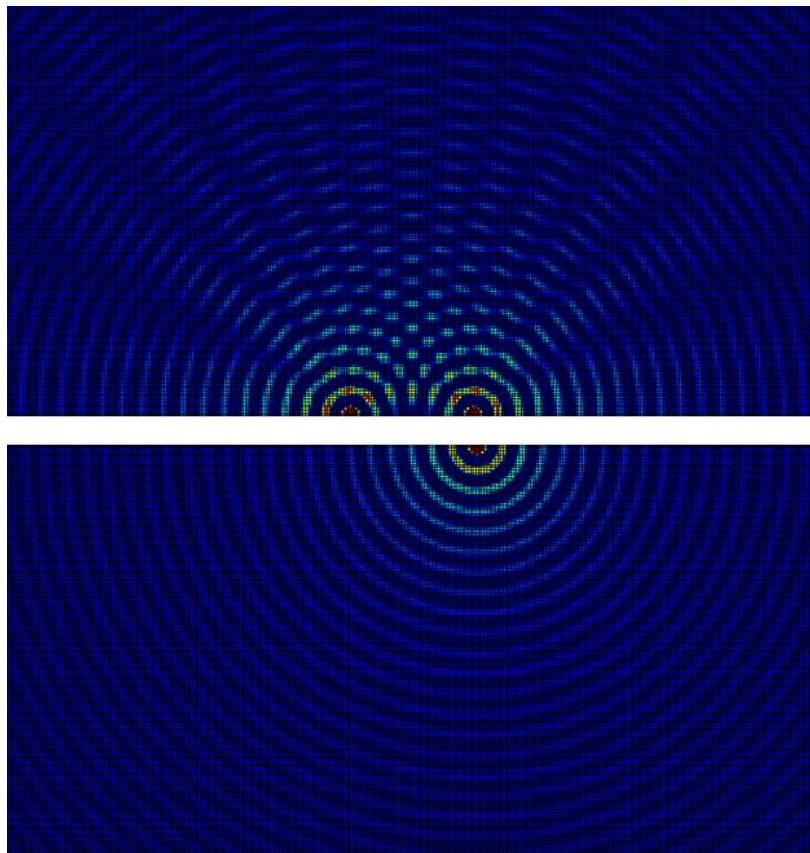


Figure 2-2. Two isotropic radiators, above, with a single radiator for comparison, below.

The interference pattern is periodic in nature, and is determined by both the phase and spacing between radiators, as will be shown later. Two radiators spaced an arbitrary distance apart, as in Figure 2-2 above and Figure 2-3 below, generate an interference or *radiation pattern* that can be calculated, but lacks any meaningful use. However, these radiators can be placed in positions relative to one another such that their combined output becomes useful.

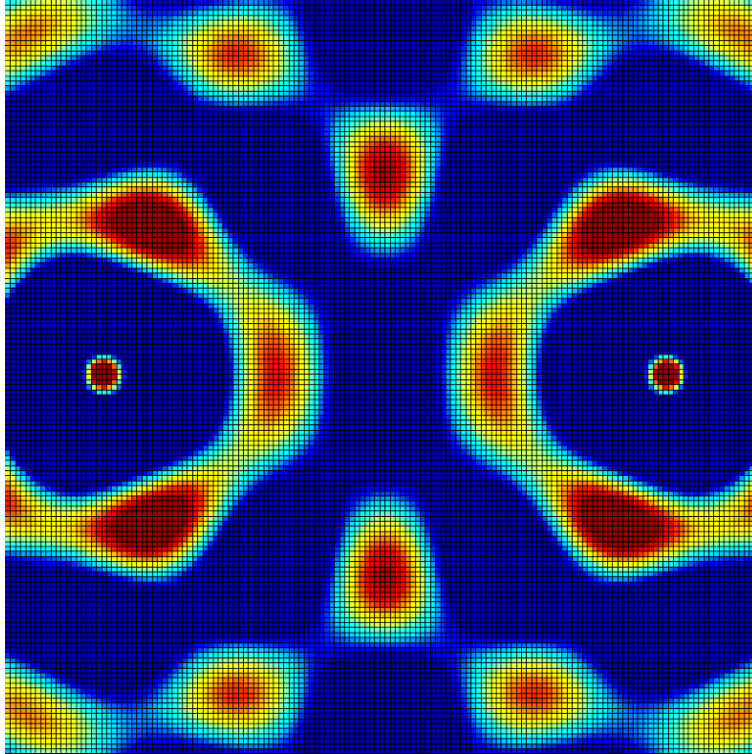


Figure 2-3. Two radiators at an arbitrary distance apart.

To understand how the radiators are positioned, it is essential to define a positioning unit. Instead of using inches or centimeters, which are *independent* of the radiator’s operating frequency, spacing is typically referred to in *wavelengths*, which is a unit of measure that is *dependent* on the operating frequency, as defined in Equation 2.1 below.

$$\lambda = \frac{c}{f} \quad (2.1)$$

Here λ is the wavelength, in meters; c is the speed of wave propagation, i.e., the speed of light for electromagnetic waves, in meters per second; and f is the frequency of the wave, in hertz. Using wavelengths as a measure of distance keeps the measurement in a real, physical unit (meters), but importantly, the unit of measure *scales* with the operating frequency and thus can be used to refer to antennas and radiators *operating at any frequency*.

Now, with a definition for positioning, comes the selection of the “best” position to put a radiator. The position of the radiators relative to one another determines how the waves collide and either combine or cancel. As seen in Figure 2-4, they can either be spaced such that their total output maximizes (top of plot), cancels (bottom of plot), or is somewhere in the middle (middle of plot). The radiators are represented with a large “X,” and their outputs are shown in blue or purple, with the combined output in green on the right.

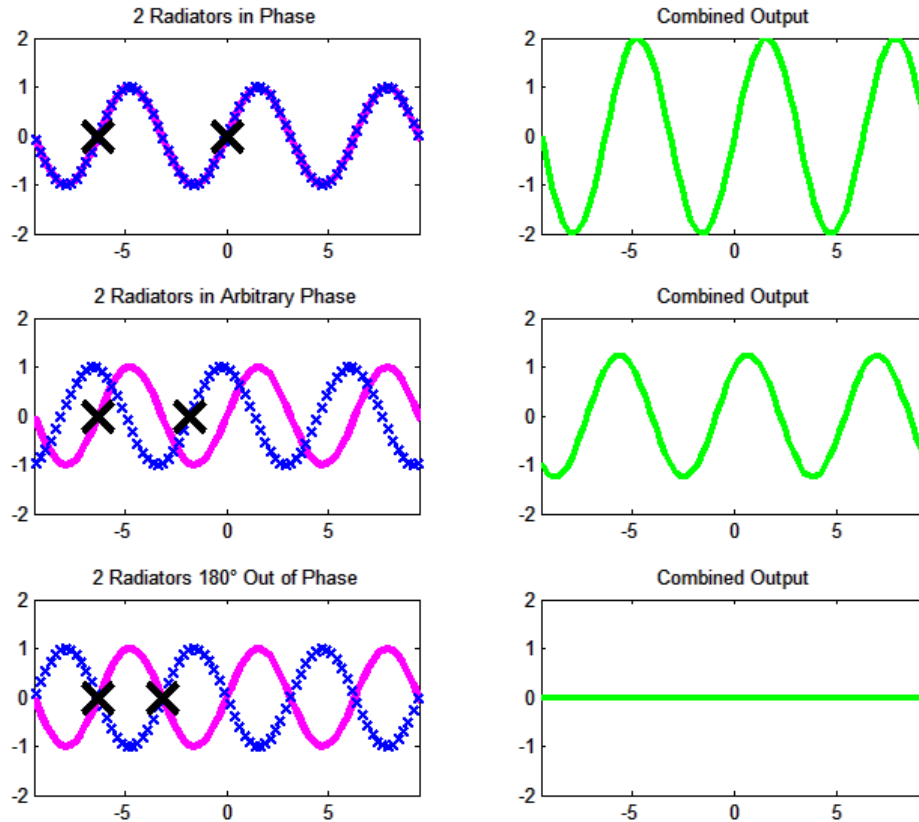


Figure 2-4. Combined outputs for two radiators at various intervals.

To help explain the selection of the ideal spacing between radiators, remember that the point of all of this is to transmit a signal *to a target*. To that end, it makes the most sense to attempt to concentrate all of the radiated energy in the direction of the target. The only signal power that can exist is that which has been emitted, and more than that, the only signal power that can exist is that which has been emitted *and not been cancelled*. There is a tradeoff in signal strength as the radiators move relative to one another - it is possible to situate a local maximum anywhere in space, but that comes at the cost of cancelling or reducing signal elsewhere.

For the moment, consider only two radiators. There will always be only one line that runs between them - the array axis. Call this the x-axis. The “broadside” location, as in nautical terminology, will always be perpendicular to the array (perpendicular to the x-axis), so call that the y-axis. It is not possible to shift either point along the y-axis, because the x-axis was *defined* as the line that connects the two radiators. This means that if you attempt to move one radiator along the y-axis, the coordinate system simply rotates until both points return to their position along the line $y = 0$.

Because these two radiators are *always* aligned on the $y = 0$ axis, assuming that they are radiating in phase (this is an important assumption that will be discussed later), they will always radiate in sync along the y-axis. If they are spaced one full wavelength apart, then their signals

will exactly overlap and they will also radiate in sync along the x-axis. But, because they have been aligned to purposefully maximize along *two* axes, they are dividing their total radiative power along *two* axes.

If, instead of being spaced to maximize along the x-axis, they were spaced with intent of *cancelling* along the x-axis, then the result would be that they could only maximize along *one* axis, and that would better focus the total energy along that axis. This can be clearly seen in Figure 2-5 below. The image on the left is an eight element array spaced at half-wavelength intervals, while the image on the right is at full wavelength intervals. On the left, the signal is still reddish orange halfway to the edge of the graphic, which represents a large magnitude signal, while the signal on the right is a bluish green, which indicates a signal close to zero.

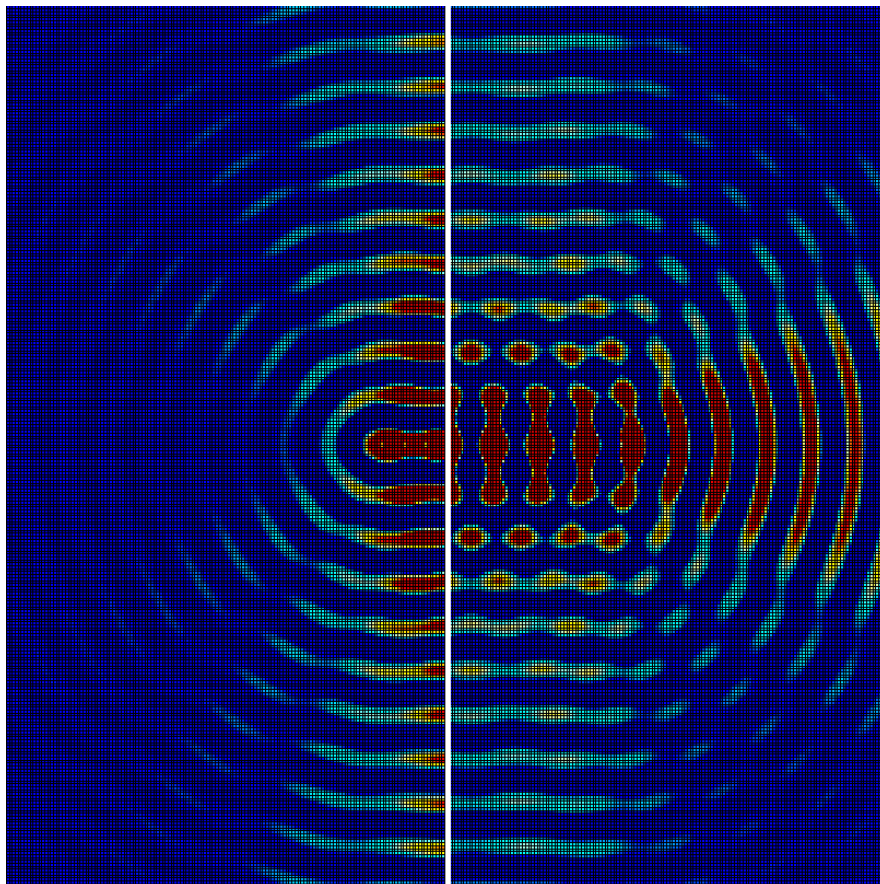


Figure 2-5. Inter-element spacing of a half wavelength, on the left, and full wavelength, on the right, for an eight element array.

CONTINUOUS AND DISCRETE APERTURES

It is possible to place isotropic radiators *infinitely close* to one another, such that their radiation patterns *almost* exactly overlay one another. This infinitely close spacing is what is used to build up the radiation pattern of real antennas. Antennas are typically imagined as real,

physical devices, through which a signal is transmitted or received. While this is true, it is also possible to send or receive a signal from an imaginary surface that *is not a physical antenna*.

Photographers are used to the term *aperture* in reference to the opening in a camera through which light can enter. The light that exposes an image *is not created* by the aperture, but nonetheless it diverges from the aperture *as though it was*. Another, easier, example to imagine is a mirror. It is possible to direct light from a flashlight or other source with a mirror. The mirror *is not creating* the light, but it doesn't matter! The light still shines from the mirror *as if it had* created the light.

Therein lies the difference between an *antenna* and an *aperture*. The word “antenna” refers to the *device* that generates or ultimately receives the signal, while the word “aperture” refers to the *surface* from which a signal is transmitted or received. For most devices, antenna and aperture are synonymous, but there are a *great many* examples where they are not.

For instance, your voice is not created in your mouth; it is generated by your vocal cords, in your throat. Your voice does not come from your throat though, nor does it come from your tongue or your teeth. Your voice leaves your body through the *imaginary surface* that exists between your lips! When you cup your hands to your mouth to be heard at greater distances, you are *not* focusing your voice with your hands, you are increasing the effective size of that imaginary surface between your lips. The focusing is done not by your palms, but by the opening at the edges of your hands. You are literally giving yourself a bigger mouth (a larger aperture).

Surfaces like your mouth, a car antenna, a mirror, and others are referred to as *continuous apertures* because they are one continuous body. This is the most common case, but apertures can also be *sampled* or *discrete*. To imagine a discretized aperture, compare a string of holiday lights wrapped around a stick to a long fluorescent light bulb. Both are about the same size, about the same length, and both may illuminate a room about the same. The fluorescent bulb has a *continuous* surface that emits light, while the holiday lights are *discrete* bulbs whose sum *approximates* the continuous light-emitting surface of the fluorescent bulb.

A discrete aperture made of elements arranged on a regular spacing can be referred to as an *array*, and how well an array approximates a continuous aperture depends on the number of elements involved and the spacing between those elements. As discussed earlier, for this purpose, the “best” inter-element spacing is every half wavelength. If the inter-element spacing is fixed and the desired aperture width is known, then the number of elements required can be quickly determined. The importance of the aperture size is discussed next.

BEAMWIDTH

The resolution delivered by the imaging system is ultimately determined by the width of the beam used by the system. Consider television or picture resolution ratings. Typically measured in “pixels” or “megapixels,” a higher pixel count means a higher resolution image, which in turn means a sharper, more detailed image. A standard definition television signal is

480 pixels across, a high resolution broadcast signals is 720 pixels across, and an ultra-high resolution signal, such as that found on a Blu-Ray disc, is 1080 pixels across.

The higher pixel count means that there are more data points in a given image with which to reproduce the initial scene. If the television or picture's physical dimensions remain constant, then a higher resolution image requires the individual pixels to be physically smaller than those of the lower resolution image. The actual dimensions of the pixels are measured with Cartesian coordinates because the pixels exist on a planar surface.

With radar systems, the image resolution is determined by the beamwidth and by the size of the increment used to "steer" the beam to a given location. The mechanics of beam steering will be discussed shortly, but suffice it to say that the output of the radar array can be pointed in a desired direction. Two radiators spaced half a wavelength apart can be seen in Figure 2-6 below.

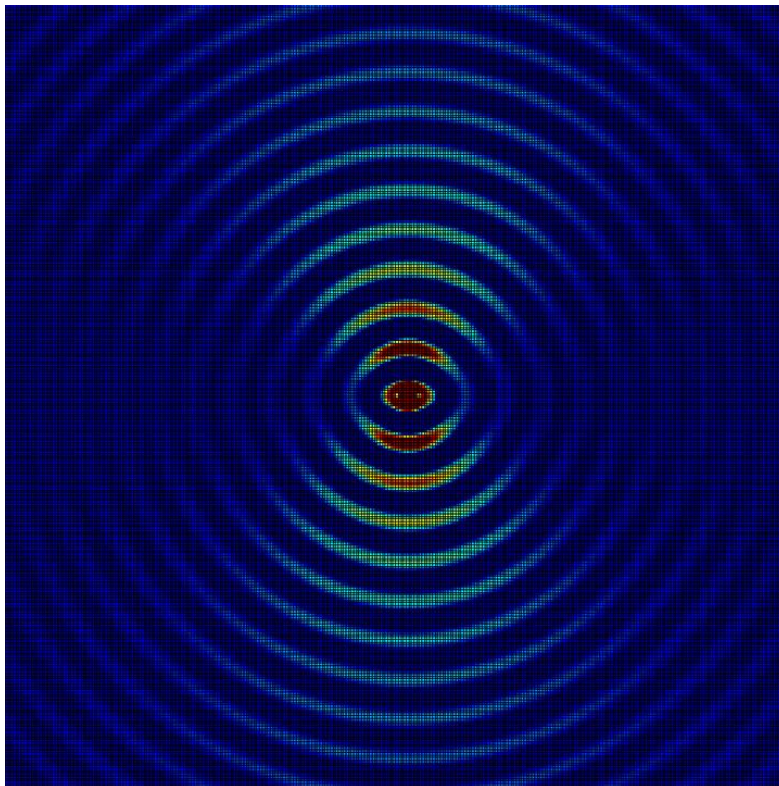


Figure 2-6. Two radiators spaced half a wavelength apart.

The output of the two element array seen above already appears to make a "wedge" or "cone" shape. The vertex of the beam actually occurs at the center of the array, and *not* at either element in the array.

No matter how narrow the beam is made, it will *always* be divergent; meaning that, unlike the pixels in a TV screen, the actual width of the beam *varies*, getting wider as the

distance from the array increases. The width at a specific distance from the array can be calculated with geometry.

Rather than attempting to recalculate actual widths at every increment using geometry and Cartesian coordinates, radar systems use polar coordinates and refer to the width of the beam in degrees rather than attempting to define a range and refer to what the widths would be at that hypothetical distance from the array. This is similar again to the unit of “pixels” – most televisions sold today are high definition, meaning that *regardless of the physical size of the television, they are always 1080 pixels across*. The physical interpretation of the unit is fixed by the size of the scene.

Returning to the two radiator array seen in Figure 2-6, the exact shape of the beam can *almost* be discerned, but not quite, because the signal tapers gradually from a maximum along the vertical axis, to near zero along the horizontal axis. There are different ways to define the “edge” of the beam, but the most common is by evaluating the angular line where the signal fades to half the power that exists at the radiator. The *half-power* beamwidth is denoted in the same way that “half power” commonly is in engineering circles – as the *-3dB* beamwidth. The -3dB beamwidth is shown in Figure 2-7 below. Another method of defining the main lobe width is the distance between the first nulls on either side of the beam. However, for a two element array, the distance between nulls is 180°! [14]

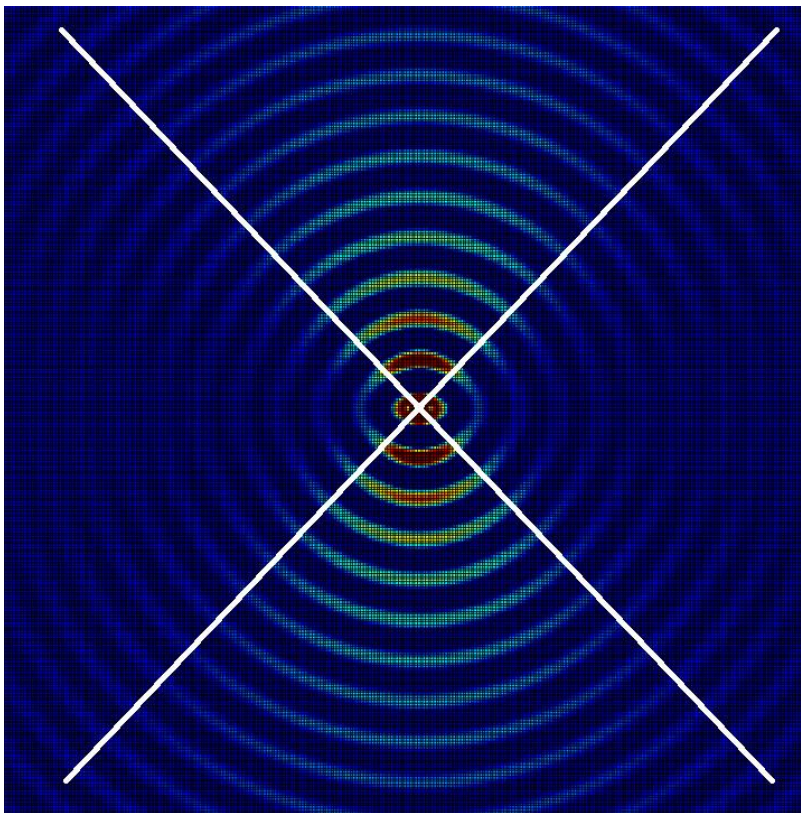


Figure 2-7. The -3dB beamwidth for a two element array.

Now, with the edge of the beam *defined*, it can be *measured*. The specific equations for determining an exact beamwidth are given in Chapter 3; this chapter is concerned with the *concepts*. Generally speaking, the beam in Figure 2-7 is very wide. If the array width is increased, then the beamwidth narrows, as seen in the four element array depicted in Figure 2-8.

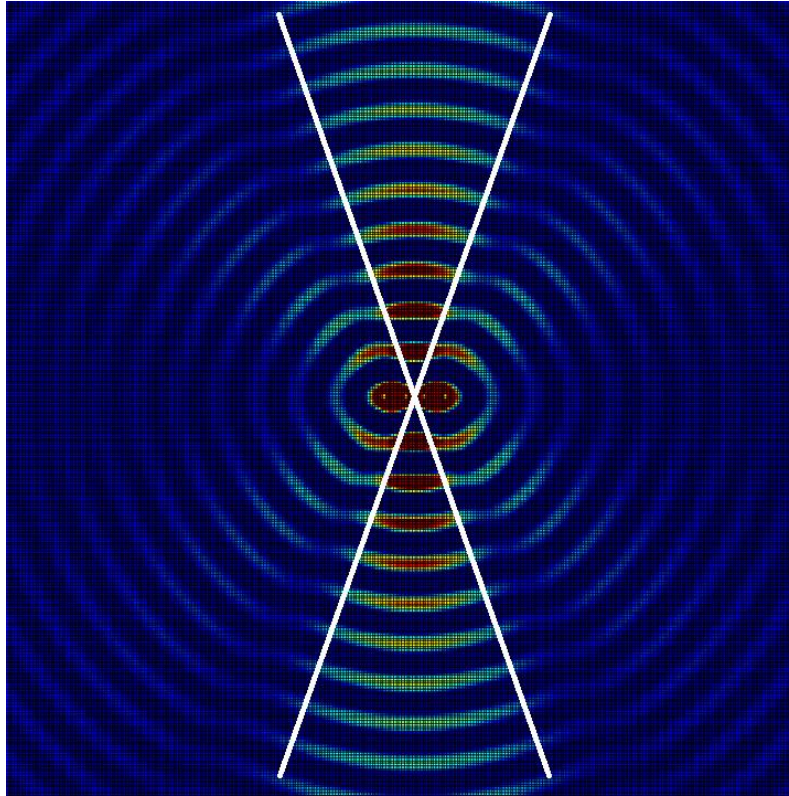


Figure 2-8. The -3dB beamwidth of a four element array.

If the array is doubled in width again, as seen in Figure 2-9, the beamwidth continues to narrow. This pattern continues – as the width of the aperture increases, the beamwidth gets narrower. As a side note, there are other array intervals that can be chosen for particular design reasons, but in general, half wavelength intervals provide a fair compromise between beamwidth and side lobe levels. Sidelobes, which will be discussed shortly, increase in magnitude as the beam is narrowed and in quantity as the aperture is widened. Sacrifices can be made to exchange beamwidth for side lobe reduction, but sidelobes are not a nuisance for the purposes of this paper, so an array spacing of a half wavelength was maintained.

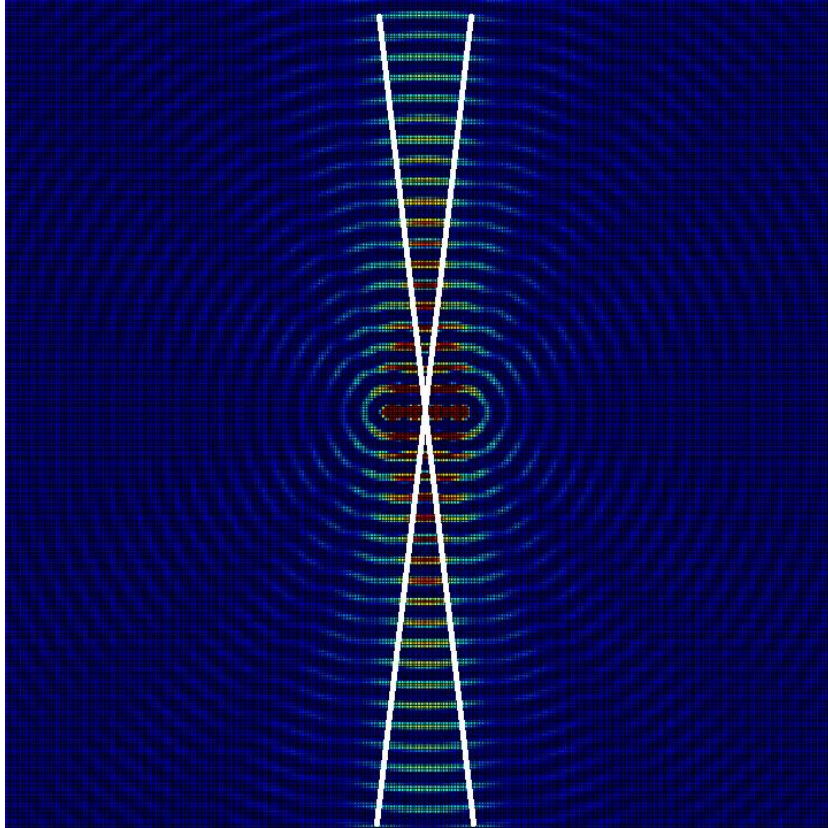


Figure 2-9. The -3dB beamwidth of an eight element array.

The figures above that show the beamwidth are intended to show the *angular width* of the beam emitted from the array. The same -3dB definition that is used to define the sides of the beam also define where the beam “ends.” At some distance from the array, signal fade and atmospheric attenuation will reduce the signal power to half of what it was when it left the array.

It is important to note that, by picking “wavelength” as the spacing unit, the *beamwidth is independent of operating frequency*. It is possible to achieve high resolution beams using any frequency. The problem with trying to get high resolution systems with low frequencies is that the wavelengths are long. At 300 kHz, the wavelength is a kilometer long! An eight element array at that frequency would span almost 2.5 miles.

Also important to note is a set of features in Figure 2-8 and Figure 2-9 that appear as pairs of signals emitting at some off-axis angle. The beams coming out of the side of the array are called “side lobes,” and the main beam coming out of the array is called the “main lobe.”

The side lobes, highlighted in Figure 2-10 below from a four element array, are a result of having more than two elements in the array when the array is spaced on half-wavelength increments. Refer back to Figure 2-2 and notice now that there are *many* lesser lobes emitting from between the two elements in the array. This is because the elements are spaced an *arbitrary*

distance from one another. Also notice that each lobe in Figure 2-2 appears to emit from the imaginary point exactly between the two real radiators.

As mentioned earlier, the total radiation pattern emitted by the array is the superposition of the output of all the elements. It is also possible to imagine the superposition as the summation of several sub-arrays because the addition process has commutative and associative properties, which means that the order and grouping in which the elements are added does not matter, as long as each base element is represented once and only once in the sum.

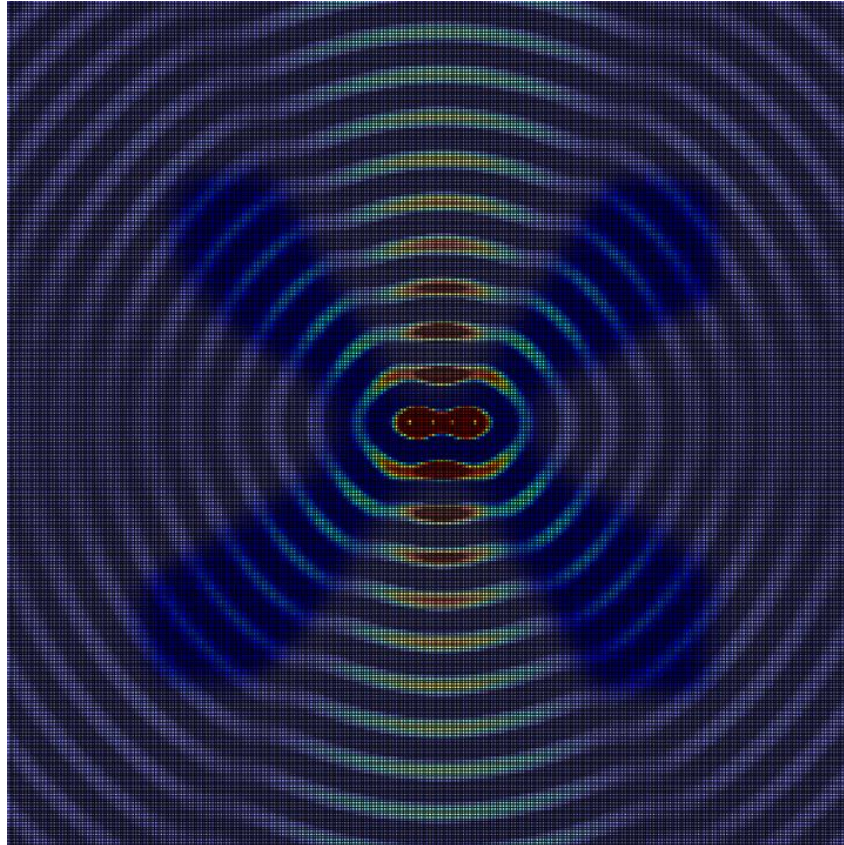


Figure 2-10. The side lobes of a four element array. The side lobes have been left with full color detail; the remainder of the image has been desaturated.

Consider, then, the four element, half-wavelength spaced array in Figure 2-12 as a two element array with one additional element on either side. Allow the elements to be numbered, left to right, as 1, 2, 3, 4. The total output of the array could then be considered as the sum of one two element array with “optimal” half-wavelength spacing (elements 2 and 3), and one two element array with “suboptimal” three-halves-wavelength spacing (elements 1 and 4).

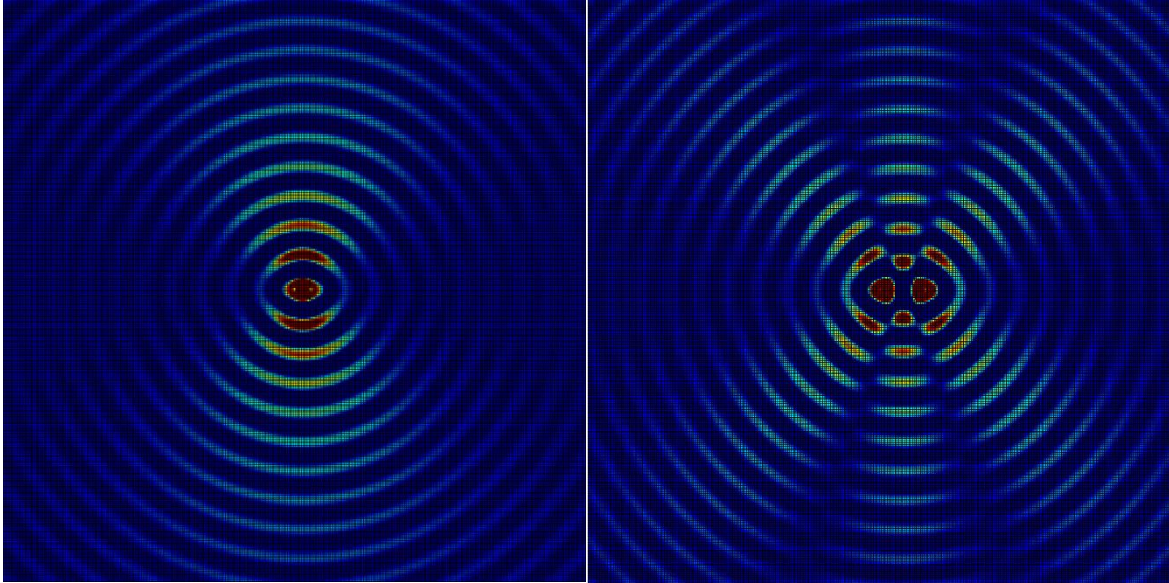


Figure 2-11. A two element array at a spacing of a half wavelength on the left, and at one-and-a-half on the right.

Consider Figure 2-11 above. The figures on the left and right are both two-element arrays, but the one on the left is spaced on a half wavelength interval while the one on the right is spaced at one and a half wavelengths. The total output of the array, seen in Figure 2-12 below, is the result of the sum of the “optimal” array with one “suboptimal” array. The suboptimal array introduces two sidelobes, but also acts to narrow the main beam. Both sub-arrays produce a signal along the broadside axis, so those broadside signals are maximized. At every other location the arrays are not *both* at peak values, so the summed output is something less than the magnitude of the main lobe.

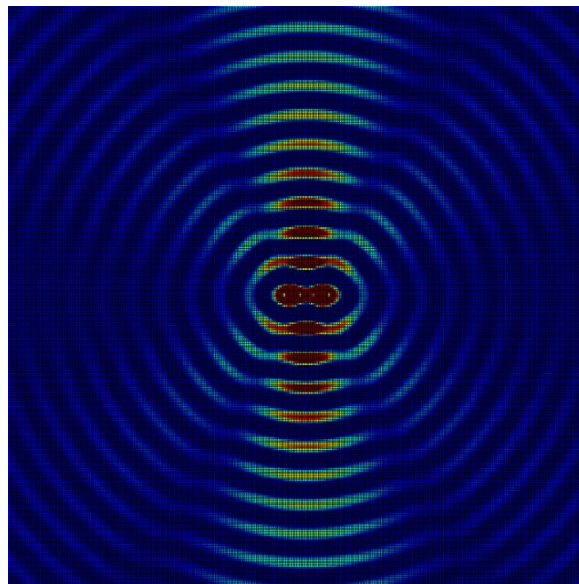


Figure 2-12. A four element array spaced at a half-wavelength interval is the summation of the two sub-arrays shown in Figure 2-11.

BEAM STEERING

The “optimal” array spacing was determined by evaluating the output of two antennas that are radiating *in phase* with one another. This assumption was made earlier, in the Multiple Radiators section, with the promise that it would be discussed later. The effects of out-of-phase radiators are discussed now.

The half-wavelength spacing between elements served two purposes. First, it ensured that the signal was canceled along the array axis, and second, by canceling along the array axis, the broadside signal was maximized. The decision to cancel along the array axis was made because there was no way to cancel along the broadside direction, because the signals could not be shifted relative to one another along the broadside axis. However, if a phase difference is introduced between the radiating elements, then the effect is *as if* they had been physically repositioned.

Now, with a phase shift, it is possible to cancel along the broadside axis! Shifting one radiator half a *cycle* in phase (180°) corresponds to moving it physically by half a *wavelength*. As discussed at length earlier, by effectively “moving” the radiator half a wavelength, the signals now cancel along the broadside axis. However, the radiator was not physically repositioned, so it is still located on the array axis, where it remains physically spaced half a wavelength from the other radiator.

Now, being shifted, one radiator is effectively half a wavelength away from the other because of the phase shift, and now it’s *also* half a wavelength away because it’s physically located half a wavelength away. That is, the radiators exist “as if” they were spaced half a wavelength apart on the broadside axis, and “as if” they were spaced a full wavelength apart on the array axis. This means that, while the signals cancel along broadside, they now combine and *maximize* along the array axis.

The transition between maximizing along the broadside axis and maximizing along the array axis is not instantaneous! If the phase difference were to gradually change, the axis of maximization would slowly move from broadside towards the array axis. If there is no phase shift, the array output is at broadside. As the phase shift increases towards $+180^\circ$, the array output “points” more towards one side. The array becomes an “endfire” array, meaning an array that emits along the array axis, when the phase shift reaches 180° .

As the phase shift is decreased towards -180° , the beam points towards the other side, becoming an endfire array along the opposite end when the phase shift reaches -180° . The particulars of which direction the beam points depend on how you, the designer, define the coordinate system and how you define a positive or negative phase shift.

PULSED VS. CONTINUOUS WAVE RADAR

The two main categories of radar systems, in terms of overall operation, are continuous wave and pulse. These systems operate exactly the way they sound – continuous wave systems have transmitters that are always on, while pulsed systems turn on the transmitters for a short period of time, then turn them off and “listen” for an echo.

Conceptually speaking, pulsed systems are the most straightforward to understand. Transmit a brief signal, and then count the time that elapses until an echo is received. The distance between the array and the target is the elapsed time multiplied by the speed of wave propagation, e.g., the speed of light for radar, or the speed of sound for sonar. The transmitter is turned off whenever the receiver is turned on, so the receiver has a “quiet” environment in which to listen for a response.

Continuous wave radar, without any form of signal modulation, *cannot determine distance* because the output is continuous. There is no reference point defining the “start” of the signal, so it is not possible to determine the time between transmission and reception. Without an elapsed time, it is not possible to calculate range.

The solution to creating a time reference with continuous wave radar is to modulate the signal such that there is a definite way with which to correlate a response to a known point in time. Frequency modulation provides the means to transform a continuous *fixed* frequency output to a *range* of frequencies. The length of time to cycle through the range of frequencies is not fixed, but it is usually a “long” time period. Here “long” means that the time that should elapse before revisiting the first frequency should be at least *as long or longer* than the time that it would take to receive a signal from the maximum range of the unit.

Consider Figure 2-13 below. The frequency modulation method is similar to a chirp signal, where the signal starts at some relatively low frequency then rises to a higher frequency before repeating the signal. If the signal repeats before a response from the maximum range could be received, then it would not be possible for the system to differentiate between a very close and a very far target. A long modulation period ensures ranging accuracy.

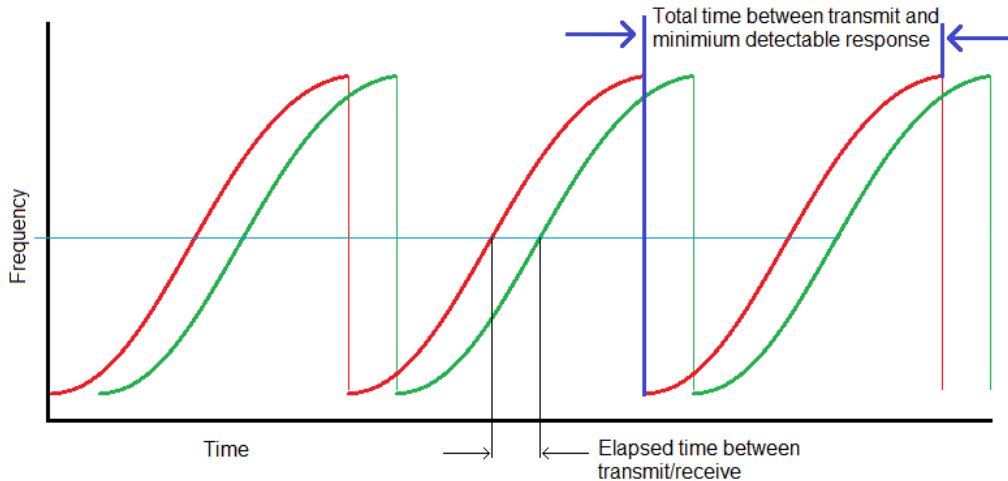


Figure 2-13. Continuous wave, frequency modulated radar signals.

Modulating the operating frequency of the radar system means that the signal that is being broadcast is not optimized for the antenna that is transmitting. The antennas are designed for a specific frequency, and it is not possible to optimize for a *band* without sacrificing performance at the center frequency.

Additionally, a continuous wave radar system is *always on* – there is no quiet time for the receiver to listen. It would be similar to trying to carry on a normal conversation with a friend on the opposite side of a stage at a rock concert. Extra components are required to invert the transmitted signal so that, when summed with the actual received signal, only the echo is recorded. This requires high accuracy electronics because any mismatch between the actual transmitted signal and the received waveform will generate “bleed through” that can quickly saturate or “rail” the receiver preamp.

The purpose of this paper is *not* to design the “best” or “optimal” ground penetrating radar, but rather to see if it is even possible to achieve the required resolution from a handheld device, and if so, to simulate what the output might look like. Given the additional complexity involved with running a frequency modulated system, the decision was made to develop a pulsed radar system. The remainder of this paper refers *only* to pulsed radar systems. For more information regarding continuous wave systems, the interested reader is referred to [15] and [16].

PROCESSING THE RETURNED SIGNAL

Data is recorded by the receiver every time the system switches from transmit to receive. This data must be processed to determine if there is an echo located somewhere in the data. The time record at which an echo is found will correspond to twice the distance between the receiver and the target because the signal had to reach the target then get reflected and return to the receiver.

The signal processing required is generally straightforward, but there are some finer points that may not be immediately obvious that will also be mentioned. Consider first a pulse that is transmitted, reflected, received, and recorded, with no noise or attenuation. At first, it may seem trivial to determine when the pulse was received – just look for the peak!

However, remember that the pulse is a high frequency signal, and that there are many peaks in a sinusoid. Figuring out which peak represents the moment the signal is received can actually be very challenging. The best way to determine the exact response is to compare what the receiver recorded with *what you know you sent*. You are the system designer! You can utilize this *a priori* knowledge of the transmitted signal to “look” specifically for that waveform.

The waveform that is received isn’t going to be *exactly* the waveform that was transmitted, though. Remember that the wave reaches the receiver only after being reflected. The reflection inverts the wave. Looking into a mirror, your left side becomes your image’s right side. Similarly, the start of the wave, which was the first to *leave* the transmitter, is the first to get reflected, and the first to *enter* the receiver. The end of the wave becomes the newest or most recent entry in the receiver data log.

Mathematically, an operation that mirrors a signal and then filters a long data record looking for the mirrored signal is called a *convolution*. The convolution process overlays one waveform (called the “window”) over another waveform (the record), and multiplies the two at every time record at which the two overlap. All of the products are then summed to produce *one* sample at the appropriate “lag” or waveform offset.

The action of multiplying then summing produces an effect that is not immediately apparent. Anywhere the window is positive and the record is negative, or vice versa, the product is negative. This represents regions where the signals do not match. Only when the window and record are the same sign, negative-negative or positive-positive, will the resulting product be positive. This represents regions where the window and record do match.

This pattern, where the output at each point is positive for a match and negative for no match, is repeated for every point in the window, and the output then gets summed. If there is a random signal, then there is an expectation that the window would *randomly* match or not match. When summed, the output is expected to be the mean for the random signal, typically zero. Only when the window “mostly” matches with the data will a positive record be produced, and the *maximum* output of the convolution corresponds to where the window *most* matches the record.

Consider Figure 2-14 above. The record is shown in blue, and the convoluted output is shown in black. Looking only at the record, it is not clear when *exactly* the waveform was received because there are *two* peaks. However, after convoluting the record with the transmitted signal, it becomes obvious that the record was received 100 “lags,” or sample periods, after the signal was transmitted. Knowing this and looking back to the record, notice that the record returns to a zero value at the 100th sample. As mentioned earlier, the newest wave sample is the

last one to leave the transmitter. That means that the waveform in blue left the transmitter 100 sample periods ago.

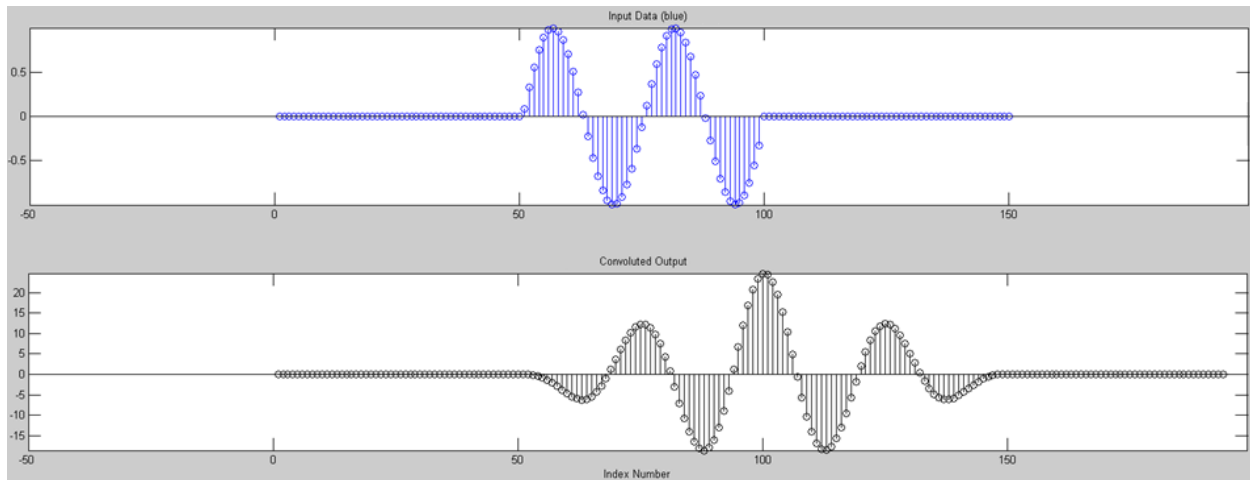


Figure 2-14. A recorded signal, in blue, and the output of the convolution, in black.

Since the receiver does not start “listening” (recording) until the transmitter turns off, the time the signal was received *does not correlate with any of the peaks in the received signal!* The time that elapsed between the end of transmission and reception actually corresponds to the start of the receiver record and the *end* of the transmitted signal. It is important to note that the convolution “automatically” located the *end* of the waveform and not just a peak, and that this scenario is unrealistically easy to work with. It is not possible to just “look for the end” of the wave form because the data will always be noisy. Refer now to Figure 2-15 below.

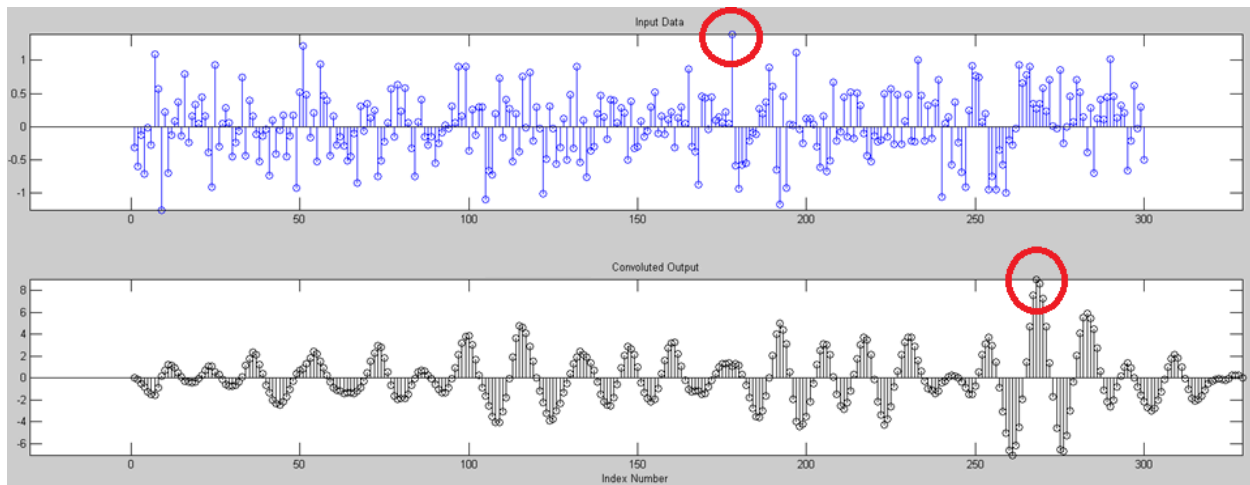


Figure 2-15. Convolved output of a realistic data set.

In the figure above, the data record, still in blue, is now *noisy*. The maximum point in the data record and convolution, in black, are both circled. In the data record (blue), the peak is due only to noise; it has no relationship to the pulse that was received. The convolution *filters* the

data, using the known waveform, and discovers the actual received signal time at approximately 270 sample periods.

The use of a convolution to *filter* data to find a *matching* signal is referred to as matched filtering. This technique improves the detectability of a signal in a noisy data set; that is, it improves the signal-to-noise ratio (SNR) of the receiver.

It is also possible to improve the signal to noise ratio by re-sampling. Assuming the noise is zero-mean, Gaussian distributed noise, a pulse could be sent several times, and the resulting series of pulses could be *averaged* or *integrated*. The random, normally distributed noise should approach the expected value (its mean, i.e., zero) as the number of pulses increases. This has the advantage of reducing the total broadcast power required to achieve a desired SNR, but comes at the cost of requiring a longer amount of time at each “look” angle.

SIDELOBES AND PHANTOM IMAGES

The last signal processing step is to determine which peak constitutes a “valid” echo. Refer again to Figure 2-15, and notice that, on the black “filtered” output, the circled peak is the highest peak, but it is not the only peak.

A threshold could be established, above which a signal could be deemed valid, but the issue with setting a fixed threshold is that the signal fades as distance increases. Compounding this problem are the side lobes. They were mentioned briefly earlier, and highlighted in Figure 2-10. The sidelobes are a *real transmission* of the array, at some angle other than the expected output angle of the array.

Consider an array that, as in Figure 2-12, has a pair of sidelobes that exist at a $\pm 60^\circ$ angle from the main lobe. Now, place the array in a void, with only one other object in existence to reflect. If the object is located at broadside and the array is not steered, the main lobe illuminates the target, and the receiver locates the echo of the main lobe and records that it found an object. Now the main lobe is steered, from 0° towards 60° . No other objects exist, so the receiver does not record any objects detected.

Once the main lobe reaches 60° , the side lobe is now pointed *directly at the object*, and the side lobe faintly illuminates the object. The matched filter still “looks for” the transmitted wave form, and it will find it, because the side lobes are *real* (but undesired) broadcast signals. The matched filter then generates a peak where the *side lobe* illuminated the target, and the receiver accepts that as a valid target. The result is an effect that is *similar to* but not the same as aliasing. If the output of the imager were shaded by magnitude of response, where black represents a zero magnitude and white represents the maximum receivable signal, then the output would look similar to Figure 2-16.

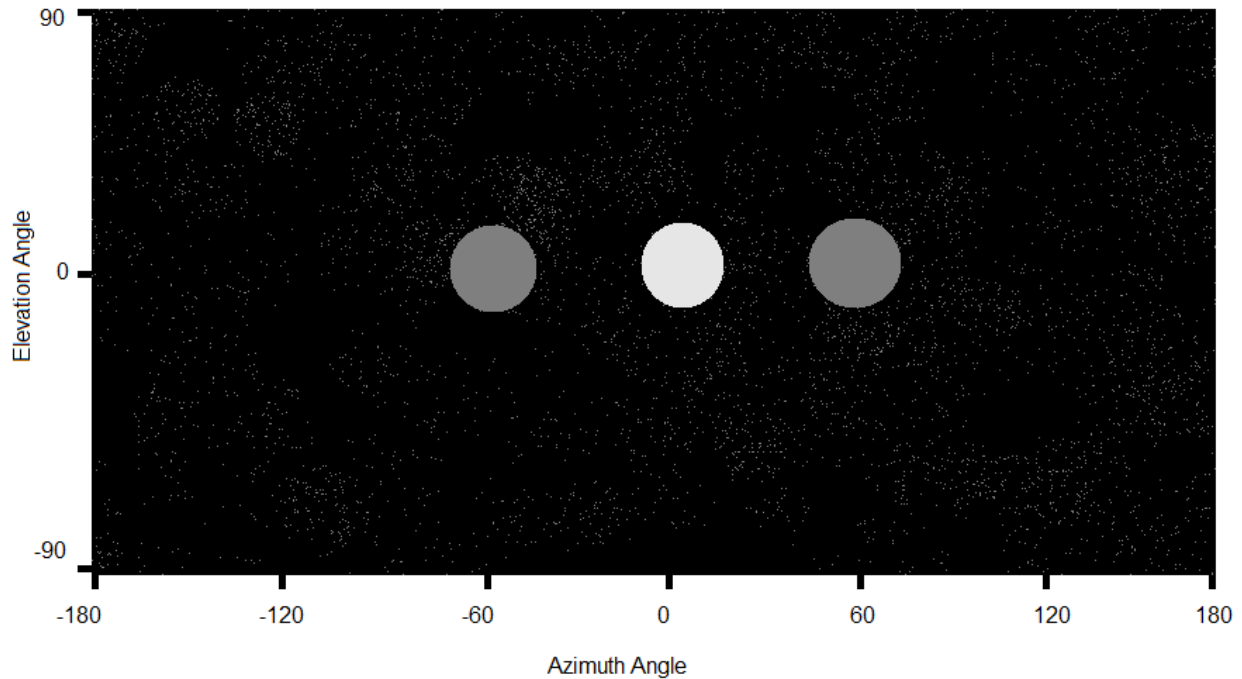


Figure 2-16. Phantom targets generated by side lobes.

The “targets” at $\pm 60^\circ$ are phantom images. As mentioned, like aliasing, these do not really exist, but they *appear* to exist because of *real deficiencies* with the radar array. Aliasing produces waveforms that appear to exist because of real deficiencies with sampling equipment. With aliasing, the sampling rate can never be high enough to capture the entire signal, so the solution is to limit the signal available to capture. This is commonly done by filtering (limiting) frequencies that are too high to be adequately sampled.

Similarly, the solution for dealing with the phantom images is to limit what is accepted as a valid target. To do so, take advantage of the fact that you know what is causing the phantom images – the side lobes! The signal from the side lobe is weaker than that from the main lobe, so a signal from a side lobe at 2 meters might be comparable to that from the main lobe at 10 meters. It is possible to differentiate where the signal came from, main or side lobe, by evaluating its estimated distance *and* its relative signal strength.

A weak signal at an estimated distance of 2 meters should be rejected, while the same signal at an estimated distance of 10 meters should be accepted. The method typically used to compare signal strengths is a method of *normalizing* the signals strengths, referred to as applying a time varying gain.

The gain that should be applied is determined by evaluating the signal loss that would occur from both fading and atmospheric attenuation. That is, a value is added to the received signal that would enlarge a main lobe's signal to the same magnitude as it was when it left the transmitter. A reflection very close to the receiver would need only a little gain to "restore" it to full power, while a reflection from very far away would need a significant amount of amplification to return to full power.

The use of the time varying gain would add only a small signal to the already weak side lobe emission, such that the "normalized" side lobe signal would be *significantly* smaller than the main lobe signal at the same point in time. Indeed, since any main lobe reflection should now exist at the same magnitude *regardless of target distance*, a threshold can now be applied to the filtered, normalized data. Any points exceeding the threshold are classified as "valid," and any points below the threshold are ignored.

SPHERICAL VS. CARTESIAN RESOLUTION

The topic of resolution was briefly covered in the Beamwidth section of this chapter. The resolution of the radar system is a description of how well the system is able to represent the scene at which it is looking. No matter the look angle, the beam *always* originates from the *center* of the array. The system does not take measurements of the scene along a line, it takes the measurements along an *arc*.

The system is steered to a particular *angle*, and measures in three dimensions along an arc, which means the logical native coordinate system for a radar (or sonar) system is a spherical coordinate system. The key difference between a radar system's spherical coordinates and a standard physics or mathematics based spherical coordinate system is that radar coordinates use an elevation angle measured from the X-Y plane, whereas most other coordinate systems measure an inclination or zenith angle from the +Z axis. All systems use an azimuth angle measured positive when counter-clockwise from the +X axis.

The difficulty in comparing resolutions comes from a familiarity with Cartesian coordinates, where a measurement in any one location is the same regardless of location. Polar or spherical coordinate systems utilize angular measurements and, from similar triangles, a linear distance between two points will increase linearly as the distance from the vertex of the coordinate system (commonly denoted "ρ") to each point increases. Two points 3 inches apart when $\rho = 10$ inches will be 6 inches apart when $\rho = 20$ inches.

In a similar manner, the ability of the radar system to determine the width of an object is dependent on the distance of that object from the array. The beam width is given as an angular

measurement, so the width of the beam *at a specific point* depends on the distance from the array. As distance to the array increases, an object of constant size is imaged more poorly because the linear width of the beam that images it has increased.

If it is desirable to achieve a specific linear beam width, as in cases where there is a specific target in mind, then the *angular* beam width should be determined by locating that target at the maximum operating range of the radar system. As the distance from the object to the array decreases, the linear width of the beam will as well. This is a conservative way to establish a beam width requirement because it ensures that the required linear width will always be achieved or exceeded.

RANGE RESOLUTION

A topic that has not been mentioned until now is *range* or *depth* resolution. Previously, all discussions regarding resolution have been about *angular* resolution, or the ability of the radar system to resolve the *width* of an object. It is also important to evaluate the *depth* or *thickness* of an object. Just as the main lobe can smear the *width of discrete objects* located inside the beam, the objects located “on top” of one another (sequentially along the beam axis) can smear the *length of the pulse*, resulting in the reflection getting averaged into one point that is located equidistant from both objects. Refer to Figure 2-17 below.

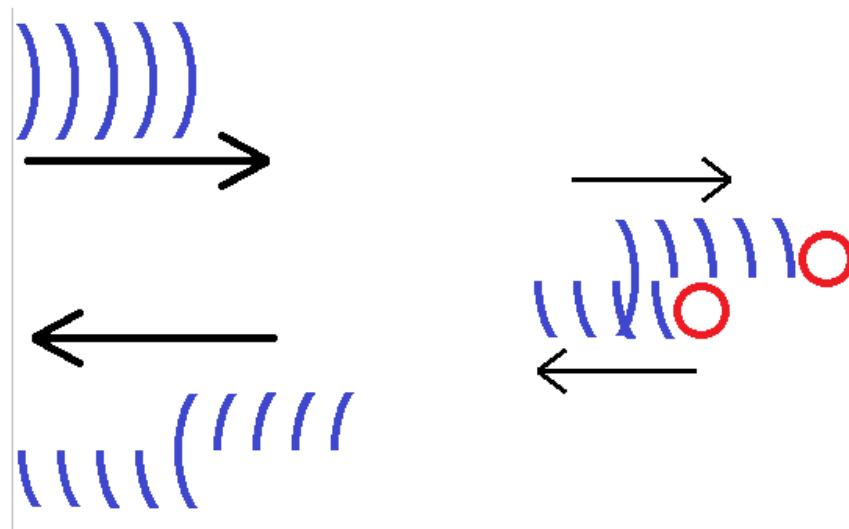


Figure 2-17. Range resolution versus pulse duration.

Figure 2-17 depicts graphically how an overly long pulse can blur two distinct objects into one. As the transmitted signal (upper left) strikes the nearer object, the wave reflects. After some period of time, the wave reflects off of the farther object as well. If the pulse is too long, the *front* of the wave reflected by the farther object can wind up riding the *end* of the wave reflected by the nearer object.

As discussed earlier and depicted in Figure 2-14, the matched filter will attempt to “find” where the signal *best* matches up with what was transmitted. In this instance, because the magnitude of the reflected wave is maximized where the waves from the near and far objects overlap, the “best” match occurs in the *middle* of the elongated reflection. The middle of this reflection corresponds with the point located between the two objects.

BASIC OPERATION RECAP

Different aspects of radar imaging have been explained individually up to this point, as understanding the different concepts involved is crucial to understanding the system as a whole. The remainder of this chapter takes a moment to explain how all of these individual parts mesh together to form the full imaging system.

First, the radar designer chooses an aperture wide enough to achieve a desired beam width. A wide aperture can be achieved by having one large antenna (see: radio telescopes), or by having an array of small antennas. The wider the aperture, real or discrete, the narrower the main beam will be.

Then, once a suitable beam width has been selected, a “raster” or scan of the scene begins. The beam is pointed to a given direction, and the time delay between transmission and reception is recorded. In the event that the aperture is one large antenna, the only way to point the beam is to physically move the entire antenna. There are plenty of time-lapse videos on YouTube of radio telescopes being steered. In the event that the aperture is an array, the beam can be steered by physically moving the array, by *electronically* steering the array with phase delays as discussed earlier, or a combination of the two.

Finally, the receiver waits for an echo. It is not possible to discern where within the main lobe the reflector (or target) is located. It is not even possible to discern whether the echo came from the main lobe or from one of the side lobes! The only thing the radar system “knows” is in which direction it was pointed (again, physically or electronically), and how long it took to receive the signal.

Upon receipt of an echo, the portion of the device responsible for producing the image has to assume that the target was as wide as the beam width at whichever distance it was detected, because again, there is no way to tell whether the target *was* as wide as the beam, or if it was located in the center or edges of the beam. This can cause a *smearing* effect, which is discussed very well in Kenneth Rolt’s master’s thesis from MIT [17]. Smearing means that objects as large as or larger than the beam are rendered relatively accurately, while objects significantly smaller than the beam’s width are *smear*ed until they are displayed to be that wide. [17] is *highly recommended reading* for anyone interested in learning more about the imaging process. Hopefully this paper gives you *your* “breakthrough” insight into how all of this works; Kenneth’s paper (which is actually on synthetic aperture sonar) was where everything “clicked” for the author.

The process repeats: point, transmit, receive, and record a data point at the distance corresponding to the time delay between transmit/receive. Typically the data point will be given a value that corresponds to the magnitude above the threshold for a valid target. This relative magnitude information is used to *shade* the image that is produced. Every time the array is pointed in a new direction, that position is combined with the intensity or shading value and a new “pixel” is created. Once the desired scene has been scanned, the beam is typically pointed back at the starting position and the scene re-scanned. Due to the high speeds associated with radar, electronic beam steering can allow the scene to be rescanned dozens to hundreds of times every second, producing “real time” video quality image refresh rates.

Chapter 3 RADAR MECHANICS MATHEMATICAL DESCRIPTION

CHAPTER SUMMARY

Hopefully, having made it this far, you have a firm understanding of how radar arrays are setup, how the beams are steered, signals are transmitted, and echoes received and processed. Getting to this point took me *months* of work! This chapter leverages your understanding of the *concepts* to show the formulas that drive the concepts. This chapter, and all the ones that follow, should be significantly shorter than the last because there isn't the need to describe *why* something is – you already understand how it works!

This chapter does not cover any of the numeric values regarding my proposed radar imaging system; those are covered in the next chapter, along with my reasoning for choosing specific values as inputs to the equations given here. The equations shown in this chapter are discussed in detail, so they may be quickly referenced in the following chapter, with discussion there about what the results mean instead of where the equation came from.

In reading numerous research papers, experience has shown that deriving *every* equation is more tedious for the reader than for the writer. If the derivation is not original, then it is an exercise in copying and pasting. It is the opinion of the author that lengthy derivations only serve to “bulk up” a paper while adding little content, and the result is that there is more time for the reader to get distracted, disinterested, and/or confused. Therefore, the only equations shown are the ones that are meaningful and intended to be used, or *brief* derivations to help reinforce the concepts covered in this paper.

PERFORMANCE METRICS

DETECTION AND THE SIGNAL TO NOISE RATIO

Most of the discussion up to this point has been about ideal systems, with difficulties of noise being discussed only briefly in the last chapter. In reality, noise is a real concern that imposes practical limitations on the system. In a noiseless scenario, it would be possible to infinitely amplify the output of the receiver and have a limitless range on the radar unit.

Random noise creates a “noise floor,” where a small signal and random noise become indistinguishable from one another. This sets a lower limit (or floor) on the minimum detectable valid signal, as the returned signal must be greater in magnitude than the noise. The noise is assumed to be zero-mean and Gaussian in distribution. This means that, for any point in the time record, the noise could either be positive, boosting a weak (side lobe) signal above the receiver threshold, or may, very infrequently, be positive and large enough in magnitude such that the noise could exceed the threshold on its own. Conversely, negatively valued noise could mask a valid response, preventing it from exceeding the threshold for detection.

It is easy to always receive the signal and always reject the noise – just broadcast with infinite power and set the receiver threshold at infinity! In reality, there is a tradeoff between broadcast power and the rejection of false positives and negatives. False positives occur when noise *adds* to a signal, so the solution is to *raise* the threshold for detection or reduce the broadcast power. Similarly, false negatives occur when the threshold is too high or the broadcast power is too low.

Walter Albersheim derived a formula, now known as the “Albersheim detection equation,” that approximates a series of receiver operating characteristic (ROC) curves developed by Bell Labs in 1967 [18]. These ROC curves display, graphically, the tradeoff between the probabilities of detection and false alarm for a given signal to noise ratio. Albersheim’s equation, which matches the Bell Labs ROC curves within 0.2dB over almost the entire range, is given as [19]:

$$SNR = -5 \log_{10} M + \left(6.2 + \frac{4.54}{\sqrt{M + 0.44}} \right) \log_{10}(A + 0.12AB + 1.7B) \quad 3.1$$

where

$$A = \ln \left(\frac{0.62}{P_{fa}} \right)$$

$$B = \ln \left(\frac{P_d}{1 - P_d} \right)$$

and M is the number of samples, P_d is the probability of detection, and P_{fa} is the probability of false alarm. This equation is derived in [20].

Equation 3.1 above has the term $-5 \log_{10} M$ where again, M is the number of samples. This term is assuming that the multiple samples are used for pulse integration, as described in the previous chapter. Notice that the term is *negative* – as more samples are taken, the quantity becomes more negative, and the required SNR declines.

The decision for the exact values selected for P_{fa} and P_d are explained in the next chapter, but the numbers are based on statistical distributions, i.e., a value of “1” means that event will happen 100% of the time, and a value of “0” means that the event will never happen. Ideally, the probability of detection would be 1, meaning an object would always be detected, and the probability of false alarm would be 0, meaning there would never be a false alarm.

Notice that the B term shows that if the probability of detection was in fact 1, the B term would go to infinity (undefined divide by zero), so the second term in Equation 3.1 would also go to infinity, so the required SNR would also go to infinity. Similarly, if the probability of false alarm were 0, the A term would go to infinity. Mentioned in jest earlier, this equation *proves* that

a true response can always be logged and a false response always rejected by setting the signal to noise ratio equal to infinity.

THE PULSE - RANGE, RANGE RESOLUTION, PULSE REPETITION FREQUENCY AND BANDWIDTH

As discussed in the previous chapter, the length of the pulse transmitted by the radar system has a direct impact on the ability of the radar system to resolve nearby targets at different ranges. As shown earlier in Figure 2-17, which is reproduced below as Figure 3-1 for ease of reference, it is possible for a wave to reflect off of two surfaces of different ranges and for those reflections to combine into one long return signal.

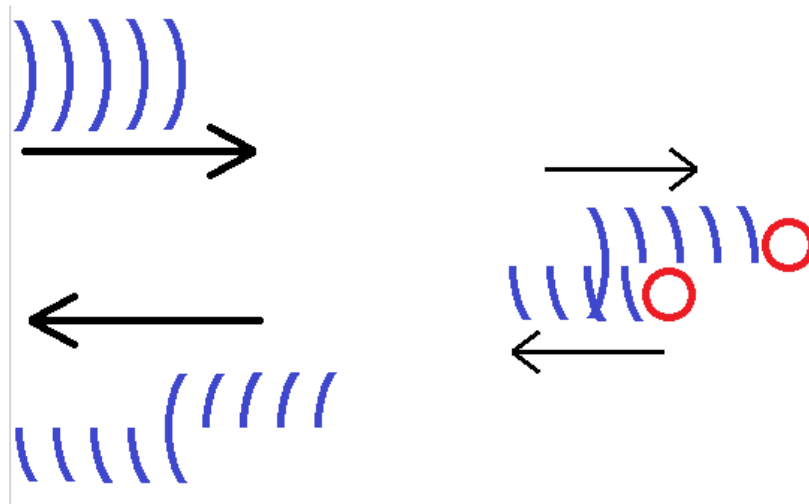


Figure 3-1. Figure 2-17 reproduced for ease of reference.

The moment the wave front strikes the nearer object, it begins the process of reflecting. During that time, if the front of the wave can propagate to the further object, reflect, and return *before* the end of the wave reaches the first object, then the wave will be elongated with no distinction (space or time delay) between returning signals.

If, however, the wave is short enough such that it is *shorter than the travel and return distance between points*, then there will be a brief period of silence between the times where the receiver detects the echoes, and instead it will log the response as two distinct objects.

Expressing the italicized line above as an equation:

$$t_{pulse} \leq \frac{2d_{resolvable}}{c} \tag{3.2}$$

where t_{pulse} is the time between the start and end of the pulse in seconds, $d_{resolvable}$ is the desired resolvable distance between objects in meters, and c is the speed of wave propagation in meters per second, e.g., the speed of light.

Another method for expressing the width of the pulse is in *bandwidth*, which would be the frequency necessary for a carrier signal or window to fully envelop the pulse. Assuming the pulse has a duration of t_{pulse} , the period of the carrier signal that exactly covers the same length of time must also be t_{pulse} , and the bandwidth of the pulse is then:

$$Bandwidth = \frac{1}{t_{pulse}} = \frac{c}{2d_{resolvable}} \quad 3.3$$

Setting the resolvable distance equal to the beam width at the ideal target position gives a reasonable approximation of a *cube* of space at the desired three dimensional coordinate. A volume at a given coordinate is sometimes referred to as a *voxel*. A 3D image can be constructed by logging the received signal strength for each voxel, to generate a shaded image, or can be logged by whether or not an object exists at all in that voxel, to generate a black and white image.

The desired maximum operating range plays a part in the radar power equation coming up soon, as farther distances require higher signal strengths, but it also determines the minimum time that can elapse between pulses. Ideally, signals reflecting just on the “far” side of the desired operating range would drop immediately to the noise floor, while signals just on the “near” side would be detectable. If this were the case, the minimum time between pulses, known as the pulse repetition frequency (PRF), would be calculated as:

$$PRF = \frac{c}{2r_{max}} \quad 3.4$$

where r_{max} is the maximum operating range in meters and c is as defined earlier. The factor of two comes from the fact that the signal must travel from the transmitter, to the target, then back to the receiver.

The frequency given in Equation 3.4 is the *highest* frequency at which the pulses may be sent. This ensures that enough time has elapsed since the previous transmission for the receiver to have gathered all of the possible reflections. Lower frequencies represent longer elapsed time between scans. NOTE: Do not confuse the pulse *repetition* frequency with the radar’s *operating* frequency.

APERTURE SIZE CALCULATION

The physical size of the aperture is irrelevant with regards to the radar system, but may have significant costs to implement in real life. As mentioned earlier, an eight element array operating at 300 kHz will span almost 2.5 miles. The total aperture size can be calculated by:

$$L = (N - 1)d \quad 3.5$$

where L is the aperture width in meters; N is the number of elements in the array; and d is the space between elements in the array, in meters. The $(N - 1)$ term comes from the fact that the array length is determined by the spacing *between* radiators – an array of one has zero length! The wavelength of a signal is related to the speed of propagation and frequency as shown earlier in Equation 2.1:

$$\lambda = \frac{c}{f} \quad 3.6$$

where λ is the wavelength in meters, f is the frequency in hertz, and c is as defined earlier. Using this equation and the definition of the array spacing $d = \frac{1}{2}\lambda$ gives the aperture length as:

$$L = (N - 1) \frac{1}{2} \frac{c}{f} \quad 3.7$$

It is usually easier and more cost effective to operate at higher frequencies than to have physical apertures yards or miles wide, so the most effective way to start the system design is to first pick the largest tolerable aperture width and then adjust the operating frequency until the desired beam width is achieved.

BEAM WIDTH CALCULATION

The formula for the width of the main lobe for an array is derived in [14] and shown here as:

$$HPBW = 0.886 \frac{\lambda}{Nd} \csc(\theta_{steer}) \quad 3.8$$

where N is the number of elements in the array, d is the inter-element spacing, λ is the wavelength, θ_{steer} is the electronically steered beam direction, and $HPBW$ stands for the half power (-3dB) beam width, *in radians*.

Notice the $\csc(\theta_{steer})$ term in Equation 3.8. This term means that the beam will gradually widen as it is steered away from the broadside axis. The beam width is at a minimum when it is not steered, then very slowly expands until it is twice as wide as the minimum width when steered to $\pm 60^\circ$, then three times the minimum width at $\pm 70.5^\circ$, then *rapidly* increasing in width as the cosecant function approaches a divide-by-zero at $\pm 90^\circ$. Assuming the array is set up on a half wavelength spacing, then $d = \frac{1}{2}\lambda$ and Equation 3.8 reduces to:

$$HPBW = 0.886 \frac{2}{N} \csc(\theta_{steer}) \quad 3.9$$

This shows the beam width is determined *solely by the number of elements in the array*. Recall, though, that the elements are still arranged on half wavelength intervals, so the operating frequency, which is inversely proportional to wavelength, will determine the physical space the array will occupy. It is important to note that the equations above give the beam width in radians. For degrees, use Equation 3.10 below:

$$HPBW = 50 \frac{2}{N} \csc(\theta_{steer}) \quad 3.10$$

The term $\frac{2}{N}$ in Equation 3.10 was purposefully separated from the 50 as a reminder that the equation only applies for the half wavelength spaced array.

OPERATING FREQUENCY SELECTION

Once the largest tolerable physical dimensions have been set and the number of elements required to achieve the desired beam width has been calculated, the lower limit on operating frequency is fixed. Substituting Equation 3.10, which gives beamwidth in terms of the number of elements in the array, into Equation 3.7, which gives the array width in terms of the number of elements in the array and the operating wavelength, gives a formula relating beam width to wavelength. Using the definition of wavelength from Equation 3.6 relates operating frequency to desired beam width:

$$f = \left(\frac{c}{L}\right) \frac{(50 \frac{2}{HPBW} - 1)}{2} \quad 3.11$$

where the half power beam width is in *degrees* and all other terms are as defined earlier. As with Equation 3.10, the term $\frac{2}{HPBW}$ is left in that form rather than multiplying out the 2 as a reminder that the equation only applies for half wavelength spaced arrays.

Notice that c is a constant, so the operating frequency is constrained by the physical size and desired beamwidth. As mentioned above, the frequency given by Equation 3.11 is the *lower limit* for operating frequency. Any frequencies lower than that given by Equation 3.11 will result in a longer wavelength, which will force a larger physical aperture. Higher frequencies allow a smaller physical size.

TRANSMITTER POWER ESTIMATION

The “radar equation” is one of the fundamental equations of radar system design, and it uses most of the antenna and performance parameters to calculate the required broadcast transmission power. The equation is derived in [22] and shown here in the following form:

$$P_t = \frac{P_r (4\pi)^3 R_t^2 R_r^2}{G_r G_t \lambda^2 \sigma} \quad 3.12$$

where P_t is the transmission power in watts, P_r is the received signal power in watts, R_t is the distance from the transmitter to the target in meters, R_r is the distance from the target to the receiver in meters, G_r is the gain of the receiver in decibels, G_t is the gain of the transmitter in decibels, λ is the wavelength of the radar's operating frequency in meters, and σ is the radar cross-section (RCS) of the target in square meters.

This brings up an important point, which has not been addressed until now. The radar system designed here is referred to as *monostatic* radar because the receiver and transmitter are, in fact, the same physical device. That is, they are both in the same (*mono*) location (or *station*). It is possible, but not addressed in this paper, for the transmitter and receiver to be located in two different places. This is more common with weapon systems, where a high power transmitter is located on the ground, and a low power (lightweight) receiver in something such as a torpedo or missile can detect (and thus home in on) reflections from a target.

Knowing that the transmitter and receiver are the same device means that the distance from the target to each must be the same, and, because they use the same antenna, each has the same gain as well. This means that Equation 3.12 simplifies to:

$$P_t = \frac{P_r(4\pi)^3 R^4}{G^2 \lambda^2 \sigma} \quad 3.13$$

where all terms are as defined above for Equation 3.12.

The wavelength was fixed in the previous section, when the operating frequency was determined. The operating frequency, in turn, was fixed by the section before that, when the beam width and physical dimensions were chosen. The gain is fixed by the choice of antenna. The operating range is also determined by the designer, so the only values left to determine are the signal power at the receiver and the target's radar cross-section.

The target's RCS is determined largely by the geometry of the target and is discussed more in the following chapter. There is no formula for the signal power of the echo *directly*, but a formula that was already covered is the signal to noise ratio. A formula for the expected noise exists, and is also given in [22]:

$$P_{noise} = kTB_r \quad 3.14$$

where P_{noise} is the noise power in watts, k is the Boltzmann constant (1.38×10^{-23} joule/degree), T is the absolute temperature of the receiver in Kelvin, and B_r is the receiver's bandwidth in hertz. The receiver's bandwidth is assumed to be equal to the pulse bandwidth to ensure the pulse is adequately sampled.

Now, with a way to calculate noise, and knowing that the signal to noise ratio is, well, the ratio of signal to noise, Equation 3.13 can be restated as:

$$P_t = \frac{(SNR)(P_{noise})(4\pi)^3 R^4}{G^2 \lambda^2 \sigma} \quad 3.15$$

where SNR is the signal to noise ratio and all other terms are as defined earlier.

THRESHOLD SELECTION

The sections above describe the characteristics of the pulse, transmitter, receiver, physical array, and beam width. As discussed in the previous chapter and in [23], the matched filter is the time-reversed and conjugated version of the transmitted waveform. Then, once the pulse has been generated, transmitted, reflected, received, and filtered, the last step is to determine at what value the recorded response is considered a true positive response.

[23] derives the formula for determining the signal power threshold:

$$T_{dB} = 10 \log_{10} \left[2N_{samples} \beta^2 (\text{erf}^{-1}(1 - 2P_{fa}))^2 \right] \quad 3.16$$

where T_{dB} is the threshold in decibels, $N_{samples}$ is the number of samples, β is the variance of the white Gaussian noise at the receiver, erf^{-1} is the inverse of the error function, and P_{fa} is the probability of false alarm.

Chapter 4 DESIGN CRITERIA, FULL SYSTEM SPECS, AND TARGETS

CHAPTER SUMMARY

This chapter discusses how the final values for system parameters are selected. Once the parameters are established, the equations from the previous chapter are used to tabulate the full system specifications. The design parameters revolve around the *minimum* detectable target, but the performance is evaluated using a set of *realistic* targets in a “crowded scene.” Following the disclosure of the full specifications, the method for approximating the realistic targets is discussed.

SYSTEM DESIGN

OVERVIEW

The concept for the radar imager is a “magic window” that the user carries at waist level that images objects in the ground as though the soil did not exist. This is depicted in Figure 4-1 below. The radar system scans and builds an image in real time, and there is no “search head” as with conventional metal detectors. The radar unit can be located on the obverse of a screen that can display the processed images.

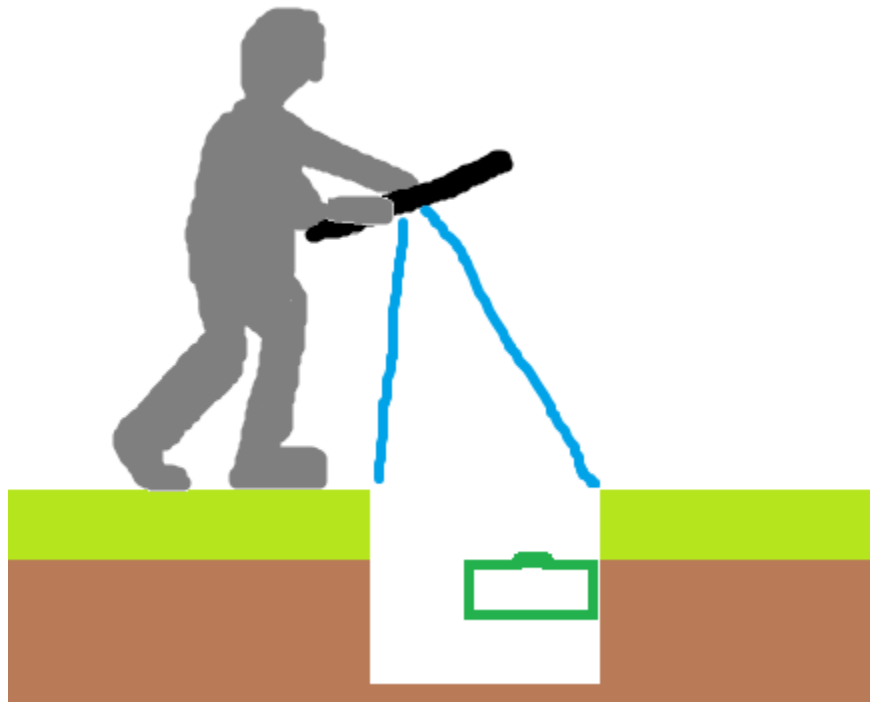


Figure 4-1. Conceptual operation.

The minimum detector distance is that from the array to the top of the soil, or about one meter. The maximum detector distance is an additional 18 inches, or approximately 0.5 meters

past the minimum distance. [24] states that anti-personnel mines, which are of primary concern in most third world countries, “are typically buried extremely shallow,” while anti-tank mines can be buried, “up to 16 in (40 cm) deep.”

The optimum scan range would be such that the imaged patch on the ground corresponded exactly to the screen. Objects on the top of the soil would be rendered in 1:1 scale in the position on the screen that they lay on the ground. The user can then look at the screen, without having to crouch, to evaluate objects discovered, and can quickly and *intuitively* determine where on the ground objects on the screen are located.

An intuitive, easy to understand interface is crucial for a device that could be shipped to nearly every country in the world. Additionally, an easily understandable interface reduces mistakes, which could be **lethal**. It is important to consider people may lose their life or limbs if they do not understand the information presented.

The last aspect of an intuitive interface is a restatement of the thesis problem – the radar system must be capable of producing images that are *identifiable*. There must not be a “look up table” or set of representative symbols for the user to interpret. The user should be able to determine what the object is based solely on its appearance on the screen. The resolution requirements are explained next.

THE MINIMUM TARGET

The ideal minimum target for the imaging system was selected by evaluating expected metal content and geometry in what is known as a *minimum metal* landmine. Minimum metal mines are specifically designed to defeat demining techniques, commonly handheld pulse induction metal detectors. Pulse induction metal detectors are the same kind used by hobby and recreational metal detector enthusiasts.

Minimum metal mines are made almost entirely of plastic, using shear pins or Belleville springs made of plastic to ensure a triggering threshold is met before detonation. The housing is also made of plastic, so the only metallic component is the firing pin that stabs the explosive. Minimum metal mines typically contain just *one gram* of metal, typically a steel tipped firing pin. Other styles of landmines are manufactured entirely of plastic, using friction-sensitive explosives or ceramics for firing pins, but even the complete lack of metal is not considered an issue because plastics reflect well in the microwave region. [25]

The landmine can be very large relative to the size of the firing pin, but, since the point of the imaging system is to be able to differentiate between mines and scrap, the firing pin was selected as the “ideal” target. The system that can adequately resolve down to one gram of steel should be able to discriminate well, and would absolutely be able to resolve the landmine in its entirety.

For the purposes of establishing a beamwidth, the one gram piece of steel was assumed to take the form of the most compact method of storing matter – a sphere. The assumption is that, if the same mass took a different shape, the cross-sectional area would only increase, making it more likely to detect the object. Additionally, assuming the form to be a sphere made radar cross-section calculations possible. The formula for radar cross section is given in [26] as:

$$\sigma = \text{Projected Cross Section} \times \text{reflectivity} \times \text{directivity} \quad 4.1$$

where σ is the radar cross section. The reflectivity and directivity can be determined experimentally, but [26] goes on to assert that, “The sphere is the unique target that the RCS is independent of the frequency.” This means that reflectivity and directivity do not need to be determined; the cross-section of the sphere alone is sufficient.

[27] gives the density of American Iron and Steel Institute (AISI) grade 302 steel to be 8060 kg/m^3 . Dividing the target mass of 0.001 kg by the density of steel gives the volume of the target as $1.24 \times 10^{-7} \text{ m}^3$. The formula for the volume of a sphere, solved for the sphere’s radius below Equation 4.2 gives the radius of the 1g steel sphere as 3.09 mm.

$$r = \left(\frac{3}{4\pi} V \right)^{\frac{1}{3}} \quad 4.2$$

Now, using the formula for area of a circle, below in Equation 4.3, the cross-sectional area of the sphere is calculated to be $3.01 \times 10^{-5} \text{ m}^2$.

$$A = \pi r^2 \quad 4.3$$

The beamwidth was calculated using the arctangent of the target radius and the expected distance from the array. These values are shown relative to each other in Figure 4-2 below. As shown, the arctangent will give *half* the required beamwidth. Equation 4.4 below gives the full beamwidth:

$$\text{Beamwidth} = 2 \operatorname{atan} \left(\frac{r_{\text{target}}}{d_{\text{detector}}} \right) \quad 4.4$$

where r_{target} is the radius of the target in meters and $d_{detector}$ is the distance of the detector from the target, also in meters. Using the radius calculated above and a detector distance of one meter, the required beamwidth is 0.355° .

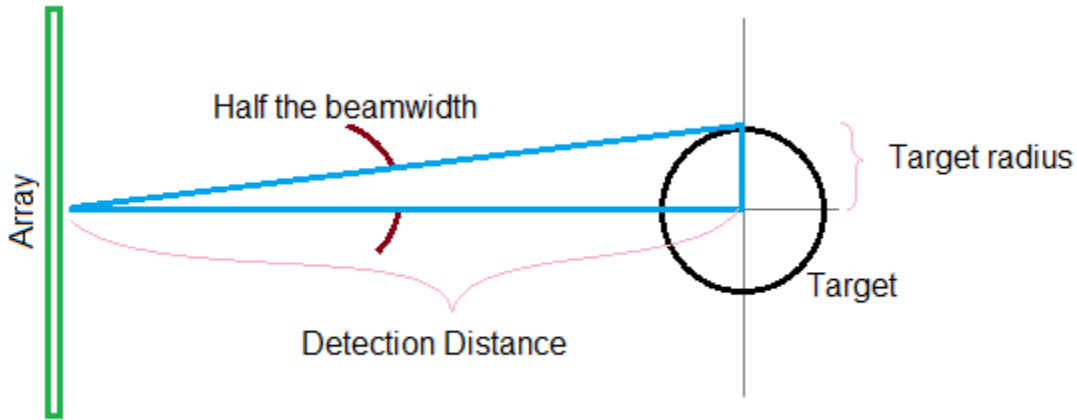


Figure 4-2. Array beamwidth and target radius, geometric setup.

As discussed in the previous chapter, the operating frequency and many other parameters become *fixed* when beam width and array sizes are selected. Because the device is supposed to be carried by one person, as seen in Figure 4-1, the *absolute maximum* dimensions on the array have been selected as 1 meter by 1 meter. Even this is a bit large, but, as discussed in the previous chapter, the array can be made smaller by increasing the operating frequency.

OPERATING FREQUENCY

Using the values above for beam width and maximum array size, Equation 3.11 shows the required operating frequency to be 43 GHz. This is the *minimum* frequency at which the desired beam width can be achieved. Higher frequencies can either produce a narrower beam, for the same array size, or can allow for a smaller array, for the same beam width. In determining what value exactly to choose for operating frequency, it occurred that, if anyone were to ever construct this device, it may be helpful to operate in a band *approved for unlicensed usage*. The hunt began for a frequency band, above 43GHz, approved by the FCC for unlicensed use.

As it turns out, there is a band allocated by the FCC for unlicensed usage in the 57-64 GHz range. [28] The center frequency for this band, 61 GHz, is also the center frequency for a band allocated for industrial, scientific, and medical use (ISM band), which typically allows for significantly higher power operation, such as microwave ovens and radio frequency (RF) plastic welders. [29]

At 61 GHz, the array could be reduced to 0.7 meters in length and width. During the calculations, the realization was made that the wavelength of a 60 GHz signal is *exactly* 0.5 cm, and that exactly 200 elements could be arranged in a line on a 0.5 meter by 0.5 meter array when

spaced at half a wavelength. Once the array has been shrunk to 0.5 meters, or about 20 inches, the device becomes *very* portable because this is also very close to shoulder width.

BEAM WIDTH

There was concerned at first that the ideal target would not be detectable with a larger beam width, but then there was the realization that, as explained in Chapter 2, an object smaller than the beam will be smeared to the same width as the beam. The transmitter power equation from last chapter, Equation 3.15, shows that a target of *any size* can be detected, if the transmitter power is set correctly. That is, even if it is not possible to *resolve* to the *dimension* of the minimum target, it can still be *detected*.

At 60 GHz, the square, half-meter array produces a beam that is 0.51 degrees wide, which is 40% wider than the beam for the ideal target, which was 0.35 degrees. However, as previously discussed, the ideal target was the *conservative* estimate for required imaging resolution. A plastic landmine would appear as a solid object [25], so achieving the 0.35° target *exactly* is not necessary. The chief performance metric is discriminatory ability in a crowded scene that would be expected in a war zone.

DETECTION PROBABILITIES

The probabilities of detection and false alarm were selected based on their physical meaning and on common values found in radar literature. As stated in the previous chapter, the best value for probability of detection is 1, meaning a valid target is always detected, and the best for the probability of false alarm is 0, meaning a false target is always rejected. Without any experience, 1×10^{-6} was selected for the probability of false alarm, as this value was given frequently in radar literature as a commonly accepted value.

For the probability of detection, 0.99 or 0.999 were commonly chosen values, but because of the life and death nature of minefield clearance, a value of 0.9999 was selected. This means that, statistically speaking, one in ten thousand valid targets will be rejected. This number seems trivial until you consider the fact that the radar is operating at the *speed of light*, and there are *tens of millions* of pulses every second.

There is no easy way to explain why this is okay without giving away values for sections discussed later in the paper. So, having said this, it is possible to cheat and give away some of the information now, and you can know that the explanations for the values are “coming soon.” There are also 9,025 pulses required to make one “scan” of the scene (akin to one “frame” of a video). So, statistically speaking, roughly one “pixel” or “voxel” should be wrongly rejected every scan.

If one pixel is incorrectly rejected every frame, then the odds of two pixels being wrongly rejected on the same *frame* are now one in ten thousand ($[1 - P_D]^2$). Take into account that these pixels could be *anywhere* on the frame, and to have two *side by side* pixels would be another 1 in 9,025. *Now* take into account that each pixel is still only 0.2° on an edge, or about 3 mm by 3

mm at target range, and *small* landmines are 2 or 3 inches in diameter, or about 50 to 75mm across, and you can understand how the odds are against an *entire mine* being wrongly rejected. Even *if* an *entire mine* were wrongly rejected in one frame, the next frame would show the target!

ANTENNA SELECTION

The last choice that needs to be made is arguably the most important – the antenna! The array is a group of discrete antennas. The antenna gain, which is typically greater than 0 dB (that of an isotropic radiator), *multiplies* the output of the array. Said another way, the *array* multiplies the output of the *antenna* (commutative property of multiplication).

For this project, it was desired to have an antenna that was simple (cheap) to manufacture, easy to work with, and produced a relatively uniform broadcast pattern such that there was no significant variation in signal strength over the intended usage range. Such an antenna was found in the form of a *patch antenna*, depicted in Figure 4-3 below.

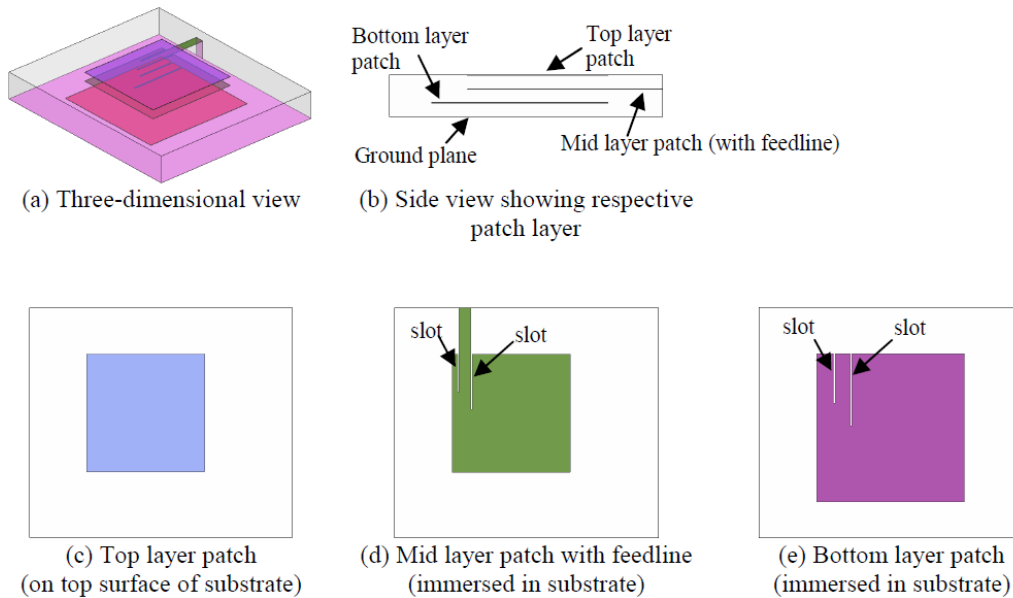


Figure 4-3. A patch antenna. Tan, Y. C. M., & Tan, Y. C. M. (2010). *Computational modelling and simulation to design 60GHz mmWave antenna*. 1-4. doi:10.1109/APS.2010.5562035. Used under fair use, 2014.

Figure 4-3 shows a variation of the very common implementation of the patch antenna. The “patch” of metal exists on an exposed face of substrate material. Typically the substrate is Duroid or another fiberglass/resin mixture used in printed circuit board (PCB) manufacture. The exact dimensions of the patch are given in [30], but in general a patch antenna is *just shy* of being a square that is a half-wavelength on either side, because the strip that carries the signal also acts as an antenna. Just as the half wavelength dimension is very important in array geometry, it is also very important in antenna geometry. This is discussed in detail in [14].

The patch antenna depicted in Figure 4-3 acts as a type of “Yagi-Uda” antenna [14], where the signal is actually generated on a patch on one of the inner layers of a multi-layer PCB. The “backwards” signal bounces off of the ground plane (referred to as the “bottom layer” in (e)), where it and the “forwards” signal are guided by a passive antenna – the patch on the surface.

The authors of [30] tested this patch antenna at 60 GHz and found the antenna to produce nearly 7dB uniformly over a range of ± 30 degrees from broadside. This means that the magnitude of the array output will not change as the beam is steered provided the steering angle remains within the $\pm 30^\circ$ band. The antenna output was visualized by [30] using ANSYS High Frequency Structure Simulator (HFSS) software. The image is reproduced as Figure 4-4 below.

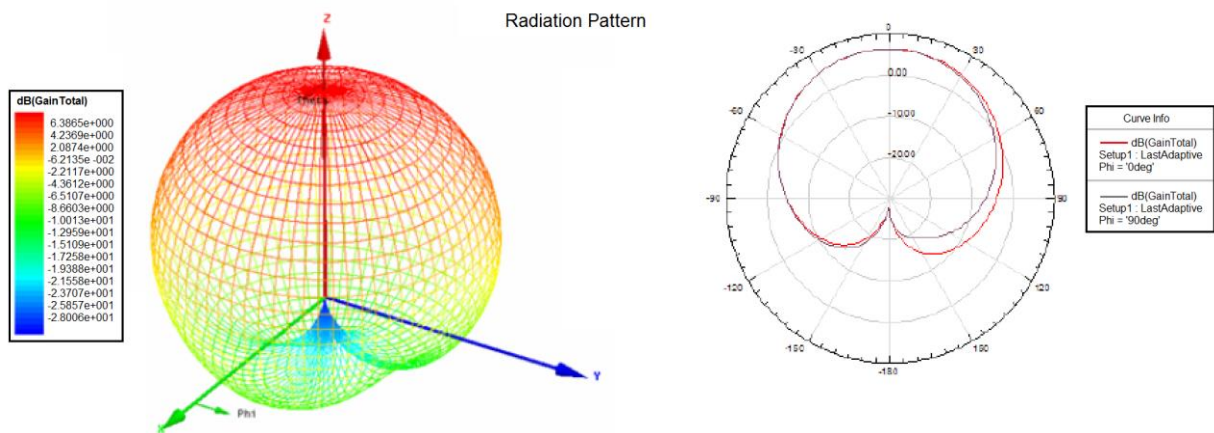


Figure 4-4. 60 GHz patch antenna radiation pattern. Tan, Y. C. M., & Tan, Y. C. M. (2010). *Computational modelling and simulation to design 60GHz mmWave antenna*. 1-4. doi:10.1109/APS.2010.5562035. Used under fair use, 2014.

The last check before calculating the full system specifications is to ensure that the scanned angles *do* remain within the ± 30 degree band. As mentioned at the start of this chapter, the system, as conceived, should image *only* the ground under the array, and *all* of the ground under the array. That is, the beam should be steered to reach ± 0.25 meters, which is the size of the array ($\pm 0.25\text{m} = 0.5\text{m}$ total, the length and width of the array), when the targets are located at the maximum range of the system, which is 1.5 meters. Using the same equation used to calculate the desired beam width, Equation 4.4, the steering range was found to be $\pm 9.46^\circ$, which is well within the $\pm 30^\circ$ band.

FULL SYSTEM SPECIFICATIONS

The next section in this chapter discusses likely targets to be found in a combat zone, the dimensions of those targets, and how they were interpreted and approximated for the radar simulations. That section is very lengthy and does not have any bearing on the design of the system as the design decisions revolved around the minimum detectable target and not the realistic targets. So, before that section begins, the full system specifications are disclosed.

Table 4-1. Full system specifications.

Target Radius	3.09	mm
Target RCS	3.00E-05	m ²
Max Distance	1.5	m
Array Size	0.5	m long
	0.5	m wide
P_{fa}	1.00E-06	
P_d	0.9999	
SNR	16.38	dB
Gain	7	dB

Beam width	0.51	degrees
$d_{resolvable}$	6.18	mm
t_{pulse}	41	ps
Bandwidth	24.3	GHz
Pulse Repeat Frequency	100	MHz
Wavelength	0.005	m
P_{noise}	1.94 E -10	Watts
$P_{transmit}$	0.109	Watts
Threshold Signal	-85.7	dB

TARGETS FOR A CROWDED SCENE

As discussed several times, the ultimate determination of system performance is target discrimination in a crowded scene. The ability to differentiate between inert shrapnel and metal waste and a live landmine is the entire purpose for creating the device described by this thesis. A “crowded scene” was generated for evaluation purposes, to test the system’s ability to differentiate between debris and to demonstrate the effects of changing key parameters.

As mentioned, the MATLAB simulation software does not allow for complex target information. On top of not being able to calculate radar cross section from material data and geometry, MATLAB does not allow for a way to input the shape of the radar cross section. The cross section of any object must be made up of the only way MATLAB can handle cross sections - with circular sub-objects.

The scene is composed of objects that could be expected to be found in a mine field. There are four 5.56 NATO M855 ball point bullets (projectile only), eight 5.56 NATO bullet casings (casings only, no slugs), one model PMN Russian landmine, and currency, in the form of one American dimes and one American quarter. The currency serves to provide scale and acts a stand-in for shrapnel, because again, non-circular cross-sections cannot be represented in MATLAB simulations.

The 5.56 NATO rounds are used because they are generally used in assault rifles in NATO-member countries. The rounds are used in rifles including, but not limited to, the U.S. M16, M4 Carbine, SCAR-L, and the squad automatic weapon (SAW) M249. The round, depicted in Figure 4-5 and Figure 4-6 below, is approximated by a series of circular sections, as shown in Figure 4-7.

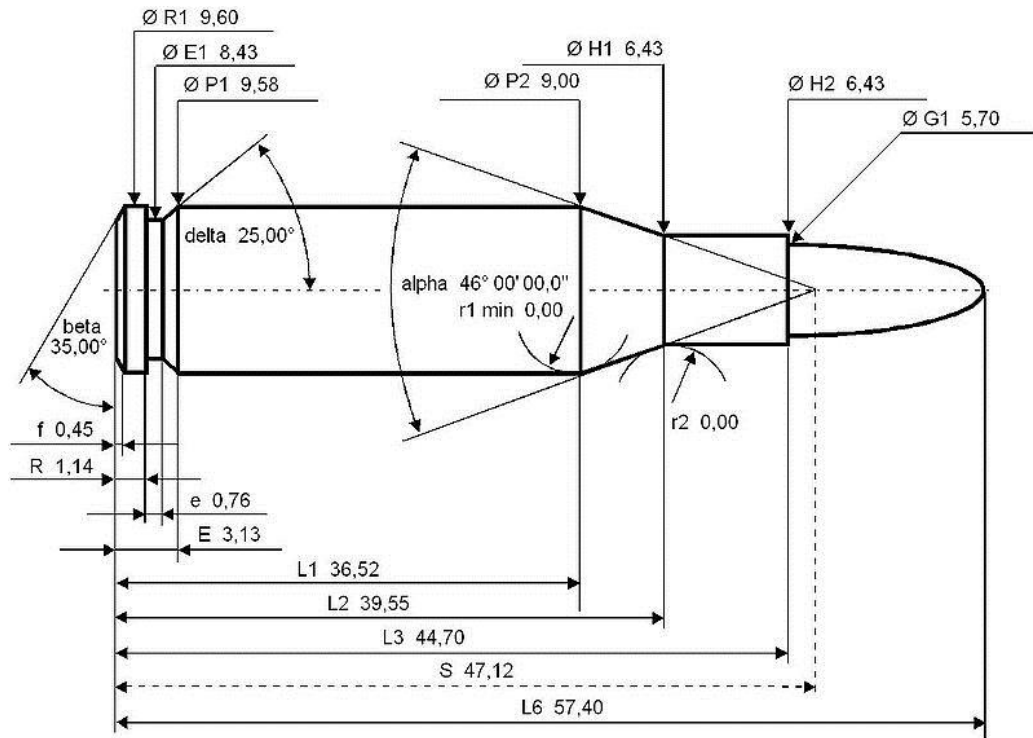


Figure 4-5. NATO 5.56 casing dimensions. Flinch, F. (Artist). (2010, November 19). 5.56 NATO Cartridge Dimensions [Web Drawing]. Retrieved from <http://ultimatereloader.com/tag/5-56-x-45mm/>. Used under fair use, 2014.

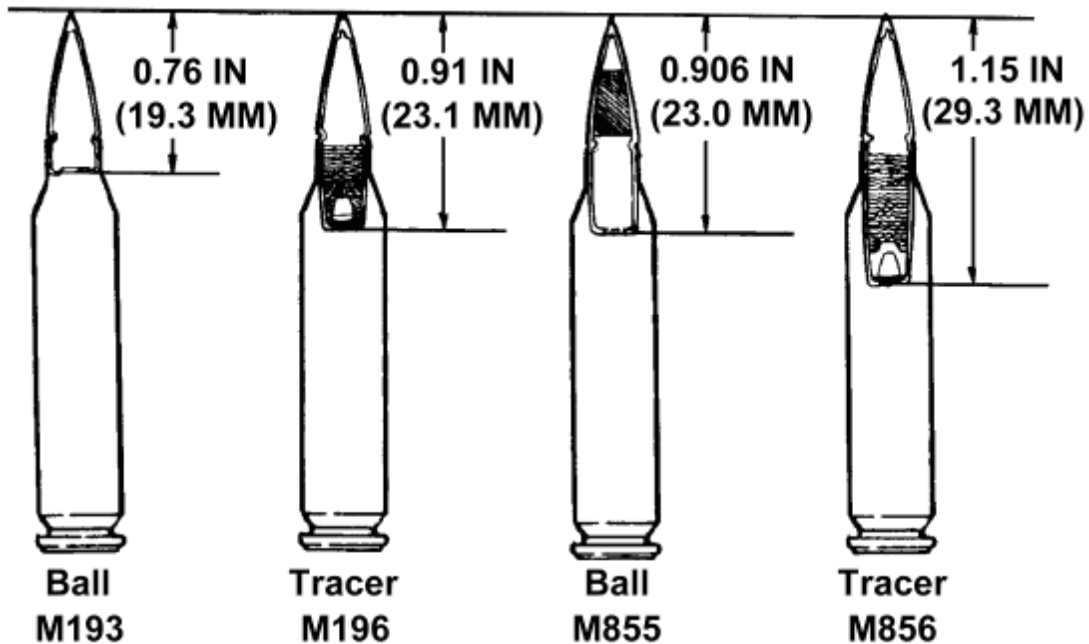


Figure 4-6. Slug lengths for different variations of the 5.56 round. Cooke, G. (Artist). (2005, May 03). 5.56 Ammo [Web Drawing]. Retrieved from http://www.inetres.com/gp/military/infantry/rifle/556mm_amm.html. Used under fair use, 2014.

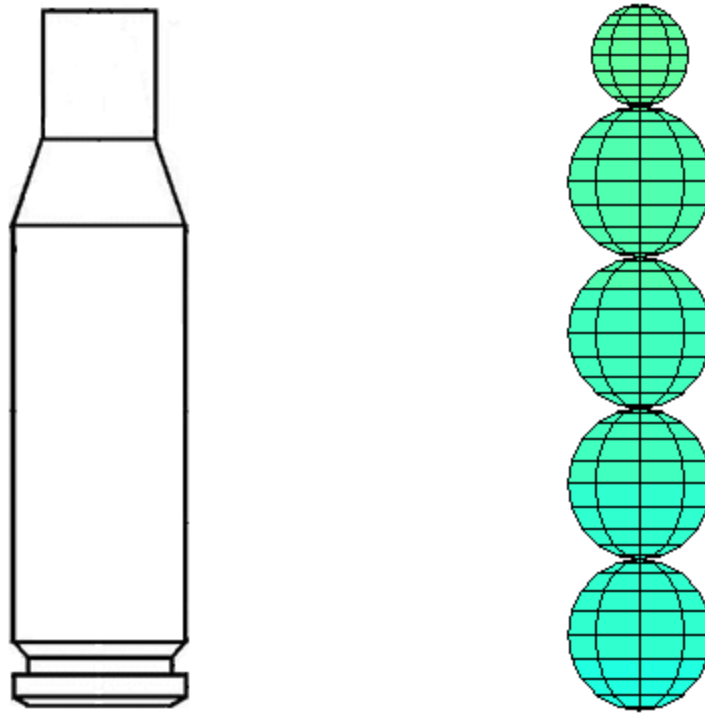


Figure 4-7. A 5.56 NATO casing and its simulation approximation. Flinch, F. (Artist). (2010, November 19). 5.56 NATO Cartridge Dimensions [Web Drawing]. Retrieved from <http://ultimatereloader.com/tag/5-56-x-45mm/>. Used under fair use, 2014.



Figure 4-8. A complete 5.56 NATO round and the slug without a shell casing. (2010, June 24). 5.56 M855A1 Enhanced Performance Round [Web Photo]. Retrieved from <http://usarmy.vo.llnwd.net/e1/-images/2011/05/08/107872/army.mil-107872-2011-05-06-190552.jpg> . Used under fair use, 2014.

The 5.56 NATO slugs are significantly longer than the tip that is exposed from the casing, as can be seen in Figure 4-8. The bullet was approximated in the simulation in a manner similar to that for the casing shown in Figure 4-7.

Simulating the landmine was more difficult. The mine selected for simulation is the PMN, a model produced by Russia since the 1950's and used in almost every conflict since. The mine has been found in Afghanistan, Cambodia, Chechnya, Egypt, Ethiopia, Georgia, Honduras, Iraq, Kurdistan, Laos, Lebanon, Libya, Rwanda, Somalia, Republic of South Africa, Sudan, Vietnam, Yemen, and more [34]. The mine is still actively used by modern armies, as can be seen in Figure 4-9.

The difficulty in simulating the mine is the fact that it is manufactured largely from Bakelite, an early predecessor to modern plastics. The mine, pictured by itself in Figure 4-10, does feature internal metallic components. When disassembled, as seen in Figure 4-11, the pressure plate and arming delay springs can be seen. While no dimensioned drawings for the mine could be found, the mine is known to be approximately 100mm in diameter. [35]



Figure 4-9. A pile of PMN landmines, found outside Fallujah, Iraq, in 2003. Gaines, D. (Photographer). (2003, June 25). EOD personnel evaluating PMN mines in Fallujah, Iraq [Web Photo]. Retrieved from <http://www.dodmedia.osd.mil/Assets/2004/Army/DA-SD-04-02138.JPG> . Used under fair use, 2014.



Figure 4-10. A Russian PMN landmine. Trevelyan, J. (2000, January 01). Photographs of pmn-2 mine. Retrieved from <http://school.mech.uwa.edu.au/~jamest/demining/info/pmn-2.html> . Used under fair use, 2014.



Figure 4-11. A partially disassembled PMN landmine. Trevelyan, J. (2000, January 01). Photographs of pmn-2 mine. Retrieved from <http://school.mech.uwa.edu.au/~jamest/demining/info/pmn-2.html> . Used under fair use, 2014.

Given the known diameter of the mine, and the relative size of the springs in the image, the larger arming delay spring was assumed to be approximately 15mm in diameter, and the smaller pressure plate spring was assumed to be approximately 10mm in diameter. Both springs

are the ones pictured still inside the unit in Figure 4-11. The mine is approximately 45mm tall [35], so the arming delay spring was assumed to be 40mm high when the unit is sealed, and the pressure plate spring was estimated to be 25mm long. The numbers of loops in the springs were determined by examining Figure 4-11, with the arming delay spring having 7 turns and the pressure plate spring having 8. The wire diameter is estimated at 1/16", or about 1.6mm.

SCANNING METHOD AND EXPECTED SIMULATION RESULTS

Before jumping straight into the results, this section will take a moment to discuss how the pulses are arranged and how those pulses are interpreted, to help explain why the results look the way they do.

The responses recorded are those coming from a *beam*. The beam is not square in cross-section, like the antenna, it is a *cone*. This means that targets are struck by and reflect a pulse that has a circular cross section. How, if the signal and reflection has a *circular* cross section, do you stack the signals to make sense of the result? How do you ensure the entire scene is observed? Consider Figure 4-12 below.

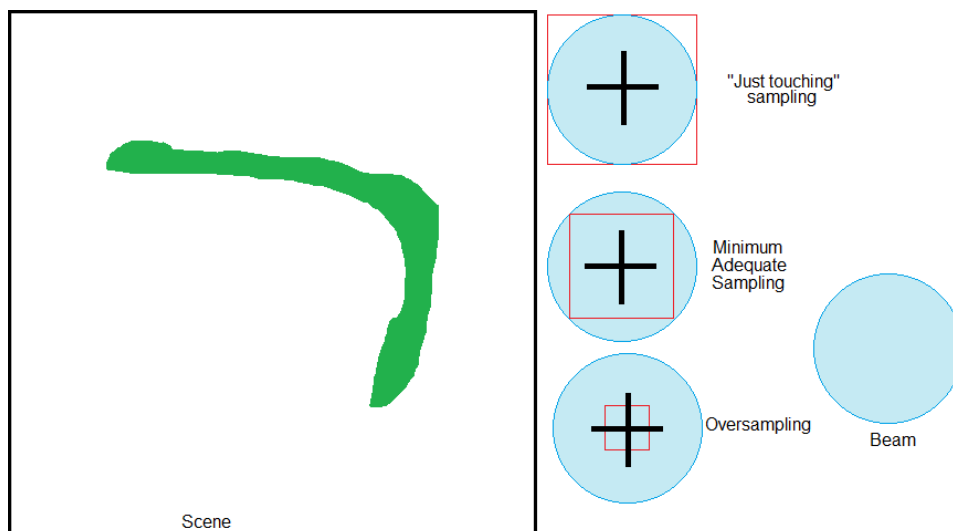


Figure 4-12. Sampling techniques.

Figure 4-12 shows how the pulses appear when they strike a surface parallel to the plane of the array. The pulses can be stacked at a “just touching” interval, where the edges of the beam *just* touch, but no part of the beam overlaps, as in Figure 4-13, or they can overlap such that no portion of the scene is left observed, as in Figure 4-14.

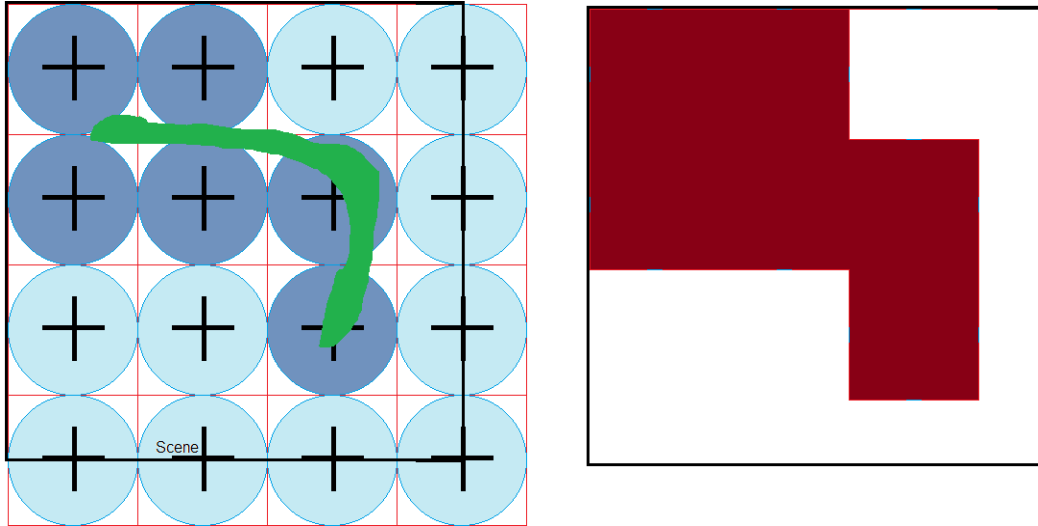


Figure 4-13. An undersampled scene.

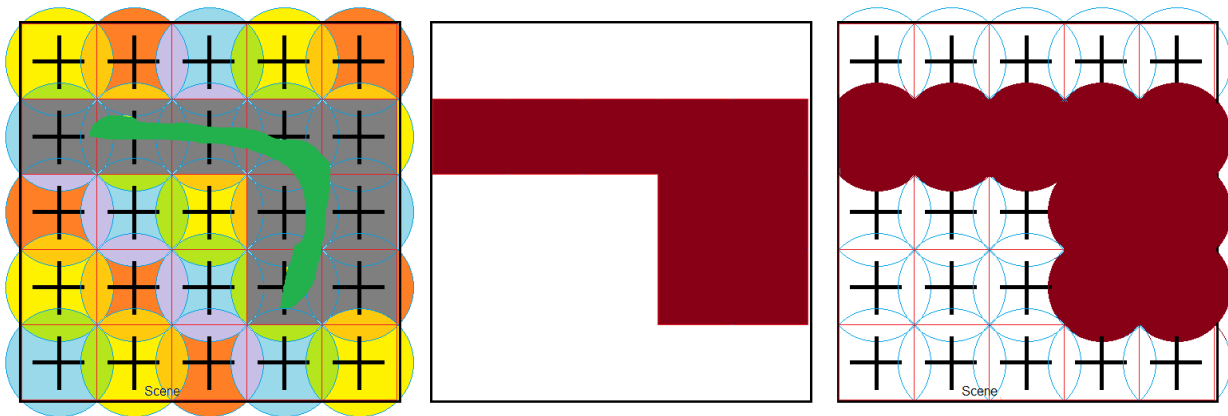


Figure 4-14. An adequately sampled scene.

Figure 4-14 shows how the pulses overlap (red and yellow overlap as orange, etc.), and gives *two* methods for handling the returned data. Do you log the returned signal as a filled “box” or do you log the returned signal as a filled *beam*? The box represents the area that is adequately sampled by the pulse, but there is some oversampling that also occurs. Take for instance the rightmost column of pulses. Their “boxes” don’t really overlap the object, but their *pulse* does, so they record the pulse as a valid response.

What has been found to produce the best quality images is to use *neither* of the options above, instead logging the pulse as a circle (sphere) that fits entirely inside the pixel (voxel). See Figure 4-15 below for reference.

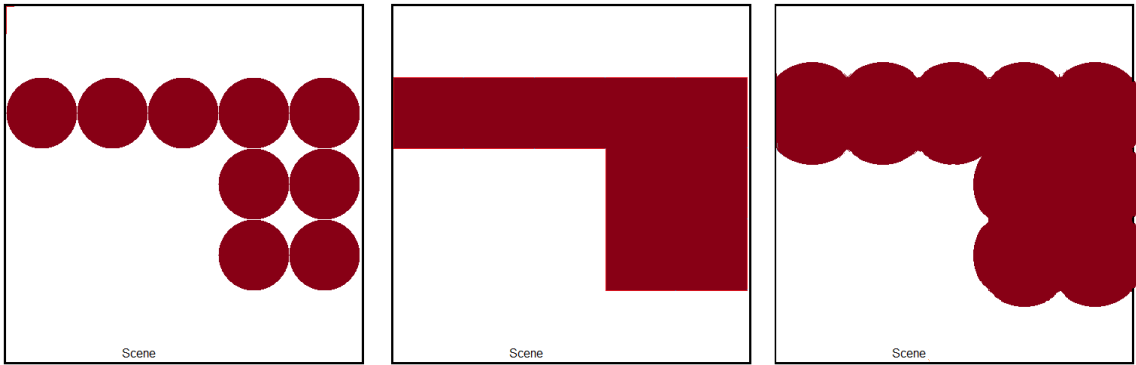


Figure 4-15. Rendering methods. Left to right: Inscribed circles, bounding boxes, circumscribed circles.

The beam isn't infinitely powerful. The beam doesn't even have the *same* power across it! Recall that the edges of the beam were defined as the point where the signal drops to *half* the power. Inscribed circles allow your eyes to round corners that are likely already rounded, and as a reminder that *the pulse is an estimate* that an object exists.

Just as the adequately sampled rendering in the middle of Figure 4-15 is better than the undersampled rendering of Figure 4-13, oversampling can improve the resolution even more, provided *only* the bounding box is shaded and *not* the entire width of the beam. See Figure 4-16 below.

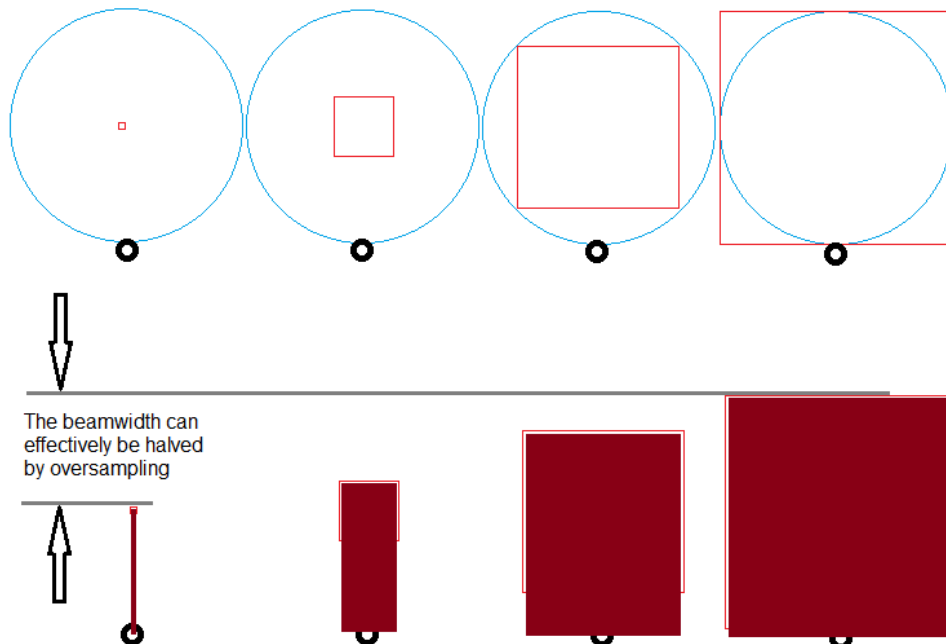


Figure 4-16. Oversampling can improve resolution, up to half of the beamwidth.

The black circles in Figure 4-16 above represent targets located *just* at the point where they would send a reflection large enough to be detected. The beams are located at the same

position away from the targets, but the pattern sampling alters from undersampled, on the far right; to adequately sampled, second from the right; to oversampled, second from the left; to extremely oversampled, on the left.

Notice that the width that the beam adds (the “smearing” effect) gradually decreases as the percentage of overlap or oversampling increases. The smallest smearing the beam would produce is if the scene is infinitely oversampled, at which point the red bounding boxes would collapse to a single point in the center of the beam. At this point, the extra distance or smearing the beam would add is reduced to the absolute minimum half-beamwidth.

This is exactly the smearing concept discussed earlier in Chapter 2. The beam is “stupid,” and has no way of “knowing” where in the beam the object that is generating a reflection is located. Chapter 2 stated that the only way to deal with this was to assume that the object existed in the *entire width* of the beam, but as you can see, if the response is logged for each *sampled area* instead of each *beam area*, then the effective resolution can be increased.

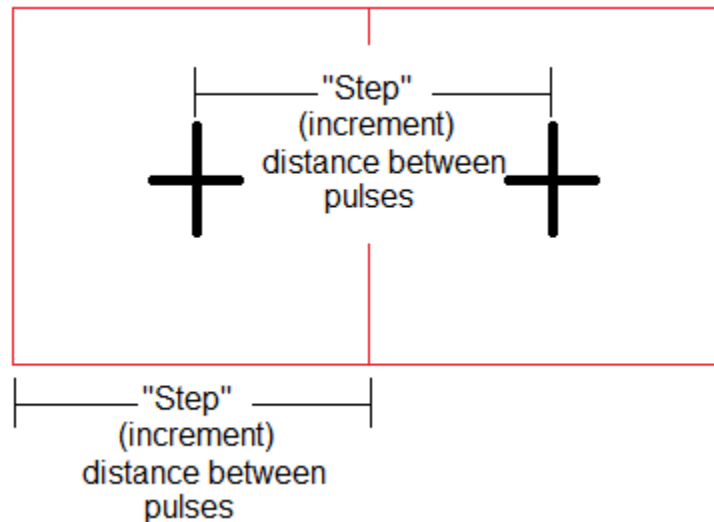


Figure 4-17. Bounding boxes (sample areas) defined in terms of step distances.

The minimum spacing to be able to adequately sample the scene is where the radii of two separate pulses are allowed to form an angle of 90° . At this point, if four pulses were arranged, no area would be left uncovered. Since the radii are forming an angle of 90° , the distance between centers of the pulses, known as the pulse step or increment, is the hypotenuse of that 90° triangle. That is, the pulse increment for the minimum adequate sampling is:

$$d_{pulse} = \sqrt{2r^2} \tag{4.5}$$

where d_{pulse} is the distance between pulses and r is the radius of the pulse. Ordinarily, these values would be given in units of *length*, but the radius of the pulse varies with broadside distance, so the scan increment is calculated in polar coordinates, the same way the beam’s width is. This means the unit of measure is *degrees* instead of feet or meters.

Using this formula, which is really just a restatement of the Pythagorean Theorem, and the radar system's actual beam width of 0.51° , the *minimum* adequate pulse spacing is 0.36° . In the simulations, oversampling has been performed by reducing the spacing to 0.2° .

The tradeoff between physical size and a frequency open to unlicensed use put the beamwidth wider than desired, but, as demonstrated above, the effective beam width can be reduced by up to half by increasing the number of samples taken. The design decisions produced a beam that is 40% larger than desired, but the use of oversampling will compensate for the increase in width, as will be seen during the discussion of the simulation results in the next chapter.

Chapter 5 SIMULATION RESULTS AND DISCUSSION

CHAPTER SUMMARY

This chapter discusses radar system simulations at length. Topics discussed include how MATLAB appears to handle targets, single target responses, and the response from a crowded scene. Also discussed are performance specifications not related to imaging capability, such as transmitter power and refresh rates.

METHOD OF SIMULATION

The simulations were performed using MATLAB and the Phased Array System Toolbox. This toolbox features many pre-built functions that significantly reduced simulation development time. The functions in the toolbox are implemented as “System Objects”. The system objects are defined with an equals sign and then used by passing the object to a `step()` function. For example, the desired wave form to be transmitted is defined by the expression:

```
hWave = phased.RectangularWaveform(...  
    'PulseWidth' , pulseWidth , ...  
    'PRF' , PRF , ...  
    'SampleRate' , samplingFreq);
```

The above expression defines only the duration of the wave, ‘PulseWidth’, how often the signal is emitted, ‘PRF’, and the sampling rate for the pulse, ‘SampleRate’. The individual data points are not generated until this object is passed to the `step()` function:

```
wave = step(hWave);
```

MATLAB recognizes the variable passed to `step()` as a system object and generates the individual data points as they would exist given the definition of the wave from the first expression. This makes development easy because it is possible to perform tedious tasks, such as sampling a waveform, by providing the definitions in broad terms, rather than having to write scripts to calculate each data point.

The Phased Array System Toolbox has other system objects that allow for easy definition of antennas, sensor arrays, array geometries, beamforming methods, and more. The difficulty in using this product is that all of the development appears to have been on the signal processing end of the radar system - there is very little included in the way of defining targets or operating environments.

The only method available to define a target is the `phased.RadarTarget` system object, which, for the purposes of this project, essentially only allows for the definition of the radar cross section. Other options exist, for fluctuating targets, but the targets for this system are

non-fluctuating, so they do not apply. While it is possible to define a radar cross section, it is not possible to input specific geometry. The impact of this will be discussed later in this chapter.

The only option for propagation is the `phased.FreeSpace` system object. This means that it is not possible to immediately simulate any environment other than a vacuum. It is not possible to simulate the effects of environmental attenuation without either writing a system object from scratch, finding a way to *correctly* manipulate the output of the array to simulate the effects, or finding a different way to simulate the system altogether. As will be discussed later, in Chapter 6, this issue was side-stepped entirely by ignoring the effects of environmental attenuation.

NON-IMAGING SPECIFICATIONS

TRANSMISSION POWER

The array was first simulated using pulse integration to determine the effects of multiple pulses on system performance. Using 16 pulses for the pulse integration, the peak power for each element was $0.2495\mu\text{W}$. With the array being a 200×200 grid of patch antennas, this means that the total array's transmit power is 9.98mW . The FCC transmitter power limit, fed into the antenna, is 500mW [28], meaning that there is plenty of headroom to increase the transmission power. This reduces the revisit time for each location, which in turn can increase the "refresh rate" of the imaging system.

Reducing the number of integrating pulses from 16 to 4 increased the peak power required to achieve an adequate SNR from a total 2.495mW to 29.5mW . Reducing it again from 4 to 1 increased the peak power to a total of 109mW , which is still well within the FCC transmission limits. Performing pulse integration may be necessary for radar units with a much larger operating range, but the limited range of this application significantly reduces the amount of atmospheric attenuation, which in turn limits the SNR required to ensure proper received signal processing.

There was no difference in imaging capability when the number of pulses to integrate was varied. This was surprising at the time, but then it quickly dawned that the *entire point* of pulse integration was to achieve the desired signal to noise ratio! MATLAB was adjusting the transmitter power automatically as the number of pulse samples was changed.

REVISIT TIME

As discussed last chapter, imaging the entire scene involves scanning $\pm 9.46^\circ$ across the width (*azimuth* scan), and $\pm 9.46^\circ$ across the height (*elevation* scan), and the scan pattern is utilizing moderate oversampling, scanning on a 0.2° increment. To scan the entire width means scanning $(9.46 \times 2) = 18.92^\circ$. With the given increment between scans, there are 94.6 pulses to scan one line. As there cannot be a fractional pulse, 95 pulses are required in each direction, giving the total number of pulses to scan the scene one time to be 9,025.

The pulse repetition frequency is 100MHz, meaning that 100 million pulses *can* be generated every second while maintaining the desired operating specifications. At that rate, given the number of pulses to scan the scene one time, the array can scan the entire scene and then return the beam back to the starting position to begin another scan in 6.76 μ s.

At this rate, the scene could be updated at a rate of 147.8 kHz. This is *far* above the traditional 30 frames per second (FPS), but does not take into account the processing time involved in calculating the next scan angle, adjusting the phase shifters, or processing the recorded data from the receivers. The low revisit time (high revisit frequency) does suggest that there is ample time to perform the actions described and still maintain a “real time” 30 fps refresh rate.

SMALL SCENE RESPONSE

Before heading straight to the crowded scene response, this section will take a moment to review the *small* scene responses under varying conditions to discuss and reinforce the radar principles that have been covered throughout this paper.

VARYING SCAN STEP SIZE

The first single target response goes a long ways towards reinforcing the discussion at the end of the previous chapter, regarding methods of interpreting pulse response data. The images below all represent the *same set of targets*, three targets in a row, but the difference is the scan spacing.

As can be seen in Figure 5-1 through Figure 5-4, oversampling can contribute a *lot* towards resolution. The impact of oversampling the scan was actually far more significant than expected before running these simulations. Oversampling generates images of far higher quality than initially estimated. Figure 5-1 is undersampled, and the targets are so poorly represented that they actually appear as four objects instead of one. Or, if the bounding box method is used instead of inscribed circles, the three objects would be represented as one wide rectangle.

Oversampling improves image fidelity by increasing the number of sample points. This improves the odds of finding a location where no object can be detected. Refer to Figure 5-4 below and notice that the objects on the left and right are separated from the one in the middle by a width of *one pixel*. Oversampling also improves the appearance of the contours of the objects because again, there are more chances to find the exact spot where the object is no longer detectable.

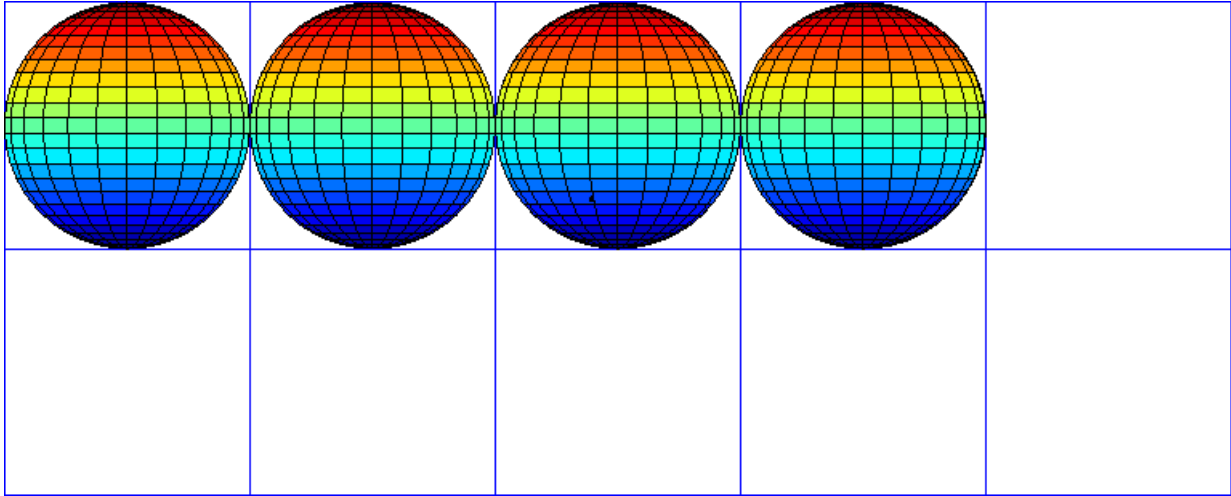


Figure 5-1. Three targets imaged with undersampled pulse spacing. Spacing is equal to the beam width.

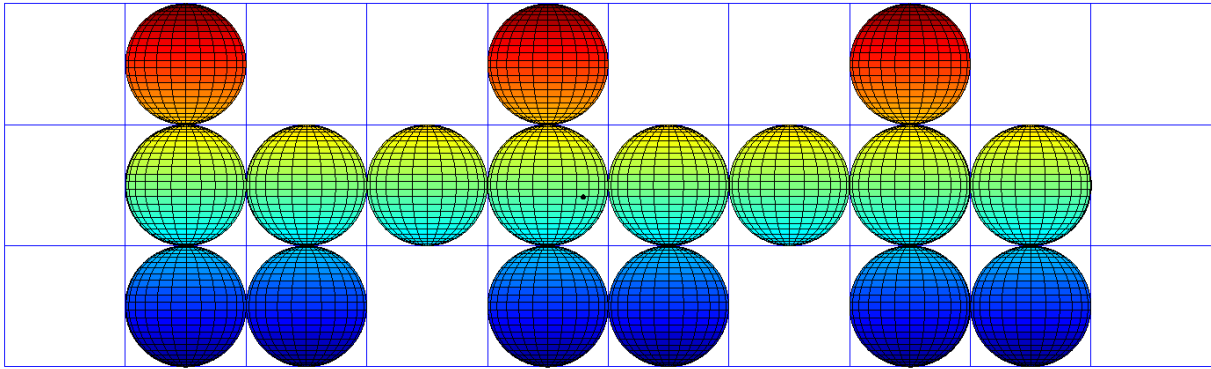


Figure 5-2. Three targets imaged on a coarse pulse spacing grid. Spacing is the minimum necessary to sample every location in the scene.

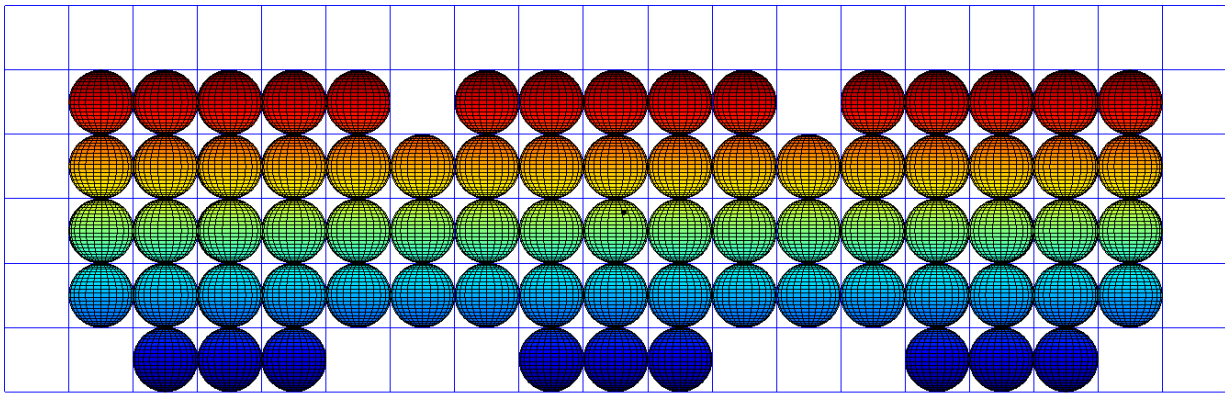


Figure 5-3. Three targets imaged on a medium pulse spacing. This figure is slightly oversampled.

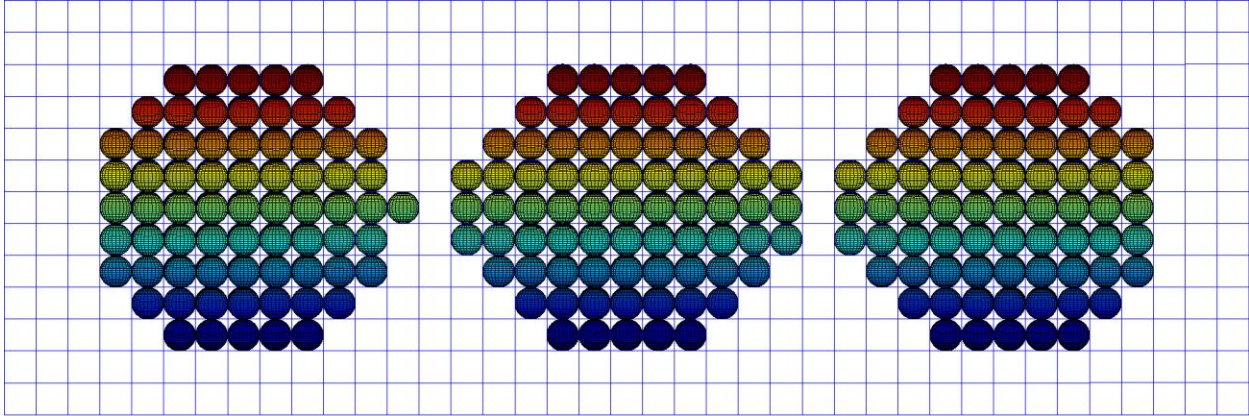


Figure 5-4. Three targets imaged on a fine pulse spacing. This figure is highly oversampled.

The spacing between the targets is 0.7° , which when compared to the beam width measurement of 0.5° , makes the fact that the system was able to detect the space between elements even more impressive. However, consider too the fact that, as the grid spacing gets finer, there are increasing odds that *one* sample will be the sample that picks up the space between targets. Look back at Figure 5-4 and notice that there is, in fact, only *one* sample separating the targets on the left and right from the target in the center.

Also notice how *eccentric* or *oval-like* the target in the center of Figure 5-4 appears. Compare its left and right edges with the left edge of the left target and right edge of the right target. Recall *again* that the beam measurements are the *half power* edges of the beam. The center target is getting smeared in width because the targets on either side are enhancing a signal that ordinarily, without enhancement, would not get detected. This is the case on the outer edges of the scene, where there are no nearby objects to boost the response.

VARYING TARGET SIZE

The results covered here were surprising. They are revealing in that they show how MATLAB handles (or doesn't) the cross-sectional areas provided as targets for the radar simulations. The conceptual explanations of how the beam width stretches or smears a target would suggest that smaller targets will get disproportionately skewed because the beam adds a constant width to all objects. The constant width is a larger percentage of smaller objects.

Figure 5-5 shows a series of objects that are small relative to the radar's wavelength. The objects are located along the top row, and the bottom row shows how those objects appear to the radar. The grid spacing is 4.88mm. Notice that the representation here works *exactly* as described in the Scanning Method and Expected Simulation Results section from last chapter (displayed in Figure 4-13 and Figure 4-14). Anywhere the object occupies any portion of the scan square, it counts as a valid response and is recorded as such.

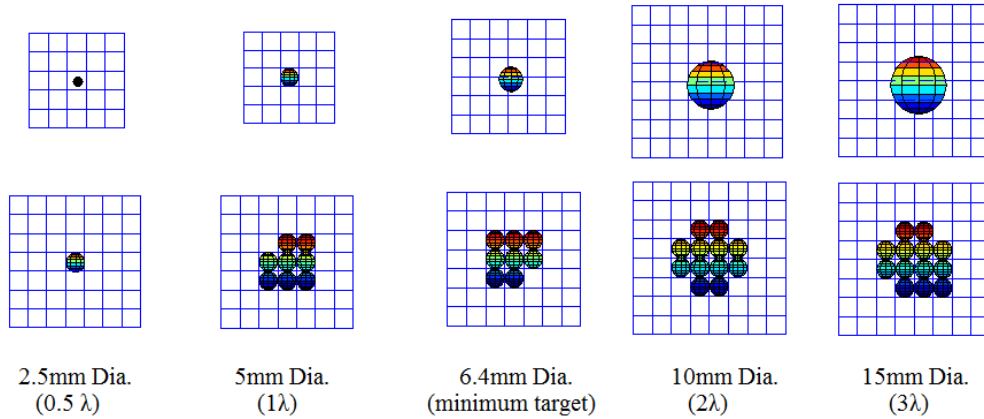


Figure 5-5. Small objects, above, and their representations, below, on a 4.88mm grid

This was the expected behavior. The hope was to be able to generate a plot that showed the percent enlargement of objects, in terms of their width in wavelengths. As larger objects were imaged, as seen in Figure 5-6, the pattern seemed to stop. The object 5 wavelengths (λ) across seemed to be represented *okay*, but the 6λ and 8λ objects appeared to be the same sizes! More than appearing the same size, the representations were *smaller* than the actual objects.

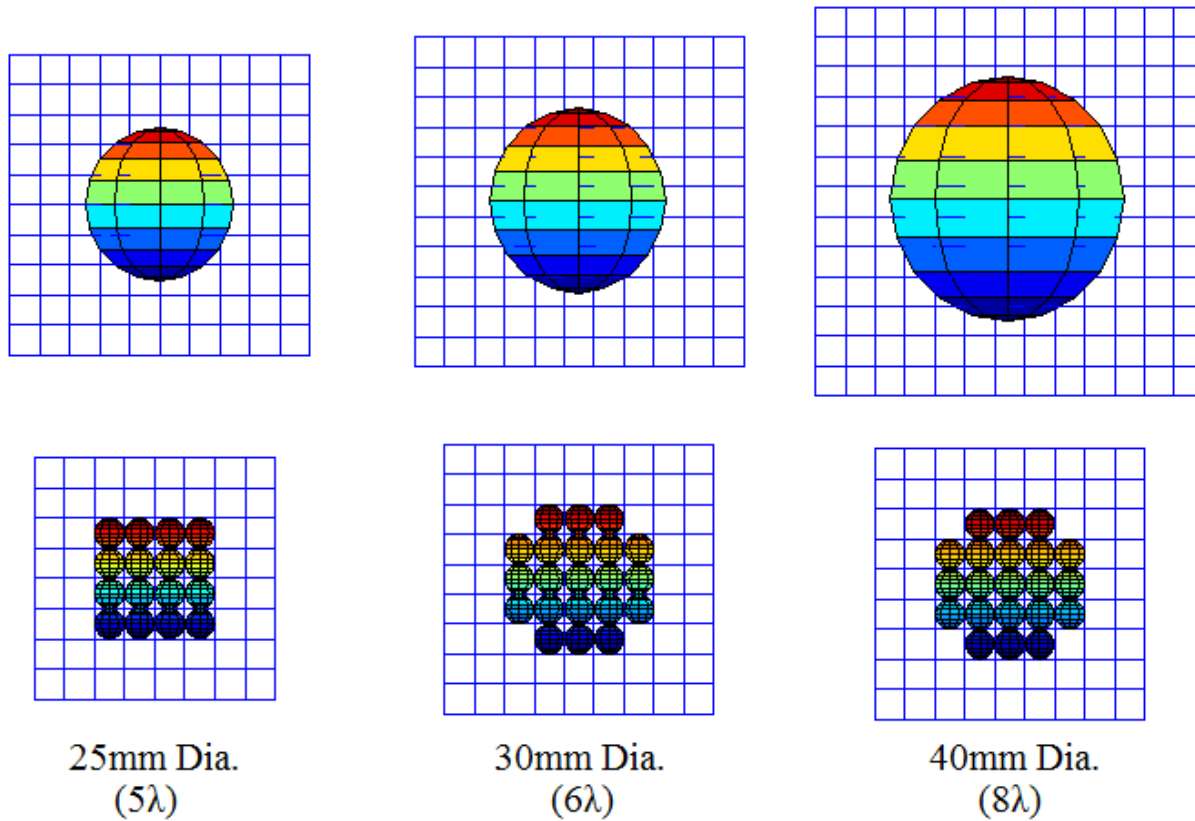


Figure 5-6. Large objects, above, and their representations, below, on a 4.88mm grid.

As the object size continued to increase, eventually phantom targets started to appear! This can be seen as the distinct points separated from the central image in Figure 5-7. This was confusing at first, as the phantom targets are occurring *inside* the span occupied by the actual target. After a *lot* of consideration, it was finally understood that there was an assumption that MATLAB was using the radar cross sections as circular cross sections, because of the statement made in [26], referenced last chapter, which asserted that reflections from spheres were *independent of frequency*.

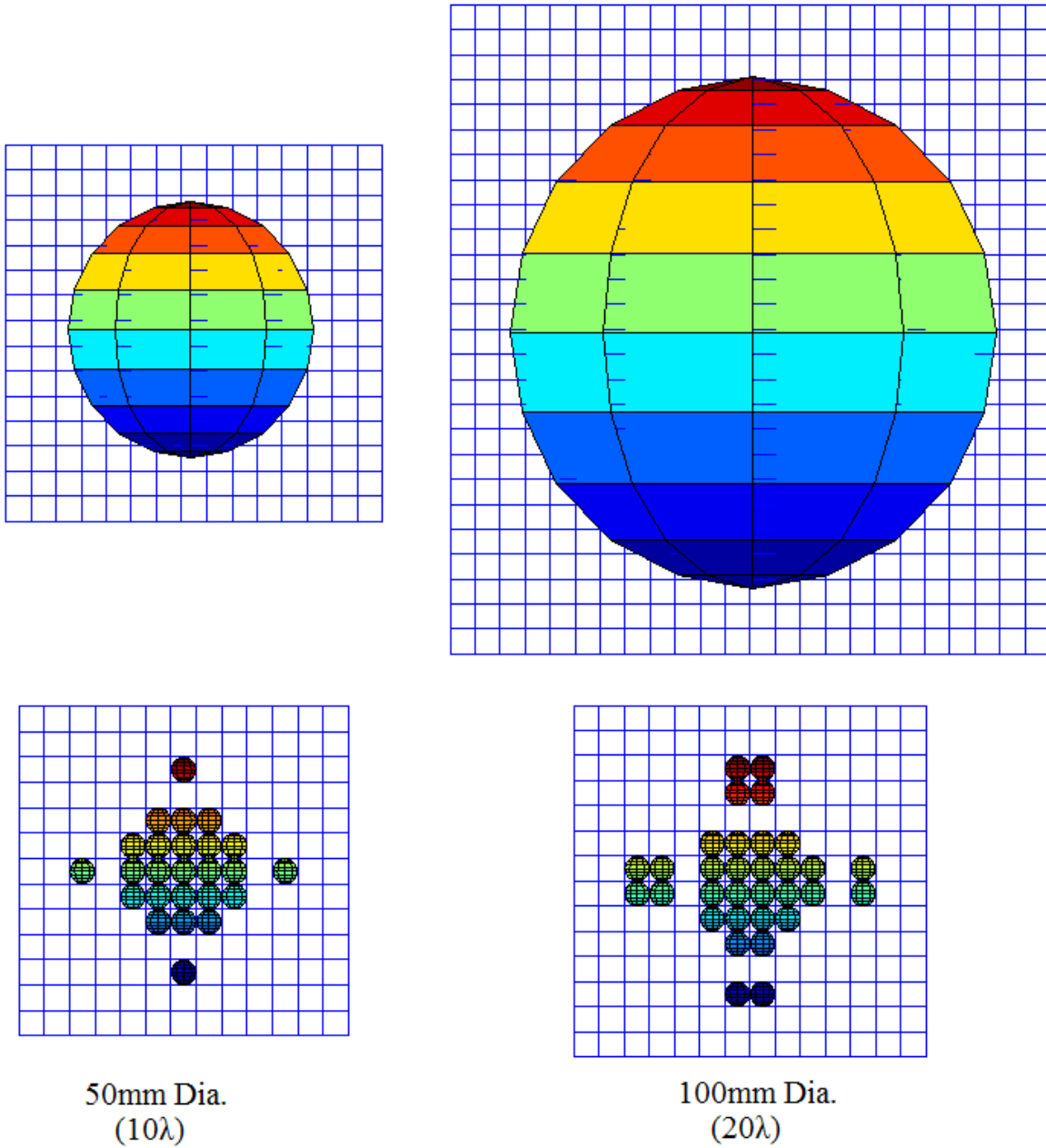


Figure 5-7. Huge objects, above, and their representations and phantom images, below. Grid spacing is 4.88mm.

Instead of assuming *any* physical shape, MATLAB is instead using the cross section as a value, and assigning that value to *one point in space*. Imagine an infinitely small reflecting *lens* of varying focusing power. The radar cross section equation, Equation 4.1, gave the formula as the physical cross section, *multiplied by a reflectivity and directivity factor*.

When the object is small, it approximates a point in space, and the representation is accurate. However, as the object increases in size, MATLAB's interpretation of the radar cross section no longer adequately represents the true target, and the result is the distortion of the target in the returned signal.

CROWDED SCENE RESPONSE

Having run through the simulation basics with the small scenes and individual targets, now it's time for the full crowded scene responses! The objects are all relatively small, so the distortion effects discussed in the last section are not an issue here, though they would be if a different target set were selected (like the *housing* of a landmine). The first figure below is the scene itself – the objects to be imaged. This image is likely not to scale for you, so sections of the figure will be removed from the image later so they may be displayed at a 1:1 scale, as they would appear on the imaging system.

The targets arranged in Figure 5-8 are as follows: NATO 5.56 shell casings are aligned vertically, NATO 5.56 slugs are arranged horizontally, the two coins, dime and quarter, are approximately centered horizontally, and the springs for the landmine are located in the bottom right hand corner.

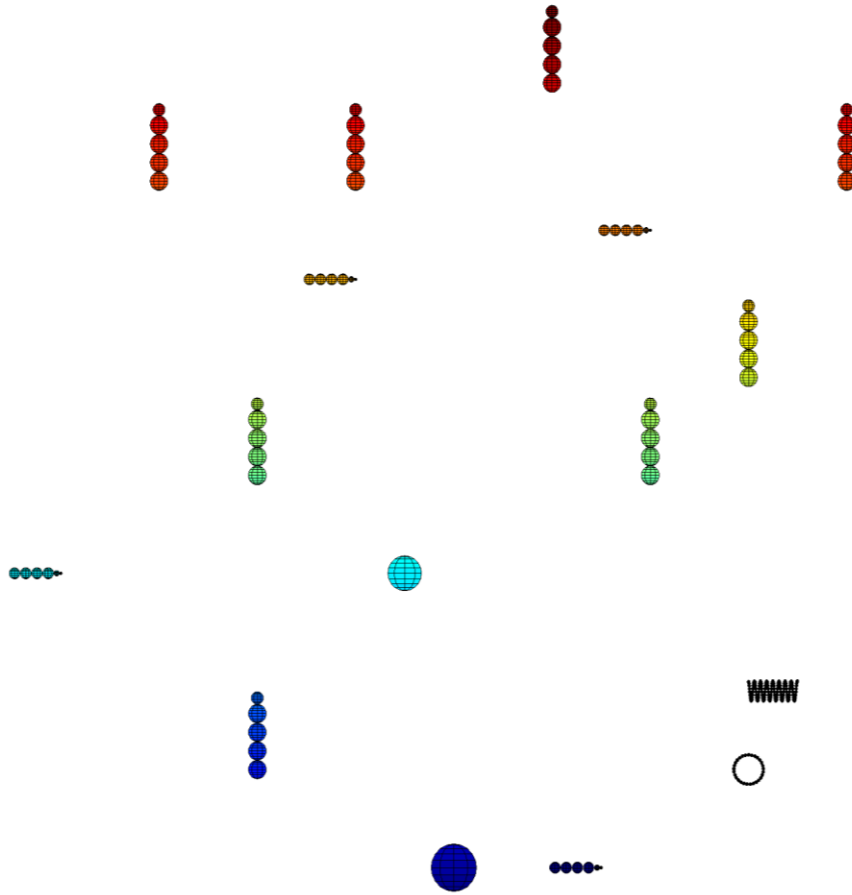


Figure 5-8. The "crowded scene".

The decision was made to leave the landmine housing *out* of the crowded scene, despite the fact that the radar system should detect it without issue, because of a desire to be rigorous in evaluating the discriminatory capability of the system. Also, as discovered later and discussed in the previous section, modeling the housing as one object would not be possible because of MATLAB's handling of very large targets. The assumption was that if the system could distinguish between a spring and a shell casing that it should be able to perform adequately. Figure 5-9 shows the results of the crowded scene simulation.

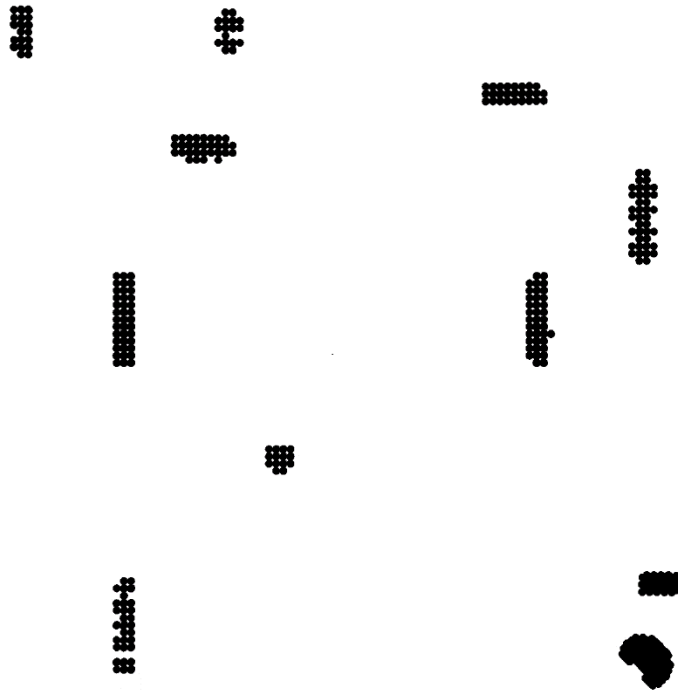


Figure 5-9. Full system results.

As a warning, the full scale results are intended to be displayed on an 18”x18” screen, and you are viewing them as a figure on an 8.5”x11” display. What is important to point out before moving to the object-by-object performance review is the fact that the system does not appear to have imaged the entire scene! This was *positively baffling* for hours when the simulation results were returned. When it was finally understood what had happened, the results were almost discarded; ultimately they were kept for a “teachable moment.”

Recall that the beam from the array emits as though it originated as *one* beam located in the center of the array, instead a conglomeration of *many* beams distributed across the array. The width of the scene (where the targets are located) was supposed to be the same size as the physical dimensions of the array. Refer to Figure 5-10 below. The simulation had the targets located near the surface, relatively far from the maximum operating range of the system. The problem is that the beam is always steered starting from the *center* of the array. The objects buried close to the surface but still under the array (designated by the dashed gray lines) were *never scanned!*

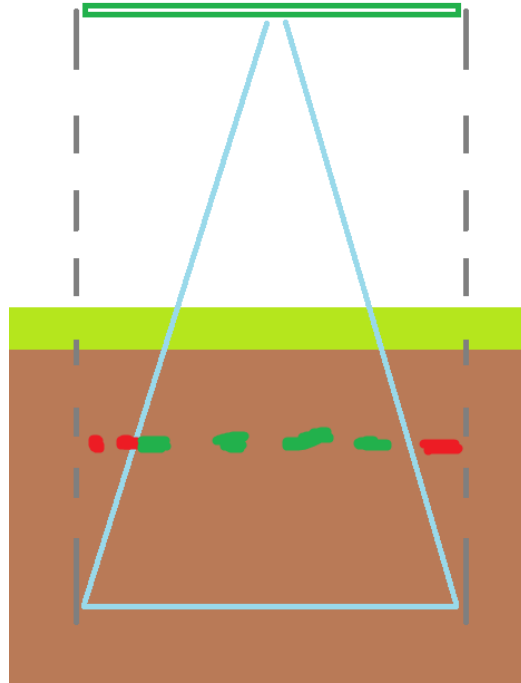


Figure 5-10. Erroneous scan width settings.

The proper way to deal with this is to have the beam scan a patch as wide as the array on the *surface* of the terrain, and discard data that exceeds the x/y coordinates of the screen when the data is converted from polar to Cartesian coordinates for display. This method would scan a patch larger than necessary and would wind up discarding a significant amount of data, but *not scanning the area the user thinks is safe could kill someone*.

An intuitive interface cuts both ways – if you make someone think they know what they’re doing and then you feed them bad information, they are worse off than if they knew they didn’t understand the information to begin with. Again, this mistake could have had lethal consequences. It’s a good thing simulations exist!

Now, with the reason for the smaller-than-expected image explained, the discussion can move on to the side-by-side comparisons. The objects shown are ordered by shell casings, then slugs, then the mine springs. On the left of the figures is a visual reference for the simulation approximation of the object, as discussed from the previous chapter. The middle shows the system results *as designed*, and the images on the right show the *same scene* as evaluated by a system that uses an array half the size, but otherwise operates on all the same specifications.

Figure 5-11 below shows how well the system portrays objects in a crowded scene. On the right, as mentioned, are images from an otherwise identical radar system using an array that is half the physical size of the ideal system (i.e., 0.25 x 0.25 meters). The images from the smaller array are unsuitable because they have “bloated” or smeared the objects too much. The smaller array has doubled the beamwidth, and even though the pulse spacing has remained the

same, the benefits of oversampling (now extreme oversampling) cannot make up for the wider beam.

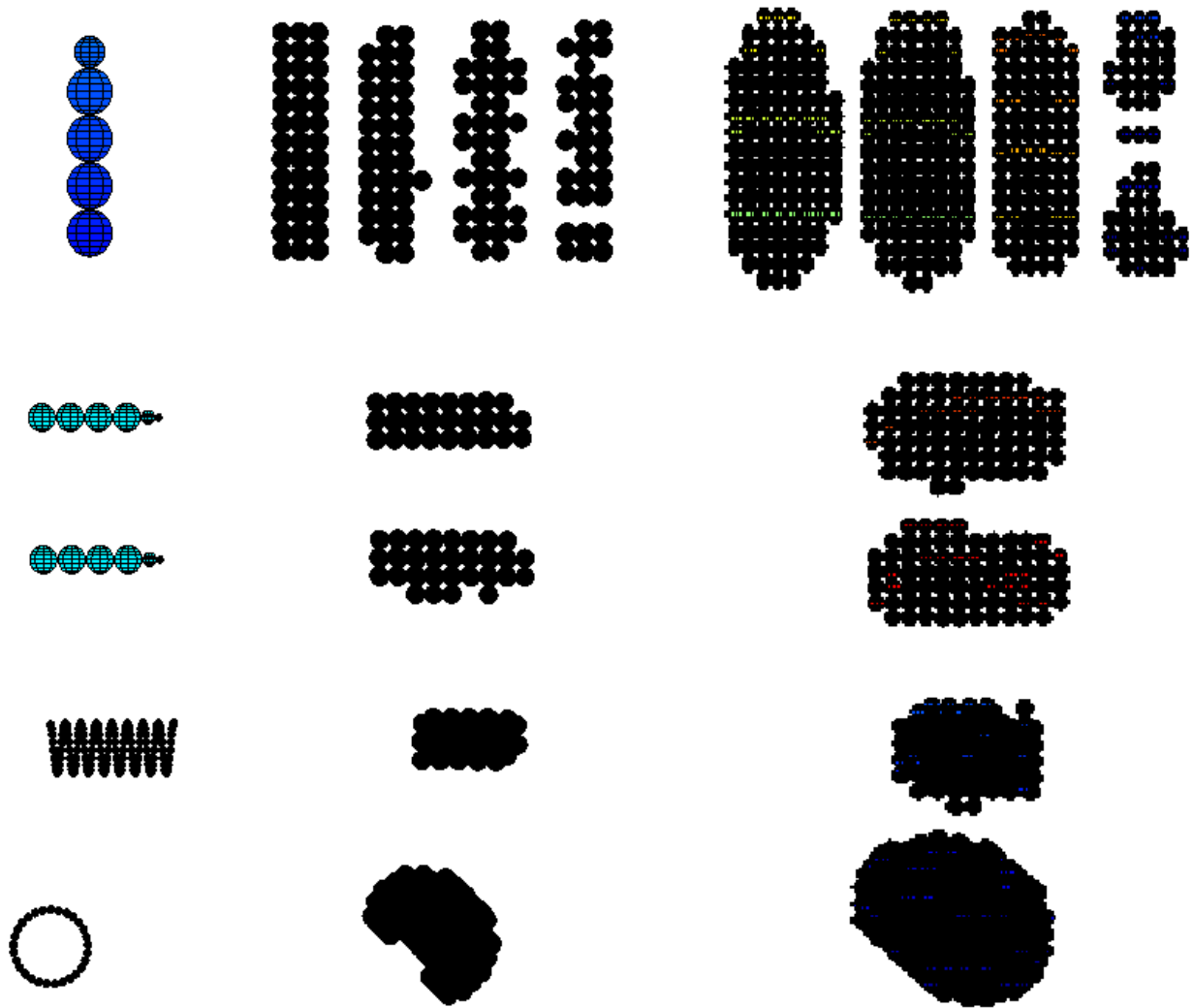


Figure 5-11. Detail of images from Figure 5-9. The images are, top to bottom, a shell casing, a slug, and the landmine springs. From left to right are the simulation models, the optimal system results, and the suboptimal system results.

It is interesting to note that, while the shell casings appear to be reproduced with relatively high fidelity, the slugs are very much enlarged, even with the “ideal” system. Also perplexing, at first, are the springs. One spring, the upper, appears to be reproduced fairly accurately, while the other is not.

Recall the image of three targets shown with highly oversampled pulse intervals, Figure 5-4. The middle image was distorted where the “pickup” from the surrounding objects was helping to reflect the signal. It is believed that a similar effect is happening with the landmine

springs. The upper spring, from the user's view (and the radar's view!) appears very much like a solid block. Indeed, to the radar, the surrounding objects will help reflect the waves and the upper spring will return a signal *exactly* like a solid block.

Meanwhile, the lower spring in the bottom center of Figure 5-11 and the slugs in center of the same figure are badly distorted. This is believed to be entirely due to the relative thinness of the objects. Recall the discussions throughout the paper about smearing. The objects' thin widths cause them to appear to have a much more significant enlargement. It was not as noticeable for the shell casings because it was a smaller *percent* increase in each direction, so the aspect ratio was left largely unchanged. Notice that the slugs appear to have the correct length; it's just the width that appears to have changed! Similarly, because the "walls" of the lower spring appear so thin they are *significantly* altered when scanned from this direction.

It is possible to increase the oversampling to correct for the extra "weight" the radar system is putting on thin objects, but this is very likely *not* necessary. The goal of this system is not to be able to identify every object in the ground! The goal is to be able to *quickly* and *with high certainty* differentiate between landmines and scrap. The landmines were simulated as springs to be able to evaluate discriminatory capability. It is expected that landmines would show up in the field as large cylinders.

Chapter 6 LIMITATIONS AND FUTURE WORK

CHAPTER SUMMARY

This chapter points out limitations on the system design, including limitations imposed by the simulation capabilities and limitations due to implementation aspects that were not considered as constraints on the system design. Health and safety considerations are discussed, and notes regarding the construction of the imaging system are addressed.

HEALTH AND SAFETY CONSIDERATIONS

The purpose of this thesis was to determine the feasibility of a high resolution, low range ground-penetrating radar. While practicality is desirable, and all operating parameters were guided by practical limits, the scope of this work was not to perform a complete analysis on a finished, physical product.

Even with such a disclaimer, the author would like to go further and clearly state that *this design has not been evaluated for fitness of use. Constructing and operating the device described in this document could lead to equipment damage, injury, and/or death.*

There has not been any research into the health effects of high frequency electromagnetic radiation, so it cannot be emphasized enough that *there could be considerable risk in operating a radar unit at waist level.*

For comparison, consider a microwave oven and a wireless internet router. It would be generally considered *dangerous* to operate a microwave oven without the shielded door installed and closed, yet most internet routers are located in occupied living spaces, typically near a computer user and/or the computer itself.

The microwave oven operates on an ISM band, at 2.45 GHz, as does the wireless router [38][39], yet one is considered dangerous while the other is not. The microwave oven operates at 1.25 kW [38], while the wireless router has a broadcast power limit of 1W [28]. Clearly the microwave oven has a significantly higher radiative output than the wireless router, but the microwave oven is contained and self-shielded. The FCC has set broadcast power limits on devices such as the wireless router so that they will not generate a signal strong enough to endanger people or disrupt electronic devices.

At some point above 1W, a 2.45 GHz signal becomes disruptive and then destructive to electronic and organic objects in the surrounding area. Similarly, there is a point at which any radiated signal will become hazardous to those around it. The array power emission was designed to stay below the FCC's 57-64 GHz band output power limit of 500 mW [28]. There is a lot of effort being put forth to shift wireless internet communications to 60 GHz [40] [41], and, "60 GHz is considered the most promising technology to deliver gigabit wireless for *indoor*

communications.” [42] It is hoped that the device would be safe, but *hope and expectations are not an acceptable substitute for a safety analysis.*

PROPAGATION MODELS AND NOISE

The primary purpose of performing this research was to determine if the necessary resolution for a handheld radar system could be achieved. To that end, the simulations were performed in an overly idealized environment - a perfect vacuum with no other objects located nearby. Signal fade was discussed briefly in Chapter 2 as being partly due to distance from the radiator and partly due to the attenuation of the signal by the environment.

For several reasons, the attenuation of the signal by the environment was ignored while performing the simulations. First, MATLAB does not have a mechanism for assigning the impedance of the environment. It is possible to simulate the effects of environmental signal attenuation by modifying the received signal data, but doing so posed a significant development task that did not contribute to the completion of the research project.

Secondly, the impedance of ground varies greatly. The net effect of impedance is that the signal is essentially shorted. Given the discussion of wavelengths earlier in the paper, for any signal, a signal with the same magnitude but opposite sign can be found half a wavelength away. For most radar systems, which are very high frequency, this represents a very small distance. For the designed system specifically, that distance is 2.5 mm.

The lower the impedance of the environment, the less resistance there is for those two negating signals to short to each other and cancel. The impedance of dry air is different than that of moist air, dry soil is different than damp soil, and impedances vary between soil types: loam, sand, peat, clay, etc.

If the effort to develop a mechanism for including environmental impedance was undertaken, it would only make sense to then use it to simulate the anticipated operating environment. The radar system could be used world-wide, from the jungles of Cambodia to the deserts of Egypt, meaning that every conceivable terrain type could be encountered. As with implementing the mechanism to begin with, this task represented a significant development effort with no contribution to the primary purpose of the research project: to determine if physics even allows such a device at all.

Along the same lines, background noise was not taken into consideration. *Thermal* noise was the only consideration for noise power when evaluation transmitter power and the required signal to noise ratio needed for reasonable system performance. In reality, objects located beyond the maximum operating range will still present reflected signals to the array, even if those signals are below the detectable threshold.

As with any noise, those faint returns can either be in-phase and constructively interfere, creating false alarms, or can be out-of-phase and destructively interfere, causing legitimate

signals to be missed. The impact of this noise and noise from other emitters was neglected for the purposes of this research project. If taken into account, this source of noise would surely require the transmission power of the radar system to be increased. Given the current transmission power of 0.11 W and the FCC broadcast limit of 0.5 W, there is a potential to boost the output power of the array by approximately 6 dB while remaining under the broadcast limits.

SIMULATION LIMITATIONS

Health and safety concerns are a key issue for anyone attempting to construct and *operate* the device described above, but a difficulty in *evaluating* the physical device would be comparing the results of an actual imaging system to the simulation results shown in Chapter 5. This is because MATLAB does not allow for complex target definitions, and thus all targets were required to be approximated.

The ideal method for defining a scene would be to specify object geometry and volume, then specify the material type or impedance, and have MATLAB simulate the wave interaction at the interface between material types.

With such a method, it would be possible to create an environment wherein the array operated in *air*, and *metal* targets were located in *soil*. This is not the case, and as such, the effect of such air/soil and soil/metal interfaces cannot be adequately simulated. These interface interactions would weaken, sometimes significantly, the wave as it passed the interface. This weakening effect would occur *both* times the wave front passed, once on transmission and once on reflection.

The inability of MATLAB to account for these interactions produced images that are surely clearer than could be expected from live data. The signal could be refined with the use of pulse integration, but the tradeoff would come at a reduced refresh rate. Given the current revisit rate of 147 kHz, there could be dozens or hundreds of pulses used for noise reduction and still maintain a 30Hz refresh rate. The radar is handheld, not on a jet, and the target is stationary, not a missile, so the extreme refresh rates needed by military radars are not necessary; 30Hz should be sufficient.

The exact gains in signal fidelity or increases in signal penetration cannot be calculated exactly because, again, the nature of the signal interaction at the interfaces is not known. A signal with no noise has an infinite (undefined) signal to noise ratio, and similarly, a known signal with an unknown noise profile has an undefined signal to noise ratio. Ultimately, the signal to noise ratio will determine effective depths, revisit (refresh) times, and overall usefulness, but this is something that would need a constructed device and extensive field testing to determine.

POTENTIAL CONSTRUCTION ISSUES

Having identified the need for constructing the imager and given the specifications to build it, this section points out several construction issues that may hinder the motivated reader. This section is not intended to be a comprehensive list of obstacles or impediments, but instead as a place to collect my thoughts on glaring, overall issues recognized during a careful consideration of construction.

As mentioned briefly in Chapter 5, it is important to view the results *with no scaling* to be able to accurately identify landmine components such as springs. The aperture width is 0.5m, which was selected as a compromise between a wide aperture, that could provide fine resolution, and a narrow aperture, which could be practically handled by one person. While this size is easily manipulated by one person, nobody would call it small.

The downside to having a large array is providing unscaled (1:1) output images in an intuitive manner. It is entirely possible to limit the scan angles such that a 4"x4" patch on the ground is imaged, and so only a 4"x4" screen would be needed to accurately render the scan information. If this were the case, the array would still be 0.5m on a side, so there would be about an 8 inch border around the screen on each side, depicted in Figure 6-1. This could cause issues where the user may not be able to tell which part of the ground the screen is referencing, which in turn could create a lot of confusion about which part of the ground to excavate.

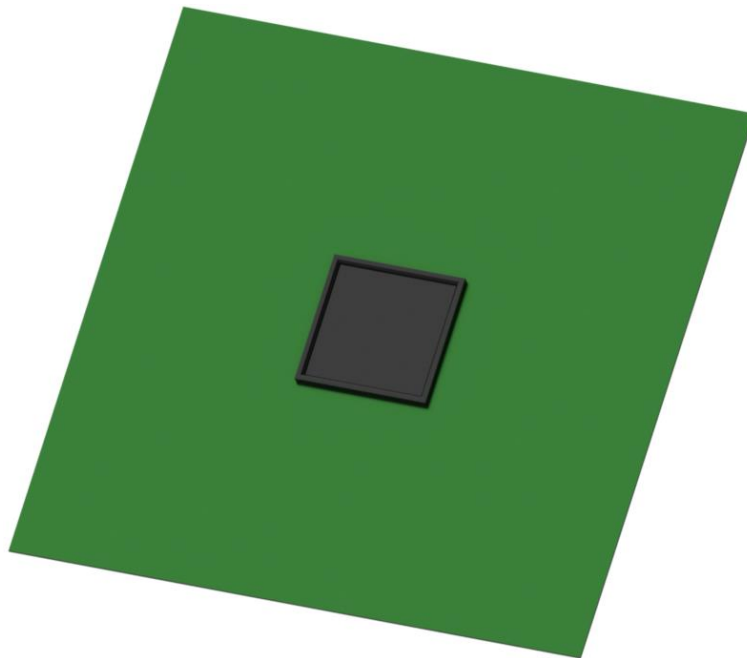


Figure 6-1. A small display screen installed on the array substrate.

The logical solution is to install a screen the size of the array, but finding one 0.5m square or similarly sized screen may be difficult. This may mean that, to be constructed, the designer may need to locate a great many smaller screens and split the full image to each screen

to create a mosaic-style rendering. This adds to the complexity, which means increased cost, weight, and processing power, just to drive the display.

As the intention of this device is to produce real-time images, processing power is another problem that is likely to give headaches. The electronics for forming, transmitting, receiving, and processing the signal all must be located onboard, as well as the electronics for powering and driving the display(s). Due to the nature of RF components, the transmission and reception electronics are all likely required to be mounted on the opposite side of the substrate from the antennas. The post-processing and display driver electronics could probably be located elsewhere, but if they are this would require communications transmitters and receivers, cabling, and the selection of a range-appropriate communications protocol.

The most likely target for moving off-device would be the batteries. Between the signal handling, processing, and display, it is thought that the power consumption of the imager would be significantly higher than that of a standard metal detector. The increase in power consumption should be offset by much higher demining rates, such that the power consumption per unit area of ground certified mine-free would actually be lower. Even so, a higher rate of power consumption suggests a higher heat output of the power electronics, which, in a backpack-style configuration, could become a nuisance in areas commonly associated with severe landmine problems: Southeast Asia, Northern Africa, and Central America.

The last glaring issue envisioned would involve handling by the user. The aperture is *fully* populated by antennas. There is no room on the periphery of the array for the user's fingers. This means that the entire device could not be gripped on the edges as designed. Handles could be attached to the non-antenna side of the device, but that's where the display is located. The solution here would be to extend the size of the antenna substrate such that a buffer region could be located, but the impact of the near-field interaction between a user's finger and the array was not studied. The effect, if any, could be reduced by increasing the buffer zone around the array, but any increase in the buffer zone reduces the ease of handling.

The tradeoffs between portability, ease of use, weight, etc., are all the responsibility of the industrial designer tasked with producing the end product. As mentioned several times now, practicality guided all of the design decisions made in developing the imaging system, but the decisions were not constrained by practicality. There may be some aspects of the device that are not practical for actual implementation (re-read the section above, Health and Safety Considerations, for more information).

CONCLUSION

The radar system described above was designed to be portable while achieving resolutions high enough to discriminate meaningful targets (landmines) from scrap in a cluttered "combat zone" scene. Despite the limitations, the MATLAB simulations have proven that the

output images are high quality enough to perform this task, and are far higher quality than competing systems.

It is hoped that, by repeatedly echoing concerns stated clearly in the last chapter, anyone interested would consult a professional electrical engineer before attempting to construct this device. Recall from *first page* that this is a thesis for a master of *mechanical* engineering degree. If you persist in attempting to build this system, it cannot be stressed enough how useful small scale testing is – don't commit to building the full device until you can get a sub array working! Don't build a sub array until you can get one antenna working! *Don't do anything until you know it is safe to do so!*

Ultimately, with the simulation limitations, there's no way to fully validate the design without constructing the imaging unit. This would involve a *considerable* investment in time, material, and test equipment. It is believed that if a suitable partner could be found, one who may already possess the required test equipment, it could well be worthwhile to pursue this project through at least to a prototype.

What became a secondary goal for this project was to ensure that this paper did not turn into one of the *very many* papers that was read and discarded while researching. Most of the literature reviewed had started with the assumption that the reader already understood the fundamentals of radar imaging, or attempted to explain the mechanics in terms of derivations from Maxwell's equations! The most frustrating aspect about all of that was that nothing was written for someone from a mechanical background.

It is hoped that, in addition to showing that this design is *feasible*, a document was created that explains, *in lay terms*, how an imaging radar system works, then *after* the explanation shows the radar equations *and how to use them*. It is sincerely hoped that this gives *everyone*, from *every background*, a fundamental conceptual understanding of radar imaging. If you enjoyed this, then there's a mountain of resources on the next page to jump further into radar systems.

REFERENCES

- [1] Associated Press. (2011, December 11). *Vietnam weapons of war: Over 42,000 killed by leftover mines, bombs*. Huffington Post. Retrieved from http://www.huffingtonpost.com/2011/12/05/vietnam-weapons-of-war-casualties_n_1128791.html
- [2] Associated Press. (2013, August 14). *Vietnam war bombs still killing people 40 years later*. Huffington Post. Retrieved from http://www.huffingtonpost.com/2013/08/14/vietnam-war-bombs_n_3755066.html
- [3] Bruschini, C. (2000). *Metal detectors in civil engineering and humanitarian demining: Overview and tests of a commercial visualizing system*. Informally published manuscript, Institute of Electrical Engineering, School of Engineering, École Polytechnique Fédérale de Lausanne & Vrije Universiteit Brussel, Brussels, Belgium. Retrieved from <http://citeseerx.ist.psu.edu/viewdoc/download?doi=10.1.1.72.9870&rep=rep1&type=pdf>
- [4] United Nations. Department of Humanitarian Affairs, United Nations Mine Clearance and Policy Unit. (1997). *Landmines factsheet*. Retrieved from website: <http://www.un.org/cyberschoolbus/banmines/facts.asp>
- [5] Candy, B. H. (2009). U.S. Patent No. 7,579,839. Washington, DC: U.S. Patent and Trademark Office.
- [6] Borgwardt, C. (1996). High-precision mine detection with real-time imaging. , 2765(1) doi:10.1117/12.241232
- [7] HILTI. (Photographer). (2009). HILTI Ferrosan [Web Photo]. Retrieved from <https://www.hilti.com/data/product/prodlarge/62304.jpg>
- [8] Port of London Authority. (Photographer). (2013, June 03). Dornier Do 17 bomber [Web Photo]. Retrieved from http://eandt.theiet.org/news/2013/jun/images/640_german-plane-sonar-cropped.jpg
- [9] Port of London Authority. (Photographer). (2013, May 07). Dornier Do 17 bomber [Web Photo]. Retrieved from http://a57.foxnews.com/global.fncstatic.com/static/managed/img/Scitech/660/371/PossibleDo17_Wessex_Archaeology_side_scan.jpg?ve=1&tl=1
- [10] Daniels, D. J., & Institution of Electrical Engineers. (2004). *Ground penetrating radar*. London: Institution of Engineering and Technology.
- [11] Ditch Witch. (2007, December). 2450gr operator's manual. Retrieved from <http://www.ditchwitch.com/sites/default/files/manual-pdfs/2450GR-manual.pdf>

- [12] US Radar, Inc. (n.d.). P-1000 ground penetrating radar specifications. Retrieved from <http://www.usradar.com/ground-penetrating-radar-gpr/utility-locating-cart-systems/high-resolution-utility-locator>
- [13] Ditch Witch. (Photographer). (2007, December). Ditch Witch 2450GR [Web Photo]. Retrieved from http://www.ditchwitch.com/sites/default/files/styles/popup/public/pictures/ditch-witch_2450GR_master_03.jpg
- [14] Stutzman, W. (1981). *Antenna theory and design*. (p. 129). New York: John Wiley & Sons.
- [15] Komarov, I. V., & Smolskiy, S. M. (2003). *Fundamentals of short-range FM radar*. Boston: Artech House.
- [16] Ricny, V. (2009). *Maximum available accuracy of FM-CW radars*. *Radioengineering*, 18(4), 556-560.
- [17] Rolt, K. D. *Ocean, platform, and signal processing effects on synthetic aperture sonar performance*. Massachusetts Institute of Technology).
- [18] Robertson, G.H. (1967) Operating characteristics for a linear detector of CW signals in narrow-band noise. *Bell System Technical Journal* (April 1967), 755-774.
- [19] Tufts, D. W., & Cann, A. J. (1983). *On Albersheim's detection equation*. *IEEE Transactions on Aerospace and Electronic Systems*, AES-19(4), 643-646. doi:10.1109/TAES.1983.309356
- [20] Davenport and Root. (1958) *Random Signals and Noise*. New York: McGraw-Hill, 1958.
- [21] Hornung, J. L. (1948). *Radar primer*. New York: McGraw-Hill Book Co.
- [22] Skolnik, M. I. (1962). *Introduction to radar systems*. New York: McGraw-Hill.
- [23] Richards, M. A. (2005). *Fundamentals of radar signal processing*. New York: McGraw-Hill.
- [24] Siegel, R. (2002). *Land mine detection*. Piscataway: IEEE-Inst Electrical Electronics Engineers Inc. doi:10.1109/MIM.2002.1048979
- [25] Bruschini, C., Gros, B., Guerne, F., Pièce, P., & Carmona, O. (1998). Ground penetrating radar and imaging metal detector for antipersonnel mine detection. *Journal of Applied Geophysics*, 40(1), 59-71. doi:10.1016/S0926-9851(97)00038-4

- [26] Miacci, M. A. S., Nohara, E. L., Martin, I. M., Peixoto, G. G., & Rezende, M. C. (2012). Indoor radar cross section measurements of single targets. *Journal of Aerospace Technology and Management*, 4(1), 25-32. doi:10.5028/jatm.2012.04014711
- [27] Moran, M., & Shapiro, H. (2008). *Fundamentals of engineering thermodynamics*. (6th ed.). Hoboken: John Wiley & Sons.
- [28] (2009). *Code of federal regulations* (47 CFR Ch.1 §15.247(b)(3)). Retrieved from Government Printing Office (GPO) website: <http://www.gpo.gov/fdsys/pkg/CFR-2009-title47-vol1/pdf/CFR-2009-title47-vol1-part15.pdf>
- [29] (2009). *Code of federal regulations* (47 CFR Ch.1 §18.301). Retrieved from Government Printing Office (GPO) website: <http://www.gpo.gov/fdsys/pkg/CFR-2007-title47-vol1/pdf/CFR-2007-title47-vol1-sec18-301.pdf>
- [30] Tan, Y. C. M., & Tan, Y. C. M. (2010). *Computational modelling and simulation to design 60GHz mmWave antenna*. 1-4. doi:10.1109/APS.2010.5562035
- [31] Flinch, F. (Artist). (2010, November 19). 5.56 NATO Cartridge Dimensions [Web Drawing]. Retrieved from <http://ultimatereloader.com/tag/5-56-x-45mm/>
- [32] Cooke, G. (Artist). (2005, May 03). 5.56 Ammo [Web Drawing]. Retrieved from http://www.inetres.com/gp/military/infantry/rifle/556mm_ammo.html
- [33] (2010, June 24). 5.56 M855A1 Enhanced Performance Round [Web Photo]. Retrieved from <http://usarmy.vo.llnwd.net/e1/-images/2011/05/08/107872/army.mil-107872-2011-05-06-190552.jpg>
- [34] Smith, A. (2010). PMN anti-personnel blast mine. Retrieved from <http://www.nolandmines.com/minesPMN.htm>
- [35] ORDATA - U.S.S.R. Landmine, APERS, PMN-4. (2013). Retrieved from <http://ordatamines.maic.jmu.edu/displaydata.aspx?OrDataId=1171>
- [36] Gaines, D. (Photographer). (2003, June 25). EOD personnel evaluating PMN mines in Fallujah, Iraq [Web Photo]. Retrieved from <http://www.dodmedia.osd.mil/Assets/2004/Army/DA-SD-04-02138.JPEG>
- [37] Trevelyan, J. (2000, January 01). Photographs of pmn-2 mine. Retrieved from <http://school.mech.uwa.edu.au/~jamest/demining/info/pmn-2.html>
- [38] Panasonic. (2010). *Operating instructions, microwave oven*. Shanghai: Panasonic Home Appliances Microwave Oven. Retrieved from <http://service.us.panasonic.com/OPERMANPDF/NNSN797.PDF>

- [39] Netgear. (2010). *N600 wireless dual band router wndr3400 setup manual*. San Jose: NETGEAR, Inc. DOI: ftp://downloads.netgear.com/files/WNDR3400_SM_23MAR2010.pdf
- [40] Kalfas, G., Markou, S., Tsiokos, D., Verikoukis, C., & Pleros, N. (2013). *Very high throughput 60GHz wireless enterprise networks over GPON infrastructure*. 873-878. doi:10.1109/ICCW.2013.6649357
- [41] Clive Akass. (2008). *Wireless battle over 60GHz*. *Personal Computer World*.
- [42] Yang, L. (2008). *60GHz: Opportunity for gigabit WPAN and WLAN convergence ACM*. doi:10.1145/1496091.1496101

APPENDIX A.1 – MAIN SIMULATION CODE

```
%%%%%%%%%%%%%%%%%%%%%%%%%%%%%%%%%%%%%%%%%%%%%%%%%%%%%%%%%%%%%%%%%%%%%%%%
%
%   High Resolution Radar Simulation   %
% MATLAB Script Supporting a Thesis for %
%
%           Master of Science           %
%           Mechanical Engineering       %
%
%           Charles Saunders            %
%           Spring 2014                 %
%           Virginia Tech               %
%   Dr. Al Wicks, Committee Chair      %
%
%%%%%%%%%%%%%%%%%%%%%%%%%%%%%%%%%%%%%%%%%%%%%%%%%%%%%%%%%%%%%%%%%%%%%%%%

%% Initialization

clear;
clc;
tic
plotNum = 0;
warning('off','phased:system:array:SizeConventionWarning')
% Note: This code requires the MATLAB Phased Array System Toolbox to be
% installed to function. The script will fail with errors if the toolbox is
% not installed.

%% Configurables

% Detector Options
probDetection = 0.9999;           % Probability of detection
probFalseAlarm = 1e-6;           % and false alarm
maxRange = 1.5;                  % Meters
rangeResolution = 3.1e-3;        % Meters
                                   % Note: Size of a 1g
                                   % stainless steel ball.
nPulseInt = 1;                   % Number of pulses to
                                   % integrate

% Target Options
taregetMass = 1e-3;              % Kilograms
specificWeight = 76e3;           % N(m^-3), Note:
                                   % 18-8 stainless steel

% Array Options
arrayWidth = 0.5;                % Array width, in meters
arrayHeight = 0.5;               % Array height, in meters
centerFrequency = 60e9;          % Center frequency, in Hz
arraySpacing = 0.5;              % Array spacing, in
                                   % wavelengths

%% Definitions

% Physics definitions
```

```

v = physconst('LightSpeed');           % m/s
gravity = 9.8;                          % m(s^-2)
lambda = v/centerFrequency;            % Meters

% Array definitions
arraySpacing = arraySpacing*lambda;     % Meters
yElements = floor(arrayWidth/arraySpacing); % Array width, in elements
zElements = floor(arrayHeight/arraySpacing); % Array height, in elements
rows = zElements;
cols = yElements;
nElements = yElements * zElements;

% Target definitions
density = specificWeight/gravity;       % kg(m^-3)
targetBulk = taregetMass/density;       % m^3
targetRadius = (targetBulk*(3/4)/pi)^(1/3); % Meters
targetRCS = pi*(targetRadius^2);        % m^2 (radar cross-section)

sceneWidth = arrayWidth;
sceneHeight = arrayHeight;
totalAZ = rad2deg(2*atan2(sceneWidth/2,maxRange));
totalEL = rad2deg(2*atan2(sceneHeight/2,maxRange));
% Note: The above 4 lines define the scan area for the radar system. The
% default scan area, as coded above, scans an area equivalent to the array
% dimensions. This may take a very long time, so if only a small object is
% evaluated, it may be desirable to adjust the scene height and width.

%% Transmit Pulse Setup

pulseBW = v/(2*rangeResolution);        % Hz
pulseWidth = 1/pulseBW;                 % Seconds
PRF = v/(2*maxRange);                   % Hz
samplingFreq = 2*centerFrequency;       % Hz
adjuster = ceil(samplingFreq/PRF);       % See NOTE below
samplingFreq = adjuster*PRF;

hWave = phased.RectangularWaveform(... % Define the pulse.
    'PulseWidth' , pulseWidth , ...
    'PRF' , PRF , ...
    'SampleRate' , samplingFreq);

% Note: MATLAB will not allow a sampling frequency that is not an exact
% multiple of the pulse repetition frequency. This ensures that the instant
% the pulse is transmitted will always occur on an integer value of the
% sampling frequency. In reality, it is possible to have any sampling
% frequency and trigger the samples based on the start of the pulse. The
% "adjuster" variable selects the next sampling frequency above the Nyquist
% sampling frequency that is also a multiple of the PRF.

%% Receiver Setup

noiseBW = pulseBW;
receiverGain = 7;                        % dB, based on literature
noiseFigure = 0;                          % dB

```

```

hRX = phased.ReceiverPreamp(...           % Define the receiver amp
    'Gain' , receiverGain , ...
    'NoiseBandwidth' , noiseBW , ...
    'NoiseFigure' , noiseFigure , ...
    'SampleRate' , samplingFreq , ...
    'EnableInputPort' , true);
% Note: See my thesis, "High Resolution Ground Penetrating Radar Design and
% Simulation" (Saunders, 2014, Virginia Tech) for more information
% regarding the selection of the 7dB receiver gain.

%% Transmitter Setup

tx_gain = receiverGain;                   % dB, same as the receiver
                                           % gain (reciprocity).
minSNR = albersheim(probDetection , probFalseAlarm , nPulseInt);
peak_power = radareqpow(lambda , maxRange , minSNR , pulseWidth , ...
    'RCS' , targetRCS , ...
    'Gain' , tx_gain);                    % Define peak transmitter
                                           % power.

hTX = phased.Transmitter(...             % Define the transmitter.
    'Gain' , tx_gain , ...
    'PeakPower' , peak_power , ...
    'InUseOutputPort' , true);

%% Antenna Setup

hElement = phased.IsotropicAntennaElement(...
    'FrequencyRange' , [(centerFrequency-5e9) , (centerFrequency+5e9)]);
                                           % Define the antenna

hAntPlatform = phased.Platform(...
    'InitialPosition' , [0 ; 0 ; 0] , ...
    'Velocity' , [0 ; 0 ; 0]);            % Define the antenna
                                           % platform position and
                                           % motion

hRadiator = phased.Radiator(...
    'Sensor' , hElement , ...
    'OperatingFrequency' , centerFrequency); % Define the radiator

hCollector = phased.Collector(...
    'Sensor' , hElement , ...
    'OperatingFrequency' , centerFrequency , ...
    'Wavefront' , 'Plane');              % Define the collector

% Note: The radiator and collector refer to the actual transmitting and
% receiving device. For this purpose, it's the monostatic radar, so the
% receiving and transmitting antennas are the same device. It is possible to
% have one antenna broadcast and another receive, but that's a different
% project!

```

```

%% Array Setup

hArray = phased.URA(... % Not surprisingly, the
    'Element' , hElement , ... % array is composed of a
    'Size' , [yElements , zElements] , ... % bunch of antennas.
    'ElementSpacing' , [arraySpacing , arraySpacing]);

hArray.Element.BackBaffled = true; % See NOTE below.

hRadiator.Sensor = hArray; % With the array defined,
hCollector.Sensor = hArray; % this redefines the
hRadiator.WeightsInputPort = true; % transmitter/receiver to
% use the _array_ instead
% of an individual antenna

% Note: The ...BackBaffled statement is used to "inform" MATLAB of the
% existence of the ground plane behind the patch antenna. See the written
% thesis for more information.

%% Power Setup

hAG = phased.ArrayGain(...
    'SensorArray' , hArray , ...
    'PropagationSpeed' , v); % Defines the array gain,
% given the array setup and
% antenna elements used

ag = step(hAG , centerFrequency , [0;0]); % Calculate the new gain

peak_power = radareqpow(lambda , maxRange , minSNR , hWave.PulseWidth , ...
    'RCS' , targetRCS , 'Gain' , hTX.Gain + ag); % Given the _array gain_,
% This finds what the new
% peak power is

hTX.PeakPower = peak_power; % Sets the transmitter
% power to the new peak
% power

%% Scan Setup

maxAZ = totalAZ/2;
minAZ = -maxAZ;
maxEL = totalEL/2;
minEL = -maxEL;

beamWidth = radtodeg(sqrt(4*pi/db2pow(ag))); % Calculates the actual
% beam width

%scanInterval = radtodeg(2*atan2(tgt_radius,max_range));
scanInterval = 0.2; % The commented out line
% above sets the scan
% interval to the width of
% the minimum target

```

```

scanStep = -floor(1000*scanInterval)/1000;           % This rounds the scan
                                                    % increment to the
                                                    % thousandths

scanAZ = (maxAZ + scanStep/2):scanStep:minAZ;       % Define azimuth and
scanEL = (maxEL + scanStep/2):scanStep:minEL;       % elevation scan points

nAZ = length(scanAZ);                               % The number of azimuth and
nEL = length(scanEL);                               % elevation scans

nScans = nAZ*nEL;
nPulses = nPulseInt*nScans;

currentPoint = 1;
populatedAZ = zeros(1,nPulses);
populatedEL = populatedAZ;
for i=1:1:nEL
    for j=1:1:nAZ
        for k=1:1:nPulseInt
            populatedAZ(currentPoint) = scanAZ(j);
            populatedEL(currentPoint) = scanEL(i);
            currentPoint = currentPoint + 1;
        end
    end
end
end                                                    % This set of loops expands
                                                    % the azimuth and elevation
                                                    % scans (vectors) into full
                                                    % arrays. This is done so I
                                                    % can pass the pulse number
                                                    % into the "populated"
                                                    % arrays and get back what
                                                    % the azimuth and elevation
                                                    % "look" angles should be

revisitTime = nPulses/PRF;                           % Revisit time is how long
                                                    % it takes to complete a
                                                    % scan of the entire scene

%% Target Setup
[hTarget , hTargetPlatform , plotNum , targetDepth] = ...
    getThesisTargets(...
        1 , targetRCS , centerFrequency , plotNum , scanAZ , scanEL);
                                                    % Call the
                                                    % "getThesisTargets"
                                                    % function to get targets.
                                                    % The parameters to pass
                                                    % are defined in that
                                                    % function

nTargets = size(hTarget , 2);
for i=nTargets:-1:1
    hTargetChannel{i} = phased.FreeSpace(...
        'SampleRate' , samplingFreq , ...
        'TwoWayPropagation' , true , ...

```

```

        'OperatingFrequency' , centerFrequency);
end % Get the number of targets
% and then define that the
% wave must propagate in
% two directions for each
% target.

%% Beamformer Setup

hSV = phased.SteeringVector(... % The array (hArray) is to
    'SensorArray' , hArray , ... % be steered. . .
    'PropagationSpeed' , v);

hBF = phased.PhaseShiftBeamformer(... % . . . using the phase
    'SensorArray' , hArray , ... % shift beamformer.
    'OperatingFrequency' , centerFrequency , ...
    'PropagationSpeed' , v , ...
    'DirectionSource' , 'Input port');

%% Pre-simulation Memory Allocation/Setup

% The simulations for a 0.5 wavelength grid spacing take a LONG time, even
% on a small array. This preallocates the variables needed for
% post-processing to ensure that you don't have to wait forever for the
% simulations to run, only to run out of memory when the data is processed.
% I could not simulate the full array with 4GB of RAM. I purchased 16GB of
% RAM to complete the simulations.

fastTimeGrid = unigrid(0 , 1/samplingFreq , 1/PRF , '[]');
% FastTimeGrid is the time
% grid at the sampling
% frequency that occurs
% during the pulse.

targetAngle = zeros(2,nTargets);

% A note briefly about the System Objects used by the Phased Array System
% Toolbox. The "step( )" function is what "uses" or "activates" the System
% Object. Below, "step(hWave)" is what actually generates the wave form.
% The earlier definition of hWave simply defined the parameters that would
% dictate the wave.
wave = step(hWave);

% Similarly, "step(hTX, wave)" causes the transmitter, defined by the hTX
% definition earlier, to actually transmit the wave that was just
% generated.
[signal , tx_status] = step(hTX , wave);

% "step(hAntPlatform , 1/PRF)" calculates the new position and velocity of
% the array platform given the amount of time between pulses (1/PRF).
[ant_pos , ant_vel] = step(hAntPlatform , 1/PRF);

% The antenna platform may move, and the targets can move also. This
% updates the speed and cartesian (absolute) and polar (relative) locations
% of each of the targets.
for i = nTargets:-1:1

```

```

    [tgt_pos(:,i) , tgt_vel(:,i)] = step(hTargetPlatform{i} , 1/PRF);
    [~, targetAngle(:,i)] = rangeangle(tgt_pos(:,i) , ant_pos);
end

rxAZ = zeros(1,nScans);
rxEL = rxAZ; % rxAZ and rxEL provide a
              % place to log whether or
              % not an object was
              % detected. These points
              % align with the points in
              % the "populatedAX" and EL
              % variables defined
              % earlier.

nDataPoints = length(signal);
rxPulses = zeros(nDataPoints , nPulses);
receivedSignal = zeros(nDataPoints , nTargets);
% The above variables represent how the signal is handled. nDataPoints is
% the number of points in the transmitted wave. The wave will bounce off of
% each target, so the "receivedSignal" has to be nDataPoints by nTargets.
% Related, but different, is the received_pulses_, "rxPulses". Each
% received PULSE is comprised of the SUMMATION of all of the received
% signals. Each received signal is nDataPointsLong, so rxPulses is
% nDataPoints long, but it's the processed result for each pulses, so it's
% nDataPoints by nPulses.

MFIntermediatePulses = rxPulses;
MFPulses = zeros(nDataPoints , nPulseInt , nScans);
TVGPulses = MFPulses;
intPulses = zeros(nDataPoints , nScans);
% The above variables are for intermediate signal processing. This is where
% you can quickly run out of memory. These values, as initialized, aren't
% used as they are generated as the result of a function. However, if you
% wait until calling the function to allocate the memory, you could crash
% the program after waiting for the simulations to run.

pulseNotify = ceil(nPulses/100);
fprintf('Working...')
fprintf('\nPulses is %d' , nPulses)
% The above is a text tracker to help monitor the simulation process.
% Simulations of one small object and a restricted scene usually take ten
% minutes to an hour, and simulations of the full sene with many objects
% take days to over a week to run.

% The loop below is what actually simulates the radar system
for i = 1:nPulses

    if mod(i,pulseNotify)==0
        clc;
        elapsed = toc;
        fprintf('Currently %d percent complete\n', (i/pulseNotify))
        fprintf('Elapsed time is %d seconds\n' , floor(elapsed))
        fprintf('Estimated time remaining is %d seconds\n' , ...
            floor((100*elapsed/(i/pulseNotify)) - elapsed))
        fprintf('Estimated total time is %d seconds' , ...
            floor(100*elapsed/(i/pulseNotify)))
    end
end

```

```

end
% The above code looks at the time that has passed since the simulation
% started, and what percentage it thinks it has completed, and
% generates an estimate of how long it thinks it will take to complete
% the simulations.

azimuth = populatedAZ(i);           % Get the current azimuth
elevation = populatedEL(i);        % and elevation to scan

scanVector = step(hSV , centerFrequency , [azimuth ; elevation]);
weights = conj(scanVector);        % Setup the phase shift

for j = nTargets:-1:1              % For each target. . .

    targetSignal = step(hRadiator , ...
        signal , targetAngle(:,j) , weights);
    % . . . transmit the
    % signal. . .

    targetSignal = step(...
        hTargetChannel{j} , ...
        targetSignal , ant_pos , ...
        tgt_pos(:,j) , ant_vel , ...
        tgt_vel(:,j));
    % . . . then have that
    % signal propagate. . .

    receivedSignal(:,j) = step(...
        hTarget{j} , targetSignal);
    % . . . then have that
    % "bounce" off the target.
end

receivedSignal = step(hCollector , receivedSignal , targetAngle);
% Collect all received
% signals. . .
receivedSignal = step(hRX , receivedSignal , ~(tx_status>0));
% . . . amplify them. . .
receivedSignal = step(hBF , receivedSignal , [azimuth; elevation]);
% . . . apply the
% beamformer . . .

rxPulses(:,i) = receivedSignal;
% . . . and record the
% received pulse.

end

% I hope the end of this loop helps clarify what I had talked about in the
% previous section. The received signal is exists for every target. When
% the hCollector System Object is called, those multiple signals are
% "collapsed" into one signal - the returned pulse. There is some basic
% initial processing (amplification and beamforming) that is performed
% before the received wave is recorded. Post-processing occurs next.

%% Signal Processing

initialAz = maxAZ;
endAz = minAZ;

matchingCoeff = getMatchedFilter(hWave);

```

```

hMF = phased.MatchedFilter(...
    'Coefficients' , matchingCoeff , ...
    'GainOutputPort' , true);
[MFIntermediatePulses , MF_gain] = step(hMF , rxPulses);
MFPulses = reshape(MFIntermediatePulses , [] , nPulseInt , nScans);
matchingDelay = size(matchingCoeff , 1) - 1;
nMFPulses = size(MFPulses);
MFPulses = [MFPulses((matchingDelay + 1):end) , ...
    zeros(1 , matchingDelay)];
MFPulses = reshape(MFPulses , nMFPulses);
% The above code applies a matched filter to the data. See the thesis for a
% more involved discussion, but briefly, the matched filter convolves the
% data with a mirrored conjugated version of the transmitted pulse.

rangeGates = v*fastTimeGrid/2; % Range gates are just how
% far the wave could move
% in a given time
% increment. Here it's
% determined by the
% fastTimeGrid, which
% again, is the sampling
% frequency periods for the
% duration of a pulse at
% maximum operating range.

hTVG = phased.TimeVaryingGain(...
    'RangeLoss' , 2*fspl(rangeGates , lambda) , ...
    'ReferenceLoss' , 2*fspl(max(rangeGates) , lambda));
TVGPulses = step(hTVG , MFPulses);
% Again, see the thesis for a discussion of time varying gain. The code
% above applies the time varying gain.

intPulses = pulsint(TVGPulses , 'noncoherent');
intPulses = squeeze(intPulses);
% The code above performs the pulse integration.

noise_power = noisepow(hRX.NoiseBandwidth , ...
    hRX.NoiseFigure , hRX.ReferenceTemperature);
threshold = noise_power * db2pow(...
    npwgnthresh(probFalseAlarm , nPulseInt , 'noncoherent'));
threshold = threshold * db2pow(MF_gain);
% The code above finds the signal magnitude threshold for a valid response.

[I,J] = find(abs(intPulses).^2 > threshold); % Anywhere the magnitude of
% a pulse is above the
% threshold, record it as a
% valid response.

currentPoint = 1;
for i = 1:length(scanEL)
    for j = 1:length(scanAZ)
        rxAZ(currentPoint) = populatedAZ( (currentPoint-1)*nPulseInt + 1);
        rxEL(currentPoint) = populatedEL( (currentPoint-1)*nPulseInt + 1);
        currentPoint = currentPoint + 1;
    end
end
end

```

```

estRange = rangeGates(I);           % Estimated range
estAZ = rxAZ(J);                   % Estimated direction
estEL = rxEL(J);

%% Output Text

fprintf('Scan interval is: % 7.4f\n' , scanInterval)
fprintf('Actual beam width is: % 7.4f\n' , beamWidth)
fprintf('The revisit time is: % 7.4f s, or % 7.4f ms\n' , ...
        revisitTime , 1000*revisitTime)           % Display some facts about
                                                    % the scan

for i=1:1:2                             % Generate output plots!

    plotNum = plotNum + 1;
    dataPlotter(estAZ , estEL , estRange , scanStep , plotNum)
    if i==2
        gridPlot(scanAZ,scanEL,targetDepth)
    end                                     % dataPlotter and gridPlot
                                           % are both custom functions

    axis equal
    axis([0 1.5 -0.25 0.25 -0.25 0.25])
    view([-90,0])
    hold off
end

% As a final note, any custom functions (dataPlotter, gridPlot, and
% getThesisTargets) are all disclosed in Appendix A of my thesis.

```

APPENDIX A.2 – TARGET FETCHING CODE

```
function [hTarget , hTargetPlatform , plotNum , targetDepth] = ...
    getThesisTargets(style , tgt_rcs , fc , plotNum , scanAZ , scanEL)
% This cleans up my code significantly by hiding the (ugly) chunk of code
% that sets the targets. Pass a shape in, get targets out.
%
% The function is called
% [hTarget , hTargetPlatform , plotNum , targetDepth] =
%     getThesisTargets(style , tgt_rcs , fc , plotNum , scanAZ , scanEL)
%
% where the inputs are defined as:
% style:      A numeric value, 1-6, that defines the shape of the targets
%             1 = Three small targets
%             2 = Smiley face
%             3 = [deleted]
%             4 = One small target
%             5 = Several targets, in a line, of various sizes
%             6 = The crowded scene
% tgt_rcs:    The radar cross-section of the minimum target.
% fc:         The center frequency of the radar system.
% plotNum:    The current plot number
% scanAZ:     The azimuth scan vector
% scanEL:     The elevation scan vector
%
% and the outputs are:
% hTarget:    The System Object defining all targets
% hTargetPlatform:  The System Object defining the platform for all
%                 targets
% plotNum:    The current plot number (after making plots)
% targetDepth:  The depth of the targets (used for making grid
%                 overlays)
% There are no significant comments throughout the remainder of the code;
% see the thesis for more information.

sphereRes = 10;
targetDepth = 1.3;

switch style
    case 1      % Three small targets
        targets = [ [1.3 ; 0 ; 0] , ...           % [x;y;z] position in
                    [1.3 ; 0.01608 ; 0] , ...     % meters
                    [1.3 ; -0.01608 ; 0]];
        targetDepth = 1.3;
        nTargets = size(targets,2);
        plotR = [0.003,0.003,0.003];
        hTarget{1} = phased.RadarTarget(...
            'MeanRCS' , tgt_rcs , ...
            'OperatingFrequency' , fc);
        hTargetPlatform{1} = phased.Platform(...
            'InitialPosition' , targets(:,1) , ...
            'Velocity' , [0; 0; 0]);

    if nTargets>1
        for i=nTargets:-1:2
            hTarget{i} = phased.RadarTarget(...
```

```

        'MeanRCS' , tgt_rcs , ...
        'OperatingFrequency' , fc);
    hTargetPlatform{i} = phased.Platform(...
        'InitialPosition' , targets(:,i) , ...
        'Velocity' , [0; 0; 0]);
    end
end

case 2 % Smiley face
theta = 0:(pi/10):2*pi;
r = 0.08;

targetDepth = 1.1;

faceY = r*cos(theta);
faceZ = r*sin(theta);
faceX = targetDepth * ones(1,length(faceY));
faceTargets = [faceX; faceY; faceZ];

smileTheta = 0:(pi/5):pi;
smileR = r/2;
smileY = 1.2*smileR*cos(smileTheta);
smileZ = -1.2*smileR*sin(smileTheta);
smileX = targetDepth * ones(1,length(smileY));
smileTargets = [smileX; smileY; smileZ];

eyes = [[targetDepth; -0.8*smileR; 0.8*smileR],...
        [targetDepth; 0.8*smileR; 0.8*smileR]];

nose = [[targetDepth; 0; smileR-0.5*smileR],...
        [targetDepth-(smileR/2); 0; (smileR/2)-0.5*smileR],...
        [targetDepth-(smileR); 0; 0-0.5*smileR],...
        [targetDepth; 0; 0-0.5*smileR]];
targets = [faceTargets , smileTargets , eyes , nose];

for i=size(targets,2):-1:1
    hTarget{i} = phased.RadarTarget(...
        'MeanRCS' , tgt_rcs , ...
        'OperatingFrequency' , fc);
    hTargetPlatform{i} = phased.Platform(...
        'InitialPosition' , targets(:,i) , ...
        'Velocity' , [0; 0; 0]);
end

case 3 % Three large objects
% Removed, superceded by Case 5.

case 4 % Single small object

targetDepth = 1.4;

%tgt_radius = sqrt(tgt_rcs/pi);
%tgt_multiplier = 2;

```

```

%tgt_radius1 = tgt_multiplier*tgt_radius;
tgt_diameter = 0.1;
tgt_radius1 = tgt_diameter/2;

my_RCS(1) = pi*(tgt_radius1^2);
plotR(1) = tgt_radius1;

targets = [targetDepth; 0; 0];

hTarget{1} = phased.RadarTarget(...
    'MeanRCS' , my_RCS(1) , ...
    'OperatingFrequency' , fc);
hTargetPlatform{1} = phased.Platform(...
    'InitialPosition' , targets(:,1) , ...
    'Velocity' , [0; 0; 0]);

case 5 % Line of objects of varying sizes
targetDepth = 1.4;

tgt_radius = sqrt(tgt_rcs/pi);
tgt_radius1 = tgt_radius;
tgt_radius2 = tgt_radius1*2;
tgt_radius3 = tgt_radius2*2;
tgt_radius4 = tgt_radius3*2;
tgt_radius5 = tgt_radius4*2;
tgt_radius6 = tgt_radius5*2;

targets = [[targetDepth; -1; 0],...
    [targetDepth; -1+1*(0.25); 0],...
    [targetDepth; -1+2*(0.25); 0],...
    [targetDepth; -1+3*(0.25); 0],...
    [targetDepth; -1+4.5*(0.25); 0],...
    [targetDepth; -1+6.5*(0.25); 0]];
plotR=[ tgt_radius1,...
    tgt_radius2,...
    tgt_radius3,...
    tgt_radius4,...
    tgt_radius5,...
    tgt_radius6];
my_RCS=[ pi*(tgt_radius1^2),...
    pi*(tgt_radius2^2),...
    pi*(tgt_radius3^2),...
    pi*(tgt_radius4^2),...
    pi*(tgt_radius5^2),...
    pi*(tgt_radius6^2)];

disp(size(targets))
disp(size(plotR))
disp(size(my_RCS))
for i=size(targets,2):-1:1
    hTarget{i} = phased.RadarTarget(...
        'MeanRCS' , my_RCS(i) , ...
        'OperatingFrequency' , fc);
    hTargetPlatform{i} = phased.Platform(...

```

```

        'InitialPosition' , targets(:,i) , ...
        'Velocity' , [0; 0; 0]);
    end

case 6 % Crowded scene
    counter = 1;
    targetDepth = 1;

    casing_body_dia = 0.0095;
    casing_neck_dia = 0.0064;

    casing_body_CS = 0.5*pi*((casing_body_dia/2)^2);
    casing_neck_CS = 0.5*pi*((casing_neck_dia/2)^2);

    casing = [ [0 ; 0 ; 0], ...
               [0 ; 0 ; casing_body_dia], ...
               [0 ; 0 ; 2*casing_body_dia], ...
               [0 ; 0 ; 3*casing_body_dia], ...
               [0 ; 0 ; 3*casing_body_dia + (casing_body_dia/2) + ...
                 (casing_neck_dia/2)]
               ];
    casing_size = [casing_body_CS , casing_body_CS , ...
                  casing_body_CS , casing_body_CS , casing_neck_CS];
    casing_dia = [casing_body_dia , casing_body_dia , ...
                 casing_body_dia , casing_body_dia , casing_neck_dia];
    myCasings = zeros(3,8);
    myCasings(:,1) = [targetDepth ; 0.1 ; 0];
    myCasings(:,2) = [targetDepth ; -0.1 ; 0];
    myCasings(:,3) = [targetDepth ; 0.05 ; 0.15];
    myCasings(:,4) = [targetDepth ; 0.15 ; 0.15];
    myCasings(:,5) = [targetDepth ; 0.1 ; -0.15];
    myCasings(:,6) = [targetDepth ; -0.15 ; 0.05];
    myCasings(:,7) = [targetDepth ; -0.2 ; 0.15];
    myCasings(:,8) = [targetDepth ; -0.05 ; 0.2];

    plotR = zeros(1,size(casing,2)*size(myCasings,2));

    for i=1:1:size(myCasings,2)
        for j=1:1:size(casing,2)
            targets(:,counter) = casing(:,j) + myCasings(:,i);
            target_sizes(counter) = casing_size(j);
            plotR(counter) = casing_dia(j)/2;
            counter = counter+1;
        end
    end
    %}

    armingSpring_coil_dia = 0.015;
    armingSpring_metal_dia = 0.0016;
    armingSpring_length = 0.040;
    armingSpring_turns = 7;

```

```

pressureSpring_coil_dia = 0.010;
pressureSpring_metal_dia = 0.0016;
pressureSpring_length = 0.025;
pressureSpring_turns = 8;

armingSpring_circumference = pi*(armingSpring_coil_dia);
armingSpring_points_per_turn = floor(...
    armingSpring_circumference/armingSpring_metal_dia);

pressureSpring_circumference = pi*(pressureSpring_coil_dia);
pressureSpring_points_per_turn = floor(...
    pressureSpring_circumference/pressureSpring_metal_dia);

nArmSpringPts = armingSpring_points_per_turn*armingSpring_turns;
nPressSpringPts = pressureSpring_points_per_turn*...
    pressureSpring_turns;

armingSpring = zeros(3,nArmSpringPts);
pressureSpring = zeros(3,nPressSpringPts);

for i=1:1:nArmSpringPts
    armingSpring(:,i) = [ targetDepth+(i-1)*...
        (armingSpring_length/nArmSpringPts); ...
        (armingSpring_coil_dia/2)*...
        sin(2*pi*(i/armingSpring_points_per_turn)); ...
        (armingSpring_coil_dia/2)*...
        cos(2*pi*(i/armingSpring_points_per_turn))];
end

for i=1:1:nPressSpringPts
    pressureSpring(:,i) = [ targetDepth+...
        (pressureSpring_coil_dia/2)+...
        (pressureSpring_coil_dia/2)*...
        sin(2*pi*(i/pressureSpring_points_per_turn));...
        -(i-1)*(pressureSpring_length/nPressSpringPts);...
        0.04+(pressureSpring_coil_dia/2)*...
        cos(2*pi*(i/pressureSpring_points_per_turn))];
end

landmine = [armingSpring , pressureSpring];
armingSpring_rcs = pi*((armingSpring_metal_dia/2)^2)*...
    ones(1,nArmSpringPts);
armingSpring_radius = (armingSpring_metal_dia/2)*...
    ones(1,nArmSpringPts);
pressureSpring_rcs = pi*((pressureSpring_metal_dia/2)^2)*...
    ones(1,nPressSpringPts);
pressureSpring_radius = (pressureSpring_metal_dia/2)*...
    ones(1,nPressSpringPts);

landmine_rcs = [armingSpring_rcs , pressureSpring_rcs];
landmine_radius = [armingSpring_radius , pressureSpring_radius];

myMines = [0; -0.15; -0.15];

```

```

for i=1:1:size(myMines,2)
    for j=1:1:size(landmine,2)
        targets(:,counter) = landmine(:,j) + myMines(:,i);
        target_sizes(counter) = landmine_rcs(j);
        plotR(counter) = landmine_radius(j);
        counter = counter+1;
    end
end

americanDime_dia = 0.0179;
americanDime_rcs = pi*((americanDime_dia/2)^2);
americanDime_radius = americanDime_dia/2;

americanQuarter_dia = 0.02426;
americanQuarter_rcs = pi*((americanQuarter_dia/2)^2);
americanQuarter_radius = americanQuarter_dia/2;

myDimes = [targetDepth; 0.025 ; -0.05];
myQuarters = [targetDepth; 0; -0.2];

for i=1:1:size(myDimes,2)
    targets(:,counter) = myDimes(:,i);
    target_sizes(counter) = americanDime_rcs;
    plotR(counter) = americanDime_radius;
    counter = counter+1;
end

for i=1:1:size(myQuarters,2)
    targets(:,counter) = myQuarters(:,i);
    target_sizes(counter) = americanQuarter_rcs;
    plotR(counter) = americanQuarter_radius;
    counter = counter+1;
end

bullet_dia = 0.0057;

bullet_body_radius = bullet_dia/2;
bullet_body_rcs = pi*(bullet_body_radius^2);

bullet_nose_radius = bullet_body_radius/2;
bullet_tip_radius = bullet_nose_radius/2;

bullet_nose_rcs = bullet_body_rcs/4;
bullet_tip_rcs = bullet_nose_rcs/4;

bullet = [ [targetDepth; 0; 0],...
           [targetDepth; bullet_tip_radius + bullet_nose_radius; 0],...
           [targetDepth; bullet_tip_radius + bullet_dia; 0],...
           [targetDepth; bullet_tip_radius + 2*bullet_dia; 0],...
           [targetDepth; bullet_tip_radius + 3*bullet_dia; 0],...
           [targetDepth; bullet_tip_radius + 4*bullet_dia; 0]];
bullet_rcs = [bullet_tip_rcs,...
              bullet_nose_rcs,...
              bullet_body_rcs,...

```

```

        bullet_body_rcs,...
        bullet_body_rcs,...
        bullet_body_rcs];
bullet_radius = [bullet_tip_radius,...
        bullet_nose_radius,...
        bullet_body_radius,...
        bullet_body_radius,...
        bullet_body_radius,...
        bullet_body_radius];

myBullets = [[0;-0.075;-0.2],...
        [0;0.2;-0.05],...
        [0;0.05;0.1],...
        [0;-0.1;0.125]];

for i=1:1:size(myBullets,2)
    for j=1:1:size(bullet,2)
        targets(:,counter) = bullet(:,j) + myBullets(:,i);
        target_sizes(counter) = bullet_rcs(j);
        plotR(counter) = bullet_radius(j);
        counter = counter+1;
    end
end

for i=size(targets,2):-1:1

    hTarget{i} = phased.RadarTarget(...
        'MeanRCS' , target_sizes(i) , ...
        'OperatingFrequency' , fc);
    hTargetPlatform{i} = phased.Platform(...
        'InitialPosition' , targets(:,i) , ...
        'Velocity' , [0; 0; 0]);
end

otherwise
    fprintf('ERROR! ABORTING!')
    return
end

nTargets = size(hTarget,2);

plotRange = [0 1.5 -0.25 0.25 -0.25 0.25];
for j = 1:1:2
    plotNum = plotNum + 1;
    figure(plotNum)
    hold on
    [x,y,z] = sphere(sphereRes);
    for i=1:nTargets
        surf(plotR(i)*x+targets(1,i) , plotR(i)*y+targets(2,i) , ...
            plotR(i)*z+targets(3,i))
    end

    if j==2
        gridPlot(scanAZ,scanEL,targetDepth)
    end
end

```

```
axis equal
axis(plotRange)
view([-90,0])
hold off
end
```

APPENDIX A.3 – CUSTOM DATA PLOTTER

```
function dataPlotter(az , el , range , scanStep , plotNum)
% This function plots the output data from my thesis script. The function
% is called:
%
% dataPlotter(az , el , range , scanStep , plotNum)
%
% where the inputs are:
%   az:          The azimuth angle, in degrees, of a target.
%   el:          The elevation angle, in degrees, of a target.
%   range:       The range, in meters, from the array to the target.
%   scanStep:    The angular increment between "look" angles, in degrees.
%   plotNum:     The current plot number.
%
% The function looks at scanStep and range to determine how wide to make
% the target, then converts from polar (range, az, el) to Cartesian
% coordinates to display the results.

nPoints = length(az);
pts = zeros(3 , nPoints);
r = zeros(1 , nPoints);
scanStep = abs(scanStep);

for i=1:nPoints
    [pts(1,i) , pts(2,i) , pts(3,i)] = sph2cart(...
        degtorad(az(i)) , ...
        degtorad(el(i)) , ...
        range(i));
    r(i) = range(i)*tand(scanStep/2);
end

sphereRes = 10;
[x,y,z] = sphere(sphereRes);

figure(plotNum)
hold on
for i=1:nPoints
    surf(r(i)*x+pts(1,i) , r(i)*y+pts(2,i) , r(i)*z+pts(3,i))
end
axis equal
hold off
end
```

APPENDIX A.4 – CUSTOM GRID OVERLAYS

```
function gridPlot(scanAZ , scanEL , dist)
% This function overlays the scanning grid at a distance specified. This
% function is intended to be used with the Phased Array System Toolbox,
% which assumes the array is in the YZ plane. For this reason, "broadside"
% is assumed to occur along the +x-axis, so the distance given by 'dist' is
% assumed to be the depth the grid should be shown along the +x-axis. The
% function is called:
%
% gridPlot(scanAZ , scanEL , dist)
%
% where the inputs are:
%   scanAZ:      1xN vector of azimuthal scan angles, in degrees, pos->neg.
%   scanEL:      1xN vector of elevation scan angles, in degrees, pos->neg.
%   dist:        Scalar value giving the distance along the +x-axis to plot.

azStep = abs(scanAZ(2)-scanAZ(1));
elStep = abs(scanEL(2)-scanEL(1));

az = scanAZ + (1/2)*azStep;

az = [az, az(end)-azStep];
el = scanEL + (1/2)*elStep;
el = [el, el(end)-elStep];

nY = numel(az);
nZ = numel(el);

rows = nZ;
cols = nY;

y = sind(az)*dist;
z = sind(el)*dist;
x = dist;

nSquares = numel(scanAZ)*numel(scanEL);

gridX = zeros(5,nSquares);
gridY = gridX;
gridZ = gridX;

hold on

for j=1:1:cols-1
    for i=1:1:rows-1
        currentPoint = (j-1)*(rows-1)+i;
        pts = [...
            x , y(j) , z(i); ...
            x , y(j) , z(i+1); ...
            x , y(j+1) , z(i+1) ; ...
            x , y(j+1) , z(i); ...
            x , y(j) , z(i)];
        gridX(:,currentPoint) = pts(:,1);
        gridY(:,currentPoint) = pts(:,2);
```

```
    gridZ(:,currentPoint) = pts(:,3);
    plot3(gridX(:,currentPoint),gridY(:,currentPoint),...
          gridZ(:,currentPoint))
end
end
fprintf('Azimuthal grid spacing is % 5.2E m\n' , abs(y(2)-y(1)))
fprintf('Elevation grid spacing is % 5.2E m\n' , abs(z(2)-z(1)))
hold off
end
```